UNIVERSITY MICROFILMS, ANN ARBOR, MICH.

L. C. Card no. Mic 58-1385

CLAUSS, Francis Jacob. THERMAL FATIGUE OF DUCTILE MATERIALS

University of Michigan

Ph. D., 1957
Engin., Metal.

Negative microfilm received from University

THERMAL FATIGUE OF DUCTILE MATERIALS

by
Francis J. Clauss

A dissertation submitted in partial fulfillment
of the requirements for the degree of
Doctor of Philosophy in the
University of Michigan
1957

Doctoral Committee:

Professor James W. Freeman, Chairman
Professor Paul Naghdi
Professor Clarence Seibert
Professor Lars Thomassen
Associate Professor Edwin H. Young

THERMAL FATIGUE OF DUCTILE MATERIALS

By Francis J. Clauss

Thermal fatigue is the process by which a material ultimately fractures after being repeatedly heated and cooled without being allowed to expand and contract freely. Though thermal fatigue failures are by no means a new problem, the trends in modern technology to higher temperatures and cyclic operations have increased their occurrence and damaging effects.

This dissertation presents the results of a program of fundamental research on the thermal fatigue process in ductile alloys. Cylindrical specimens were heated and cooled through various temperature cycles while constrained from expanding and contracting freely along their axes. Two materials, S-816 and Inconel 550, were studied.

A number of specimens were cycled until they fractured across their test sections, and other specimens were removed from thermal cycling prior to fracture and then tested in stress-rupture. A few specimens were first exposed for varying times under stress-rupture conditions and then cycled to failure in thermal fatigue. Hardness measurements and microscopic examinations were made to follow the process metallurgically and help to develop a theory of thermal fatigue.

The following conclusions were drawn for the materials and test conditions studied:

1. The maximum cycle temperature had more effect than the temperature difference on the number of cycles to failure.

2. Increasing the time of exposure at high maximum cycle temperatures increased the number of cycles to failure, whereas the same increase in time at low maximum cycle temperatures decreased the number of cycles to failure.

3. The number of cycles to failure could not be directly related to the cyclic plastic strain (i.e., to the amount of thermal strain absorbed by plastic deformation during each heating and cooling).

4. Exposure to thermal fatigue conditions strengthened one alloy (S-816) and weakened the other (Inconel 550). Under the most damaging conditions studied, Inconel 550 lost 98 percent of its original stress-rupture life as a result of prior thermal fatigue, even though the number of cycles was only one-half of that required for failure by thermal fatigue alone.

5. A theory has been tentatively proposed that divides the process of thermal fatigue into 2 stages: (1) First, a stage of strain- and/or precipitation-hardening, during which the ductility is reduced and the strength is increased; (2) Second, a stage of the destruction of the cohesive bonds and the development and propagation of cracks. Structural changes that occur during thermal fatigue are an important part of this theory.

ACKNOWLEDGMENTS

The research program has been conducted at the Lewis Flight Propulsion Laboratory of the National Advisory Committee for Aeronautics. The author wishes to express his thanks to the NACA for permission to use this work as a doctoral thesis, and to the Graduate School of the University of Michigan for permission to conduct the doctoral research *in absentia*.

The author also wishes to acknowledge the help of a number of individuals at the NACA who have facilitated the research program. He particularly wishes to acknowledge the helpful discussions with Messrs. Samuel S. Manson, G. Mervin Ault, George C. Deutsch, William F. Brown, Richard H. Kemp, John W. Weeton, and Robert W. Smith, as well as the work of Messrs. Charles H. Gresslin and Leo J. Hecht in the design and construction of the electrical equipment, the help of Miss Anne R. Kendra, Miss Frieda L. Kuhn, and Mr. William J. Waters in the metallographic work and that of Messrs. Owen T. Hickey, Steve P. Barnosky, and John Shannon in conducting the creep-rupture tests.

Finally, the author wishes to acknowledge the guidance of Professor James W. Freeman, Chairman of the Doctoral Committee.

TABLE OF CONTENTS

	Page
ACKNOWLEDGMENTS	ii
LIST OF ILLUSTRATIONS	iv
INTRODUCTION	1
PRELIMINARY CONSIDERATIONS AND LITERATURE SURVEY	3
Basic Concepts	3
Thermal Stress Tests	7
Mechanism of Failure	15
EQUIPMENT AND PROCEDURE	31
Equipment	31
Materials	33
Procedure	34
RESULTS	40
Specimens Failed by Thermal Fatigue Alone	40
Changes in Material Properties Due to Thermal Fatigue	45
Specimens Run in Stress-Rupture, Then Failed by Thermal Fatigue	48
DISCUSSION	49
CONCLUSIONS	61
REFERENCES	62

LIST OF ILLUSTRATIONS

Figure		Page
1.	Test specimen	66
2.	Diagram of equipment	67
3.	Thermocouple wires spot-welded to S-816 specimen (specimen had been cycled 200 times between 1350° and 200° F)	68
4.	Temperature profiles of test specimens	69
5.	Photograph of equipment	70
6.	Photograph of equipment	71
7.	Microstructure of heat-treated S-816	72
8.	Microstructure of heat-treated Inconel 550	73
9.	Free contraction of test section during cooling from various maximum temperatures to a minimum temperature of 200° F	74
10.	Average strain in test section during first cycle of constrained cooling from various maximum temperatures to a minimum temperature of 200° F	75
11.	Tensile stress in test section during first cycle of constrained cooling from various maximum temperatures to a minimum temperature of 200° F	76
12.	Temperature conditions during cooling	77
13.	Average strain in test section during constrained cooling from various maximum cycle temperatures to a minimum cycle temperature of 200° F at $N = 1/2\ N_f$	78
14.	Amount of bulging in specimens that had failed in thermal fatigue at various T_{max}	79
15.	Effect of T_{max} on N_f for Inconel 550 specimens thermally cycled at a constant ΔT and a constant T_{min}	80

Figure		Page
16.	Effect of T_{max} on N_f for S-816 specimens thermally cycled at a constant ΔT and at a constant T_{min} .	81
17.	Effect of ΔT on N_f for Inconel 550 specimens thermally cycled at a constant T_{max} and at a constant T_{min}	82
18.	Effect of time of exposure at T_{max} on N_f for Inconel 550 specimens thermally cycled at various T_{max} . .	83
19.	Effect of time of exposure at T_{max} on N_f for S-816 specimens thermally cycled at various T_{max}	84
20.	Variation of the number of cycles to failure of S-816 specimens with the average plastic strain per half-cycle	85
21.	Effect of prior thermal cycling on the stress-rupture life of S-816 at 1350° F	86
22.	Effect of prior thermal cycling on the stress-rupture life of S-816 at 1500° F	87
23.	Effect of prior thermal cycling on the stress-rupture life of Inconel 550 at 1350° F	88
24.	Effect of prior thermal cycling on the stress-rupture ductility of S-816 at 1350° F	89
25.	Effect of prior thermal cycling on the stress-rupture ductility of S-816 at 1500° F	90
26.	Effect of prior thermal cycling on the stress-rupture ductility of Inconel 550 at 1350° F	91
27.	Effect of prior thermal cycling without constraint on the stress-rupture life of S-816 at 1350° F	92
28.	Effect of prior thermal cycling without constraint on the stress-rupture life of Inconel 550 at 1350° F .	93
29.	Effect of prior thermal cycling without constraint on the stress-rupture ductility of S-816 at 1350° F .	94
30.	Effect of prior thermal cycling without constraint on the stress-rupture ductility of Inconel 550 at 1350° F	95
31.	Effect of prior thermal cycling on the stress-rupture life of S-816 at 1350° F (60 seconds exposure at T_{max})	96

Figure

Page

32. Effect of prior thermal cycling on the stress-rupture life of Inconel 550 at 1350° F (60 seconds exposure at T_{max}) 97

33. Effect of prior thermal cycling on the stress-rupture ductility of Inconel 550 at 1350° F (60 seconds exposure at T_{max}) 98

34. Effect of prior thermal cycling on the stress-rupture ductility of S-816 at 1350° F (60 seconds exposure at T_{max}) 99

35. Effect of the T_{max} of thermal cycling on the stress-rupture life of S-816 at 1350° F ($N = 1/2\ N_f$) . . . 100

36. Effect of the T_{max} of thermal cycling on the stress-rupture life of Inconel 550 at 1350° F ($N = 1/2\ N_f$) 101

37. Effect of the T_{max} of thermal cycling on the stress-rupture ductility of S-816 and Inconel 550 at 1350° F ($N = 1/2\ N_f$) 102

38. Effect of exposure to stress-rupture conditions on the thermal fatigue life of S-816 103

39. Effect of exposure to stress-rupture conditions on the thermal fatigue life of Inconel 550 104

40. Effect of thermal cycling on the hardness of S-816 105

41. Effect of thermal cycling on the hardness of Inconel 550 . 106

42. Microstructure of Inconel 550 after 1000 cycles at 1350/200° F 107

43. Microstructure of Inconel 550 after 1000 cycles at 1350/200° F 108

44. Microstructure of Inconel 550 after 7000 cycles at 1350/200° F 109

45. Microstructure of Inconel 550 after 2000 cycles at 1350/200° F 110

46. Microstructure of Inconel 550 after 7000 cycles at 1350/200° F 111

47. Microstructure of Inconel 550 after 7000 cycles at 1350/200° F 112

Figure Page

48. Effect of T_{max} on N_f for S-816 and Inconel 550 specimens thermally cycled at a constant T_{min} 113

49. Effect of T_{max} on the amount of hardness change of S-816 and Inconel 550 specimens that had been fractured as a result of thermal fatigue 114

50. Microstructure of Inconel 550 specimen that had been fractured by thermal fatigue at 1600/200° F 115

51. Microstructure of Inconel 550 specimen that had been fractured by thermal fatigue at 1600/200° F 116

52. Microstructure of Inconel 550 specimen that had been fractured by thermal fatigue at 1600/200° F 117

53. Microstructure of Inconel 550 specimen that had been fractured by thermal fatigue at 1550/200° F 118

54. Microstructure of Inconel 550 specimen that had been fractured by thermal fatigue at 1450/200° F 119

55. Microstructure of S-816 specimen that had been fractured by thermal fatigue at 1450/200° F 120

56. Microstructure of S-816 specimen that had been fractured by thermal fatigue at 1200/200° F 121

INTRODUCTION

Thermal fatigue is the process by which a material ultimately fractures after being repeatedly heated and cooled without being allowed to expand and contract freely. Though thermal fatigue failures are by no means a new problem, the trends in modern technology to higher temperatures and cyclic operations have increased their occurrence and damaging effects. Thus, for example, thermal fatigue complicates the operation of petroleum refineries, power plants, turbojet engines, and, most recently, nuclear reactors.

Considering its importance, there is very little fundamental information available on thermal fatigue in ductile materials. Mathematical analyses have been largely confined to brittle materials or to idealized conditions in ductile ones. Laboratory results on the relative merits of real materials in thermal fatigue have not always been consistent, nor have attempts to correlate them with service performance always been successful.

This dissertation presents the results of a program of fundamental research on the thermal fatigue process in ductile alloys. The particular purposes to which the research was directed are:

1. To study the effect of the test conditions on the thermal fatigue life of ductile alloys.

2. To evaluate the extent of changes in certain mechanical properties caused by varying amounts and conditions of thermal fatigue.

3. To correlate or explain the experimental observations on thermal

fatigue on the basis of present theories of the solid state.

In the experimental part of this study, cylindrical specimens were heated and cooled through various temperature cycles. A gripping device was used to constrain the specimens from expanding and contracting freely along their axes during the temperature cycling. Failure was defined as fracture across the test section of a specimen.

Sufficient tests were carried out to define the conditions of failure by thermal cycling alone. The factors that were studied for their effects on the number of cycles to failure were the maximum cycle temperature, the temperature difference of cycling, the time of exposure at the maximum cycle temperature, and the strain change per half-cycle (i.e., the amount of thermal strain absorbed by deformation during each heating and cooling).

A number of specimens were removed from thermal cycling prior to failure and then tested in stress-rupture to measure any changes in their life or ductility under specified conditions. The independent variables were the number of cycles, the maximum cycle temperature, and the time of exposure at the maximum cycle temperature. Control specimens were cycled with no constraint to observe any changes that might be due to temperature conditions alone.

Hardness measurements and microscopic examinations were made on many of the specimens in order to follow the process of thermal fatigue metallurgically and help to develop a theoretical understanding of it.

A few specimens were exposed first to varying times under stress-rupture conditions and then cycled to failure in thermal fatigue. This reversed the order of testing mentioned previously and gave results that aided in developing a theory of thermal fatigue.

PRELIMINARY CONSIDERATIONS AND LITERATURE SURVEY

Basic Concepts

Thermal stress. - When a solid is heated or cooled nonuniformly, the various sections tend to expand or contract in different amounts. The same is true if the temperature is changed uniformly throughout a body composed of several materials with different rates of thermal expansion. To enable such bodies to remain continuous, systems of thermal strains and associated stresses are set up internally. The magnitude of the thermal stresses will depend upon:

1. The temperature distribution within the body.

2. The properties of the material.

3. The degree of constraint, which is imposed by the continuity of the body and by external boundary conditions.

Thermal shock. - Thermal shock means either sudden heating or cooling. The thermal stresses caused by thermal shock are generally greater than those that occur during slow heating or cooling for two reasons:

1. The transient temperature distributions produced within the body during sudden heating or cooling are more severe.

2. The thermal stresses do not have time to be relieved by relaxation during sudden heating or cooling.

When the thermal stress at some point in the body exceeds the fracture strength of the material, the body will fracture at that point. Failure in a single cycle of heating or cooling occurs when the body cannot deform plastically to relieve the thermal stress, and this usually

implies thermal shock conditions, a high degree of constraint, and/or a brittle material.

Thermal fatigue. - When failure occurs after a repeated number of cycles of thermal stressing rather than on the first cycle, the process of failure is known as "thermal fatigue." This process is much more complex than when failure occurs on the first cycle. It includes certain elements present in normal mechanical fatigue at low temperatures, such as cyclic plastic deformation in tension and compression that ultimately "exhausts" the ductility of the material and causes a fatigue crack. It also includes certain elements of the normal creep-rupture process at high temperatures. Thus, while the material is at the high temperature of the cycle, annealing may occur to relieve the strain-hardening due to reversed plastic deformation, or secondary phases may precipitate along slip lines and cause additional hardening. The structural changes that occur will depend upon the material, the strain, and the temperature involved, and they may change the strength and ductility so much that the material will fracture from causes other than thermal fatigue. On the other hand, long before the material cracks or fractures, it may warp or distort to a degree that exceeds the dimensional tolerances.

Examples of thermal fatigue. - While thermal fatigue is not new, it is becoming an increasingly difficult and frequent problem that the engineer must face. This seems to be due both to the continual rise in service temperatures and to operations that are cyclic in nature. A few examples will suffice to illustrate the point.

1. Power generating plants (1,2): One of the most severe problems of thermal shock in main steam lines is the carry-over of boiler feedwater along with steam. This cools the inside of the pipes, producing

a thermal gradient in the wall. Contraction of the quenched layer is resisted by the outer layers of the pipe which are at higher temperatures, and this subjects the inside of the pipe to a tensile stress. This may cause the steam pipes to crack when they are quenched by the feedwater carry-over and may damage the equipment.

2. Petroleum refineries (3,4,5): Experience in the petroleum industry has shown that much of the trouble with high-temperature service occurs during heating or cooling. Piping systems are prone to develop leaks when equipment is brought "on stream" and is heating. When it cools, other leaks and even breaks may develop. Less trouble is reported with equipment that operates steadily at temperature than that which requires shutdowns. Unfortunately, most high-temperature equipment in refineries requires periodic shutdowns (every 90 days, for example) for cleaning and other maintenance. Also, many processes introduced into the petroleum industry in the last 10 years are cyclic. In these, the equipment operates for a period of time at one set of temperature and pressure conditions, and then for another period of time at a different set of conditions.

3. Turbojet engines (6,7,8,9,10): Thermal stresses in turbojet engines are most severe in such parts as the combustor, turbine, and tailpipe, which are subjected to direct heat. Each time the engine is started, these parts are heated rapidly to their operating temperatures. If, for any reason, flame-out (combustion blowout) occurs during flight, the parts are cooled rapidly by the inrush of cold air. Rapid heating then follows on reigniting the flame. Lesser temperature changes occur whenever the engine changes speed. During a normal shutdown, the parts are again subjected to rapid cooling. All of these conditions expose the

parts in the hot section of the turbojet to repeated cycles of thermal stressing which are added to the normal stresses of operation.

4. Nuclear reactors (11): Because of the rapid conversion of nuclear to thermal energy in the fuel elements of nuclear reactors, the thermal fluxes encountered are many times those in conventional heat-transfer equipment. Thus, the steady-state operation of a reactor is associated with high thermal fluxes and accompanying steep temperature gradients and severe thermal stresses. The transient thermal problem is even more severe. Since the nuclear control of a reactor can take place more rapidly than the control of the coolant flow, transient thermal stresses can result that are particularly large.

Reducing thermal stresses. - There are three general methods for reducing thermal stresses and their effect. These are concerned with the temperature, the geometry, and the material. In the first group are included those means for obtaining more even temperature distributions, particularly during the transient conditions when the greatest differences in temperature are produced within the body. Two effective means here are: (1) to reduce the rate of heating or cooling, (2) to increase the rate of heat transfer within the body. Thus, coatings with high reflectivity can be used to suppress radiant heating so that coated parts heat more slowly than uncoated ones. Heat transfer within the body can be speeded up by increasing the thermal conductivity, as by using a copper core (the thermal conductivity of copper is about 15 times that of high-alloy steel). In many cases, proper maintenance and operation can eliminate hot spots, such as those that occur when deposits build up on fuel nozzles and deflect the flames against restricted areas.

Designers have exercised great ingenuity in changing the geometry

of parts so as to relieve constraint and reduce thermal stresses. Floating constructions have been used in tube bundles of heat exchangers, in nozzle diaphragms of turbojet engines, and in large bridges. Bellows and loops are used to accommodate the expansion and contraction in long runs of pipe that are subjected to temperature changes, and bellows attachments are also used to fasten parts that are to be heated and cooled to other massive parts that do not undergo the same temperature changes. Hollow parts, where they can be used, may have better resistance to thermal fatigue than solid parts either because of less thermal inertia (or resistance to temperature changes), a more even distribution of temperature, or more flexibility to relieve constraints. Segmenting parts has also been used to gain flexibility. Notches and abrupt changes in cross-section that concentrate thermal stresses should, of course, be eliminated early in a design.

Reducing thermal stresses by the first two methods may prove difficult from a design point of view or impractical because of the particular operating conditions. In such a case the problem that falls to the metallurgical engineer is twofold. First, there is the presentation of experimental data on a material in such a way that the designer can evaluate its behavior under service conditions. Second, there is the development of materials with greater built-in resistance to thermal fatigue. Both of these problems are made more difficult by a lack of understanding of the thermal fatigue process. Neither the material properties nor the temperature and time variables that are most important are well understood.

Thermal Stress Tests

Material evaluation. - Laboratory tests for measuring the

resistance of materials to thermal stresses are not yet standardized and often produce results that are contradictory with one another and with actual service records. A discussion of test procedures may point out the difficulties.

In general, two methods of testing are used:[1]

1. Specimens are subjected to varying temperature changes, and the minimum temperature change that will cause the specimen to fail in a single cycle under otherwise specified conditions is measured.

2. Specimens are repeatedly subjected to the same temperature cycle, and the number of cycles that the specimens survive before failing under the specified conditions is measured.

In both of these tests, failure is usually defined either as visible cracking at the surface or as actual fracture across the cross-section. The first type of test is usually confined to brittle materials. The second type is more common with ductile materials, which seldom fail in a single cycle because of their ability to deform and relieve the stresses.

In these tests, the specimens are constrained from expanding or contracting freely by the manner and rate of heating and/or cooling, by their geometry, or by a combination of the two. External constraining forces are sometimes used but are generally absent. The specimens may be heated slowly and uniformly in a furnace to the upper temperature and suddenly quenched at a single point or plane of the specimen. In such a

---

[1]A third type of test, which will not be discussed, is one that has been standardized by the American Society for Testing Materials for classifying the resistance of refractory bricks or block to spalling. Spalling involves a weight loss due to flaking of the surface layer or to chipping of the corners of the brick, and the ASTM test classifies the bricks on the basis of the percentage weight loss after a specified spalling test.

test, the specimen has more freedom to expand uniformly during heating than to contract uniformly during cooling, and, as a result, the specimens generally fail in tension during the cooling part of the cycle at the point where the cooling is most rapid. In other tests a flame is directed against a spot on the specimen for a given period of time or until the specimen has heated to a definite temperature, and the flame is then removed and the specimen cooled by a stream of air. Specimen shapes that concentrate the thermal stress at a single point or plane are frequently used because they reduce the number of cycles to failure and thereby shorten the testing time required.

The severity of such tests depends upon the temperature change, the rate and manner of heating and cooling, and the geometry of the specimen. Unfortunately, the stress and strain distributions are too complex to calculate or measure, and the severity can be defined only by specifying the test conditions. A second drawback is that the tests are based on the definition of failure either as the appearance of macroscopic cracks at the surface or as fracture of the specimen. As ordinarily conducted, they give no measure of any damage that might have built up in the specimen long before failure. Such damage might reduce the strength of the material so that it would fail under complex service conditions much sooner than it would fail because of thermal fatigue alone. A knowledge of such damage as measured by, say, the reduction in strength or ductility would greatly aid in developing a theory of thermal fatigue, as well as provide important engineering data.

Within these limitations, thermal shock tests have been conducted and have produced valuable basic information, in addition to evaluating the relative merit of several materials. The following literature review

is intended to illustrate briefly the important points that have been established.

Literature review. - The results of an early German study of the resistance of high-temperature alloys to repeated thermal shock are described in an English survey by Bentele and Lowthian (12). Wedge-shaped specimens of various materials were heated in a flame for 1 minute and then cooled in still air for 3 minutes. The specimens were cycled to two flame temperatures--one at 650° to 700° C (1202° to 1292° F), the other at 850° to 900° C (1562° to 1652° F). Specimens failed either by severe distortion of the edge or by the formation of cracks. The number of test cycles to failure varied with the materials and temperatures as follows:

Material*	Number of cycles to 650°-700° C before onset of distortion or cracking	Number of cycles to 850°-900° C before onset of -	
		Distortion	Cracking
W.F.200	1800	--	364
DVL.30	1645	--	56
P.193	1393	--	83
DVL.32	1280	--	44
DVL.31/4	1130	60	137
B.7M	1050	--	94
ATS	1023	40	---
SAS.8	858	--	---
W.F.100.D	834	--	360

*Information on the chemical compositions and properties of these materials was not available for comparison with U. S. alloys.

These tests demonstrated the following:

1. Excessive distortion, as well as cracking, is an important criterion of serviceability.

2. The number of cycles to failure falls off very rapidly as the temperature difference (or maximum cycle temperature) is increased.

3. The relative merit of several materials can change with the test conditions. Therefore, tests for rating materials must closely approach the conditions of the intended service or the results can be misleading.

The authors were unable to find any clear relation between the resistance to thermal shock and such material properties as tensile or creep-rupture strength.

Whitman, Hall, and Yaker (13) conducted tests at the NACA to measure the resistance of six cast high-temperature alloys (S-816, S-590, HS-21, 422-19, X-40, and Stellite 6) to thermal shock. Specimens were cast in the form of wedges and were heated to a uniform temperature of 1750° F for 1 hour and then quenched in water along a 1/32-inch edge. When the specimens were cool, they were removed from the quenching apparatus, the oxide films were carefully removed from the narrow edges, and these edges were microscopically examined for cracks. Failure was arbitrarily defined as the presence of an opening across the entire width of the quenched edge.

The average number of cycles to failure varied from 98 for S-816 to 4 for Stellite 6. No correlation was found between the thermal properties (coefficient of linear expansion, thermal conductivity, and specific heat) and the resistance of the alloys to thermal cracking. Since the thermal properties of the six alloys did not vary over a wide range, the investigation demonstrated that materials with similar thermal properties can have widely different resistances to thermal cracking.

Besides cracking, the specimens also warped so that the quenched edges bowed in a concave manner. The amount of bowing increased with

the number of cycles, the rate of bowing decreasing as the number of cycles increased. Although the rates of bowing were different for the alloys, the greater the number of cycles to failure, the greater was the amount of bowing at failure. Two relations were derived, namely,

$$n = 4198\ \Sigma_b^{1.318} \tag{1}$$

and

$$n = 0.002 \left(\frac{h}{\alpha}\ \Sigma_b\right) 1.370 \tag{2}$$

where

n = number of cycles to failure

Σ_b = deformation strain in wedges at failure

$h = \frac{k}{\rho_c}$ = thermal diffusivity, ft^2/hr

α = coefficient of linear expansion, in./in./^oF

Both equations gave good correlations. The authors concluded that the ability of a material to absorb strains is important in determining its resistance to cracking under repeated thermal stresses.

Tests similar to the NACA test in which wedge- or triangular-shaped specimens were heated and/or cooled along one edge have been used by many other investigators. At Allegheny-Ludlum Steel Corporation, for example, the thermal shock test involved repeatedly heating the edge of a triangular shaped sample in a propane-air flame to a maximum temperature of 1800^o F and then suddenly cooling this edge to 800^o F in a blast of compressed air (14). Failure was considered reached when a crack had progressed completely across the 1/32-inch edge of the specimen. The average number of cycles to failure varied for different alloys as follows:

Alloy	Approximate number of cycles to failure
Cast vitallium	6300
Wrought S-816	5400
Wrought L-605	4150
Wrought S-590	4050
Cast X-40	3600
Cast S-816	2900
Wrought V-36	2700
Wrought M-252	2500
Cast HE-1049	2250
Wrought Waspalloy	2250
Cast GMR-235	950
Cast Guy Alloy	500

These data show that cast HS-21 and X-40 were superior to cast S-816, whereas they were both inferior to cast S-816 in the tests of Whitman, Hall, and Yaker cited above (13). This discrepancy may have been due to differences in the lots of material or in the test conditions.

The significance of the differences between the alloys in the thermal shock test as related to actual service behavior was not determined in the Allegheny-Ludlum study, nor were attempts to correlate thermal shock resistance with other common properties successful.

Coffin (15,16,17,18) recently presented a most interesting and detailed study of the thermal fatigue of thin tubular specimens of Type 347 stainless steel. These specimens were constrained longitudinally by being gripped in a rig that clamped on to flanges at their ends. In most cases, the specimens were initially stress-free and clamped at the upper temperature limit. (Coffin found no difference in the thermal fatigue life regardless of whether the specimens were clamped at the upper or the lower temperature limit.) The effect of the ΔT of cycling was studied by varying ΔT from 200° to 500° C while holding the mean temperature constant at 350° C; that is, T_{max}/T_{min} varied from 450°/250° C

to 600°/100° C (842°/482° F to 1112°/212° F). The average temperature was held constant in order to minimize the effect of temperature on the material and to measure only the effect of varying amounts of thermal strain associated with the various ΔT's. The frequency of cycling was 4 cycles per minute, which is unusually fast for thermal fatigue tests, and failure was defined as complete or nearly complete separation of the specimen. Under these conditions, the thermal fatigue life of annealed specimens dropped from about 40,000 cycles to 1800 cycles as the ΔT was increased from 200 to 500° C.

The effect of cold-working was studied by prestraining specimens in tension or torsion. At high ΔT's, prior cold work reduced the life; for example, at a ΔT of 400° C, a 360° twist in the specimen reduced its life to 650 cycles, as compared to 3800 cycles for the annealed material. As the ΔT was reduced, the damaging effect was less, and in several cases the cold-worked material became better than the annealed material at low ΔT's; thus the curve for 360° pretwist crossed that for annealed material at a ΔT of about 300° C. Coffin found that the kind of prior cold work was not important in thermal cycling. Specimens cold-worked by torsion or by tension withstood the same number of cycles of thermal stressing, so long as both were worked to the same amount of effective strain.

Coffin also studied the effect of mean temperature on thermal fatigue by testing specimens at mean temperatures of 250°, 350°, and 450° C while maintaining the ΔT at about 300° C. Because of the slight change in the expansion coefficient with temperature, the free thermal expansion for a ΔT of 300° C was greater at a mean temperature of 450° C than at the lower mean temperatures and the ΔT's were therefore

adjusted slightly to maintain constant strain amplitudes. An increase in mean temperature under these conditions decreased the thermal fatigue life from about 15,000 cycles at a mean temperature of 250° C to 8,000 cycles at 450° C.

In another series of tests cycled between 200° and 500° C, the time that the specimens were at 500° C was varied. While there was considerable scatter in these results, increasing the hold time from 6 to 180 seconds appeared to decrease the number of cycles to failure from about 10,000 to 7,000, with a possible minimum for a hold time of 60 seconds. Coffin felt that, from a practical point of view, the decrease in the number of cycles to failure with increased hold times was small and pointed out that the life was actually increased if the total elapsed time of the tests was used rather than the number of cycles.

Mechanism of Failure

The results of the thermal fatigue studies cited in the preceding section emphasize the complexity of the thermal fatigue process. Many of its features are difficult to incorporate into a working theory, and, in fact, no completely satisfactory theory of thermal fatigue has yet been developed.

The review of the literature in the following section is intended to consider those factors in the deformation of metals that may be important in developing an understanding of the behavior of materials during reversed deformation under cyclic temperatures. The review starts with theories of low-temperature deformation, and includes brief discussions of the Bauschinger effect, high-temperature creep, and both mechanical and thermal fatigue.

Dislocation theory of deformation. - In ductile materials, fracture

is preceded by plastic deformation, and this deformation is generally accepted to occur by the movement of dislocations. The deformation is not uniform; certain crystals and planes that are favorably oriented undergo more plastic flow than do other crystals or other planes. Additional dislocations are produced during deformation. The dislocations that move through these crystals under stress are thought to pile up at grain boundaries and other barriers where they exert a backward stress. A complex network ("forest") of dislocations results that opposes the further movement of dislocations, and the material is said to strain-harden. Its ductility, or ability to absorb further deformation without fracture, is reduced.

Besides deforming by slip along glide planes, some metals and alloys deform by twinning. Nickel alloys, in common with a number of other alloys and metals, are particularly prone to twin formation. Bruckner (19) believes that mechanical twinning in alpha-iron is related to the incidence of cleavage fracture and that twinning may on occasion be directly responsible for the onset of cleavage. There are many others who consider mechanical twinning as merely incidental to brittle fracture. Bruckner has shown photomicrographs of recrystallized grains appearing at twin boundaries as evidence of the strained regions about the twins, and he has postulated that cleavage fracture is initiated when a propagating twin meets an effective barrier and its energy is diverted into producing slip.

Bauschinger effect. - The Bauschinger effect is an important phenomenon in reversed stressing. It is commonly interpreted as follows: The strain in a material that is stressed beyond its elastic limit is not uniform, and certain crystals and planes deform more than others.

This sets up residual strains when the load is released. If the original stress was tensile, some crystals and/or planes become loaded in compression when the tensile load is released. If the material is then loaded in compression, the residual compressive stresses add to the external load, and plastic flow begins at a lower stress than if the material were reloaded in tension.

Zener (20) suggests that the Bauschinger effect is due to microscopic residual stresses associated with the individual slip bands in the crystals, while Elsesser, et al. (21,22), attribute it to residual atomic forces around flaws and disordered regions. Heating at relatively low temperatures can provide enough energy for the dislocations or vacancies to diffuse out of these highly strained regions and eliminate the Bauschinger effect.

Theories of creep. - The dislocation model of plastic deformation has been applied to creep at elevated temperatures by assuming that the rate-controlling process for creep consists of the thermal activation of dislocations over barriers. While the main driving force is due to thermal movement, a preferential direction is given by the influence of the applied stress. These ideas have been formalized mathematically by several investigators (see reference 23 and references cited therein).

More recently, attention has been directed to the role of vacancies in deformation, particularly in creep at high temperatures. Thus, overall activation energies for rupture of pure metals that have been computed by Dorn and his co-workers (24) are nearly the same as the activation energies for self-diffusion, and vacancies are widely accepted as playing a dominant role in diffusion. At any given temperature, there is an equilibrium number of vacancies that exists within the crystal

lattice. The movement of suitable dislocation jogs during plastic deformation can generate vacant lattice sites (and possibly interstitial atoms) in excess of the equilibrium number (25).

The excess of vacancies would tend to revert to the equilibrium amount. At very low strain rates, the concentration of vacancies would remain substantially at their equilibrium value, whereas at much higher strain rates, larger degrees of supersaturation could be maintained. These ideas are supported by the results of Buffington and Cohen (26) on the self-diffusion of alpha-iron at 890° C (1634° F), assuming that diffusion occurs by a vacancy mechanism. These investigators found that the diffusion coefficient increased (linearly) with the strain rate, which they interpreted to mean that the number of vacancies also increased with strain rate, as postulated by Seitz (25). As a measure of the magnitudes involved, the rate of diffusion at 890° C (1634° F) was increased by a factor of 10 for a strain rate of 0.18 in./in./hr, which corresponded to a stress of only 1300 psi.

In order to remove excess vacancies from the crystal lattice and maintain the equilibrium concentration, the vacancies must come together, either within the lattice or at the grain boundaries, and form voids. There are several schools of thought as to the mechanism of void formation (27 to 36), but that which appears most acceptable is their heterogeneous nucleation by preexistant nuclei. Machlin (32) suggests that the nuclei may be identified as submicroscopic voids or cracks produced during solidification or working, supercritical sized particles containing cracks, or gas pockets. Fissures starting from local regions of high stress concentrations are also thought to influence void formation (31,34,35).

Numerous investigators have drawn attention to the minute cavities or pores formed in metals undergoing creep at elevated temperatures (37, 38,39,40,41). Jenkins, Bucknall, and Jenkinson (37) referred to the formation of "distortion cavities" in the grains and grain boundaries of a Cu-Ni-Si alloy as a result of excessive local distortion at discontinuities such as inclusions and particles of a brittle constituent. Greenwood, Miller, and Suiter (40) made a very thorough study of intergranular cavitation in copper, alpha-brass, and magnesium over a range of strain rates and temperatures. They noted that under the conditions used the disordered lattice at the boundary acted as a trap in which holes readily formed. The crystal lattice was a continuous source of vacancies, generated by dislocation motion, and the grain boundary cavities were continuous sinks.

Cavitation appeared more readily under conditions that caused a change in emphasis from deformation by slip to deformation by grain translation (i.e., lower strain rates and higher temperatures), though this might have been a cause rather than an effect. Thus, a sliding movement at the grain boundaries would probably cause localized distortion of the lattice that would aid cavities to form, whereas, on the other hand, the nucleation of large numbers of cavities would weaken the boundaries and therefore aid movement in those regions. As deformation proceeded, more vacancies would be absorbed by the existing cavities, and these would grow in size. The cavities would also be spread by tensile stress concentrations. Their growth, coupled with the applied stress, would ultimately cause the cavities in a boundary to link together. The grains would then part and an intercrystalline crack would be formed.

Mechanical fatigue. - In many respects thermal fatigue is similar to mechanical fatigue, and one can reasonably expect that the mechanism for high-temperature mechanical fatigue will, with some modification, apply also to thermal fatigue.

A number of theories have appeared through the years to explain the failure of metals by fatigue (43,44,45,46,47). While most of them have long been discarded, they all agree that the fatigue of metals is associated with a slip process similar to that involved in unidirectional extension. Thus, Gough and his collaborators (46 and 47) found that the same slip planes and slip directions operated for both repeated cyclic stressing and monotonic loading. They also found that fatigue was invariably accompanied by evidence of strain-hardening. Slip bands developed early under cyclic stressing and were accompanied by strain-hardening, but they did not cause cracks to form so long as the stresses were below the endurance limit. At stresses above the endurance limit, cracks formed in the regions of slip and slip bands continued to form and broaden even after fatigue cracks had appeared. Single crystals and polycrystalline specimens both appeared to behave in the same manner, although there were differences in degree which were associated with grain boundaries that acted to inhibit slip and influenced the rate of propagation of fatigue cracks.

Coffin, in his work on thermal fatigue (16) pictures the reversed straining as due to the movement of dislocations back and forth from one barrier to another with each stress reversal. A certain amount of energy is required to generate the dislocations and to move them back and forth from barrier to barrier; this energy is continuously dissipated into the lattice as thermal vibration and is responsible for the hysteresis loop

found under cyclic stressing. Certain factors cause this process to be irreversible and cause it to move to neighboring planes so that the region of dislocation reversal grows.

The quantitative theory of fatigue presented in 1939 by Orowan (48) considered local plastic slip and subsequent strain-hardening as the principal cause of fatigue, and assumed that a fatigue failure would occur when the "total plastic strain" (i.e., the sum of the absolute values of all positive and negative strains) reached a characteristic finite value. Orowan's argument proceeds as follows:

1. Stress distribution is more or less inhomogeneous in all materials because of the unavoidable presence of small cracks and structural inhomogeneities (e.g., grain boundaries and inclusions) as well as inhomogeneities created by plastic flow.

2. If the material is brittle, fracture occurs when the stress at the point where the stress concentration is highest reaches the true strength of the material.

3. If the material is plastic, it will yield at the stress peaks (i.e., at the points where local maxima of stress occur) before the true strength is reached. Further increase of load causes more plastic strain at these points, but the stress does not increase appreciably beyond the yield point. The surplus stress is taken over by the (more or less elastic) surroundings of the stress peak, and, in this way, the stress distribution is smoothed out.

4. If the load is alternating, the local plastic yielding will not come to an end but will alternate, and this will produce a progressive strain-hardening at the stress peaks. Consequently, the stress at which plastic yielding begins increases in the course of the load fluctuations,

the smoothing out of the stress distribution becomes less effective, and the maximum stress at the stress peaks rises until finally a crack is formed when the stress reaches the strength of the materials.

5. For plastic materials, the condition of fracture can be regarded as the attainment of either a critical stress (σ_f, the strength) or a critical strain (ε_f). In the case of alternating deformation, the total strain (i.e., the sum of the absolute values of all positive and negative strains suffered in the sourse of the stress cycles) has a characteristic value at fracture, provided that there is no considerable strain-hardening recovery.

6. The plastic strain amplitudes of consecutive cycles decrease approximately as the terms of a geometric series; thus, the total strain produced by an infinite number of cycles is always finite without respect to whether the strength is finite or not. If this limiting value of the total plastic strain is smaller than the critical strain, ε_f, failure will not occur.

After sufficient cycling, a fatigue crack is produced in a region of intense slip. The mechanism for the crack formation is not clear, but it must ultimately depend upon the concentration of the reversed dislocation motion on certain planes. Coffin (16) suggests that it is due to a running together of dislocations as they are halted at the barriers. Wood and Davies (49) suggest that it is due to a clustering together of the lattice vacancies generated by the dislocation motion.

Orowan emphasizes that his treatment deals with the formation of the fatigue crack, not with its propagation to complete fracture of the specimen. The propagation of a crack is assumed to take place by plastic deformation and progressive fracture at the growing tip. Therefore,

whether a fatigue crack forms early or late in the fatigue life, the ease or difficulty of dislocation movement is likely to exert a controlling influence (50).

One should also note that the plastic distortion caused by cyclic stressing is not necessarily damaging, as evidenced by the phenomenon of "understressing," which increases the fatigue strength at subsequent higher stress cycles. Moreover, the progress of the distortion, as observed by microscopic slip lines or by X-ray diffraction studies, is not necessarily a measure of crack formation, particularly in the early stages of fatigue, but may be due to mere cold working (strain-hardening) of the material.

Hancock's observations on the fatigue behavior of high-strength aluminum alloys (51) suggest that precipitation-hardening alloys are unstable under cyclic stresses, which cause precipitation or over-aging in the localized regions of intense deformation. Although the static strength as a whole may not be impaired, the localized bands of precipitation produced by cyclic stressing are regions of low-strength in which fatigue cracks form. Thus, the amount of precipitation-hardening and the relative stability of the precipitates are important factors to be considered.

Freudenthal (52) contends that fatigue is not inseparably associated with plastic slip, but that the real fatigue effect is a large-scale expression of the progressive destruction of cohesive bonds in the material. Plastic deformation and strain-hardening are assumed to be essential features only insofar as they modify both the intensity and rate of bond destruction. According to Freudenthal, the destruction of the cohesive bonds cannot be satisfactorily detected in what appears to

be undamaged material by a metallographic examination of slip lines, by hardness, or by X-ray diffraction studies of submicroscopic lattice breakdown. Long before any submicroscopic crack can be observed, fatigue has already been initiated by the severance of a number of cohesive bonds. The assumptions that the "separation strengths" of the cohesive bonds have a statistical distribution and that the stress caused by an applied load varies inhomogeneously within the material are the basis for the statistical treatment by Freudenthal.

Thermal fatigue. - Efforts to correlate and explain experimental results from thermal fatigue tests have emphasized the similarity to ordinary mechanical fatigue and the role of strain-hardening. The basic postulate of these efforts seems to be that failure occurs when the ductility of the material has been exhausted so that it is no longer able to absorb the reversed deformation.

As a first estimate, the sum of the absolute values of the tensile and compressive strains during each cycle multiplied by the number of cycles to failure might be thought to equal the amount of strain at failure measured in a simple tensile or compression test. Experimentally this is not true, and, in fact, even the summation of only the tensile components of plastic flow during cycling is greater than the ductility of the initial material in the conventional tensile test. Repeated increments of plastic flow thus appear to improve the subsequent behavior. Experiments also show that the summation of the components of tensile and compressive flow during cycling varies with the test conditions, and that the greater the number of cycles to failure, the greater is this summation. Manson (53) proposed the following relation in 1952 to express this:

$$N_f = K\epsilon_p^{-n} \qquad (3)$$

where

N_f = the number of cycles to failure

ϵ_p = the plastic strain, and

K and n = constants

Manson applied his proposed relation to mechanical fatigue data on 24ST aluminum at room temperature (54) and estimated that the value of the exponent in equation (3) should be about 3. Coffin (18) later derived an equivalent expression to equation (3) and used it to correlate the same fatigue data on aluminum. Whereas Manson found that the number of cycles to failure was inversely proportional to (approximately) the cube of the strain per cycle, Coffin's analysis of the same data indicated that the number of cycles to failure was inversely proportional to the square of the strain per cycle.

Although Manson and Coffin obtained different values for the exponent "n" in equation (3), the important point demonstrated was that the number of cycles to failure appeared to bear a simple relation to the amount of strain per cycle in mechanical fatigue. Manson further suggested (53) that this relation might prove valuable in thermal fatigue, and he used it to illustrate the drastic reduction in the number of cycles to failure that might be expected from increasing the ΔT of cycling. For example, assume an ideally plastic material with the following properties, independent of temperature:

$$\alpha = 10\times10^{-6} \text{ in./in./}^{o}\text{F}$$

$$E = 30{,}000{,}000 \text{ psi}$$

$$\sigma^* = 90{,}000 \text{ psi (yield strength in tension and compression)}$$

Such a material would deform plastically when the strain exceeded 0.003 in./in. It would undergo reversed plastic deformation on cycling when $\alpha\Delta T \geq 2(0.003)$; this gives $\Delta T \geq 600^{\circ}$ F. The strain per half cycle, ε_p, would then be given as

$$\varepsilon_p = 10\times10^{-6}\,\Delta T - 0.006 \qquad (4)$$

The number of cycles to failure, relative to 1000 cycles at a ΔT of 800° F, would then be as follows:

ΔT, $^{\circ}$F	ε_p, in./in.	ε_p^3	$N = K\varepsilon_p^{-3}$ (Relative to N = 1000 at $\Delta T = 800^{\circ}$ F)
600	0.000	0	∞
800	.002	8×10^{-9}	1000
1000	.004	64×10^{-9}	125
1200	.006	216×10^{-9}	37
1400	.008	512×10^{-9}	15.6
1600	.010	1000×10^{-9}	8.000
1800	.012	1728×10^{-9}	4.630

If these values are compared with the data quoted on page 10, the predicted effect of temperature difference on life is seen to compare favorably with that observed experimentally.

Going from an ideally plastic material to a real material introduces a number of changes in the behavior from that of the ideal model analyzed above. For example, the following must be considered:

1. Strain-hardening, by which prior deformation increases the yield strength and reduces the amount of reversed plastic flow
2. The Bauschinger effect, by which plastic flow in one direction reduces the stress at which plastic flow occurs in the opposite direction

3. The temperature dependence of the mechanical properties
4. The temperature dependence of the thermal properties
5. The time dependence of the mechanical properties, as the effect of strain rate on the yield point
6. Time effects such as creep and stress-relaxation, which become especially important at high temperatures

Microstructural changes that alter properties may also occur during cycling, particularly if the temperatures are high. These will increase the list of factors to be considered as follows:

7. Recovery, recrystallization, and grain growth
8. Matrix transformations
9. Aging, precipitation-hardening, overaging, and spheroidization
10. Anisotropic effects
11. Corrosion
12. Formation of cracks, which can reduce the load-bearing area or act as stress raisers

Finally, the practical case may add the following changes to the simple bar model described:

13. Nonuniformity of temperature over the cross section and length of the specimen
14. Nonuniformity of cross-sectional area over the length of the specimen
15. Stress concentrations
16. Incomplete constraint due to yielding of the supports
17. Size effects

Despite these limitations, Coffin (15,16,17) had considerable success in applying the relationship originally suggested by Manson to his

experimental results on thermal fatigue failures. Thus, Coffin correlated his results on the thermal cycling of annealed type 347 stainless steel by the relation

$$N^{1/2} \varepsilon_p = 0.36 \tag{5}$$

or, its equivalent form

$$N = 0.1296 \varepsilon_p^{-2} \tag{6}$$

When the specimens were strain cycled at a constant temperature equal to the mean temperature of the thermal cycling tests, the relation was

$$N^{0.43} \varepsilon_p = 0.28 \tag{7}$$

or

$$n = 0.05177 \varepsilon_p^{-2.326} \tag{8}$$

The quantity ε_p in these relations is the plastic strain change per cycle. Since this changes during cycling, due to strain-hardening or softening, Coffin used a calculated plastic strain change at one-half the number of cycles for failure. The calculation was based on the relationship

$$\varepsilon_{thermal} + \varepsilon_{elastic} + \varepsilon_{inelastic} = \varepsilon_{net} = 0 \tag{9}$$

which states: (1) the net strain of the tubular specimens was zero, since the ends were held fixed (or very nearly so) in a gripping device; and (2) the free thermal expansion or contraction was offset by an equal and opposite flow made up by an elastic and a plastic component. The quantity $\varepsilon_{thermal}$ could be determined either by measuring the free expansion or contraction that occurred when the specimen was unclamped or by calculating it as equal to $\alpha\Delta T$, where α is the average coefficient of thermal expansion. Actually, as Coffin points out, the quantity $\alpha\Delta T$ was not exactly equal to the thermal strain because of longitudinal heat

transfer, which caused the ends of the specimens to be colder than the middles.

The elastic strain, $\varepsilon_{elastic}$, was determined from the stress change per cycle at one-half the number of cycles to failure and from the modulus of elasticity. The constrained expansion and contraction of the specimens caused a very slight strain in the massive bars that connected the end plates holding the specimens. The strain in the bars was measured by SR-4 strain gages cemented to them and was converted to stress by multiplying by the modulus of elasticity of the bar material. Multiplying this stress by the ratio of the areas of the bars and specimen gave the stress in the specimen. The stress in the specimen was then divided by its modulus of elasticity to give $\varepsilon_{elastic}$. The modulus of elasticity would, of course, have to be an average modulus for the temperatures involved, and the strain would be an average strain over the length of the specimen. The values of $\varepsilon_{thermal}$ and $\varepsilon_{elastic}$ were then inserted into equation (19) to give $\varepsilon_{plastic}$. While the procedure involves some simplifying assumptions, the final correlations appear remarkably good.

The success of equation (3), as well as other experimental observations, led Coffin to believe that the strain change is the dominant factor controlling thermal fatigue, and that temperature effects are not so important. He points out, however, that differences may be encountered under temperature conditions where phase changes, marked strain-aging, or anisotropic effects occur. Coffin adds that "Except for the possibility of some transformation of gamma-iron to alpha-iron with extreme cold work none of the above effects can occur for Type 347 stainless steel. It appears then that temperature cycling has only a secondary effect on

the fundamental aspects of the problem." (16). As added proof, Coffin points out that there is no change in the stress-strain behavior of annealed Type 347 stainless steel if it is thermally cycled without constraint for 10,000 cycles between 200° and 500° C (that is, if it is exposed to the temperature conditions without straining). However, as one must realize, structural changes are influenced by both temperature and strain; changes that do not occur under temperature or strain alone may occur when both are present. Also, the drop-off in life with the temperature level of testing at constant strain amplitude (see page 15) challenges the hypothesis that temperature effects are not important.

In summary, although plastic deformation and strain-hardening appear to be well established as important factors in thermal fatigue, the importance of the temperature level of cycling remains undefined. In view of the tremendous effect that temperature has on the properties of materials, it is unreasonable to expect that the role of temperature should be a minor one. In addition, time becomes a factor in the behavior of metals at high temperatures, and the frequency of cycling would therefore be expected to effect the number of cycles to failure. If these factors are important, the correlations of the number of cycles to failure with the amount of plastic deformation per cycle may need to be modified by including the effects of both temperature and time in order to have general applicability. Information on these effects should also aid in understanding the mechanism of thermal fatigue.

EQUIPMENT AND PROCEDURE

Equipment

The equipment and procedure were such as to minimize thermal stresses in other than the axial direction of the specimens. Figure 1 shows the specimen design. The center section was heated and cooled through the desired temperature cycle by passing high amperage - low voltage current through it by means of water-cooled, copper leads that attached to the adjacent shoulders. The specimens were constrained from expanding and contracting axially by gripping them tightly about the shoulders at opposite ends.

The block for gripping the specimens is shown in figure 2. This was a 7 inch square by 3 inch thick steel block with a 2.50 inch diameter hole drilled out through the center of the faces and a 0.50 inch diameter hole running from top to bottom. The block was split into two halves that were fastened together on the specimens by four bolts. Tightening the bolts caused the block to grip the specimen tightly on the end shoulders. The specimen and block were electrically insulated from each other by 0.002-0.004 inch paper.

A single chromel-alumel thermocouple was spot-welded to the center of the test section to measure temperatures, and the temperatures were recorded continuously on a Brown recording potentiometer. Small diameter thermocouple wires were used to minimize heat conduction from the specimen. Tests indicated that spotting the thermocouples on the specimens did not interfere with the results. Figure 3 shows the thermocouple

wires spotted on a specimen that had been removed from thermal cycling before failure. Note that the manner of attaching the thermocouple had no apparent effect on the material other than causing a very small amount of recrystallization immediately below the couple.

The test section of a specimen was raised to the desired temperature by electric resistance heating. During cooling, the power input was reduced and heat was removed from the test section by conduction through the shoulders to the water-cooled copper leads and by transfer to still air. Both the copper leads and the gripping block were included in the cooling-water circuit. Because the shoulders of the specimens were maintained at relatively low temperatures, the temperature was not uniform along the length of the test sections, as shown in the temperature profiles in figure 4. Both S-816 and Inconel 550 showed the same variation in temperature. The cycle temperatures reported in this study are those at the center of the test section.

Suitable electric controls were provided so that the specimens could be heated and cooled automatically between the desired temperatures and in the desired times.

The expansion and contraction of the test section caused the shoulders adjacent to it to deflect slightly. The amount of this movement was measured by a mechanical strain gage with knife edges that rode on the shoulders, as shown in figure 2. A mirror mounted at the other end of the strain gage reflected the readings from a graduated scale into a telescope placed next to the scale and several feet from the specimen. As the shoulders of the test section moved, the mirror rotated, and the amount of movement was measured by the change in the scale readings received at the telescope. The lever arms and scale-to-mirror distance

were such that the movement of the shoulders was magnified about 500 times. The movement of the shoulders corresponded to the change in the total length of the test section, and this change was not uniform because of the temperature gradient along the axis of the test section.

Figures 5 and 6 are photographs of the actual equipment.

Materials

Two materials were studied, namely S-816 and Inconel 550 alloys. These are both high-temperature "superalloys" that are used mainly at temperatures on the order of 1350° to 1500° F. Of the two alloys, S-816 is weaker at elevated temperatures but has more ductility than Inconel 550. S-816 is a cobalt-base alloy, while Inconel 550 is nickel-base; their nominal compositions are as follows:

Alloy	Percents by weight									
	C	Cr	Ni	Co	Mo	W	Nb	Ti	Al	Fe
S-816	0.4	20.0	20.0	Bal.	4.0	4.0	4.0	----	----	5.0 Max.
Inconel 550	.04	15.0	Bal.	----	---	---	---	2.50	1.15	6.70

The alloys were obtained from the manufacturers as 5/8-inch diameter wrought bar stock. This was cut into $5\frac{1}{2}$-inch lengths which were then heat treated as follows:

S-816: Solution treated 1 hour at 2150° F and water quenched;
Aged 16 hours at 1400° F and air cooled.

Inconel 550: Solution treated 1 hour at 2150° F and air cooled;
Aged 4 hours at 1600° F and air cooled;
Aged 4 hours at 1350° F and air cooled.

The microstructures of the two alloys after heat treatment are shown in figures 7 and 8. Both alloys have an austenitic (face-centered

cubic) matrix structure in which precipitates have formed - carbides in S-816 and an $Ni_3(Ti,Al)$ intermetallic compound in Inconel 550. The specimens were machined from the heat-treated lengths of bar stock.

Procedure

The cycle through which the specimens were heated and cooled was divided into 4 parts: (1) heating to the maximum temperature, T_{max}; (2) holding at T_{max}; (3) cooling to the minimum temperature, T_{min}; and (4) holding at T_{min}.

In starting a run, a specimen was held in the gripping block with only the lower two bolts tightened. The upper two bolts were loose so that the specimen could expand and contract freely while the initial adjustments were being made. After the power inputs during the various portions of the cycle had been adjusted to give the desired temperatures, the free expansion and contraction of the test section was measured by noting the change in scale readings when the temperature changed from T_{max} to T_{min}. The free contractions of S-816 and Inconel 550 specimens that were cooled from various T_{max} to a T_{min} of 200° F are plotted in figure 9. Note that the two alloys contracted by nearly equal amounts under the test conditions; the free expansion or contraction of Inconel 550 was about 2 percent more than that of S-816.

Usually about 10 cycles were required to make the adjustments and initial readings, and the upper bolts were then tightened. In all tests in this investigation, the upper bolts were tightened while the specimen was at T_{max}. This induced the maximum possible tensile stress in the specimen on cooling to T_{min}. In most of the tests, T_{min} was constant at 200° F, so that the maximum tensile stress would be developed at the same temperature regardless of T_{max}.

The total amount of tensile deformation along the length of the test section was measured by the difference between the change in scale readings when the specimen was cooled while loose and while constrained. (In other words, let the scale reading change A units when the specimen is cooled while loose and B units when the specimen is cooled while constrained; then the specimen must flow elastically and plastically in tension an amount proportional to (A - B) units in order to absorb the thermal strain.) Multiplying this difference by the magnification factor of the strain gage gave the amount of deformation in the test section, and dividing the amount of deformation by 1/2-inch, which is the length of the test sections, gave the average strain in the test section. The average strain is plotted versus temperature in figure 10.

The tensile stress developed at T_{min} on the first cooling varied with T_{max} in the manner shown in figure 11. (The tensile stress was calculated by multiplying the scale change B by the magnification factor; then dividing by 2 inches, which is the total length of the shoulders adjacent to the test section, in order to get the strain in the shoulders; then multiplying by the modulus of elasticity to obtain the tensile stress in the shoulders; and finally multiplying by the ratio of the cross-sectional areas of the shoulders and test section to get the stress in the test section.) Ideally, one would expect that the greater the temperature difference of cooling (or, in this case, the higher T_{max} since T_{min} was constant), the greater would be the tensile stress at T_{min}, whereas figure 11 indicates that this was not so. The behavior shown in figure 11 is due to the temperature conditions of the test method and to the variation of the yield strength of the two alloys with temperature.

The effect of the temperature conditions follows from the manner in which the temperature gradients changed during cooling, as shown schematically in figure 12. In figure 12(a), the specimen starts cooling from a T_{max} equal to T_1 and reaches a lower temperature T_2 shortly thereafter; in figure 12(b), the specimen starts cooling from a T_{max} equal to T_2. Due to the water-cooled leads attached to the shoulders of the specimen, heat is extracted through the ends of the test section, and the ends cool more rapidly than the center of the test section. This means that when the midpoint of the first specimen has cooled from T_1 to T_2, the other parts of its test section have cooled to lower temperatures than in the second specimens when the midpoint has just started cooling from T_2. The tensile stresses set up by the contraction of the cooler sections in the first specimen can be relieved by yielding near the midpoint, provided that this portion is still at a sufficiently high temperature for the yield strength to be low. During cooling from T_2 to T_{min} there is less total contraction in the first specimen than in the second, and hence the final stress at T_{min} can be less in the first specimen than in the second, depending upon the amount of yielding in the hot portion of the test section. This, in turn, depends upon the temperature and the material.

Data on short-time tensile properties show that the yield strength of S-816 is not significantly reduced by temperatures up to about 1400° to 1500° F, but that the yield strength of Inconel 550, although higher than that of S-816 at a given temperature, begins to fall off with temperature at much lower temperatures. Thus, as figure 11 shows, the tensile stress developed in S-816 increased as the temperature difference of cooling increased until T_{max} was sufficiently high to cause a

decrease in the yield strength and to allow the hot center of the test section to yield and absorb the contraction of the cooler sections. When this T_{max} was exceeded, the tensile stress developed on cooling to T_{min} fell off as T_{max} was increased further. On the other hand, the tensile stress developed in Inconel 550 fell off with temperature for the complete range of T_{max} studied, in accordance with the drop-off in its yield strength at these temperatures. However, the tensile stress developed in Inconel 550 on cooling from a given T_{max} was always greater than that developed in S-816, due to the greater yield strength of Inconel 550.

During the first few cycles, material changes occurred that altered the electrical resistance, so that the power inputs had to be adjusted to prevent the temperatures from wandering from their proper values. The specimens soon approached an equilibrium condition, however, and there was little drift in temperatures thereafter. Strain gage readings were taken at intervals during thermal cycling, and the average strain over the test sections was found to drift slightly during cycling. The amounts of average strain absorbed by the test sections after 50 percent of the number of cycles for failure are shown in figure 13 versus the maximum cycle temperature. Note from figure 13 that up to about 1350° to 1400° F, the two alloys deformed almost equally, and at higher temperatures S-816 deformed more than Inconel 550. At the higher T_{max}, a significant portion of this deformation was compressive creep. This creep could be noted by the drop-off in scale readings as the temperature approached or was held at T_{max}, and it occurred at lower temperatures for S-816 than for Inconel 550.

In a number of tests, thermal cycling was continued until the

specimens failed. Failure was defined as actual fracture across the test section, and generally occurred at or very near to the center of the test section. Immediately before failure, there was a period in which T_{max} increased, due to overheating as a result of cracking. This overheating period lasted for five to ten cycles at high T_{max} and increased in duration as the T_{max} was lowered. No further heating could occur after failure, and the number of cycles to failure was easily determined from the charts of temperature versus time.

In a number of other tests, thermal cycling was interrupted before the specimens failed, and the specimens were removed for metallographic examination or stress-rupture testing. In these cases, the bolts constraining the specimens were loosened after the desired number of cycles while the temperature was at a T_{min} of 200° F. Thus, all of these specimens were removed just after having been subjected to a tensile stress at the same temperature.

The diameters of the specimens were measured with micrometers both before and after removal from thermal cycling, whether after failure or not, and any changes were noted. Most of the specimens were bulged at the center of the test section due to compressive yielding and creep at T_{max}. The amount of bulging increased as T_{max} increased, as shown in figure 14, and was offset by a slight thinning to either side of the bulge.

In the case of specimens removed for stress-rupture testing, the diameters of the test sections were ground to a depth of about 0.002 to 0.004 inch to remove any bulges and any surface defects that might influence the stress-rupture strength. All of these specimens were zygloed after grinding, and in no cases were any surface cracks detected.

Threads were also ground on the end shoulders for holding the specimens in the stress-rupture machines. Stress-rupture tests were conducted principally at 1350° F, although one series of specimens was tested at 1500° F. The stresses were selected to cause failure in roughly 100 hours on virgin material. Both time to rupture and reduction in area at the fracture were determined.

Microstructures and hardnesses were also studied. Specimens for these metallographic studies were prepared by carefully machining flat surfaces through the central planes. Hardness was measured with a microhardness tester, using a Vickers diamond penetrator and a 1 kg. load. Measurements on fractured specimens were made 0.01 inch below the fracture edge.

RESULTS

Specimens Failed by Thermal Fatigue Alone

The results from specimens that were cycled to failure under varying conditions of thermal fatigue indicated the following effects of the cycle variables on the number of cycles to failure.

Effect of T_{max} and ΔT. - For the conditions of testing, N_f was governed more strongly by T_{max} than by ΔT. This is shown in figures 15 and 16. The solid curves at a constant ΔT of 1150° F in these figures show the variation in N_f with T_{max} alone, and the dashed curves at a constant T_{min} of 200° F show the variation in N_f under the combined effects of T_{max} and ΔT. If ΔT were the sole factor controlling N_f, the solid curves would be straight, vertical lines intersecting the dashed curves at a common point (T_{max} = 1350° F, T_{min} = 200° F, ΔT = 1150° F)[1]; in other words, N_f would be constant as long as ΔT was constant. The actual curves at constant ΔT are not vertical, and the amount by which the actual curves deviate from the vertical indicates the effect of different T_{max}. For both alloys, the decrease in N_f due to

---

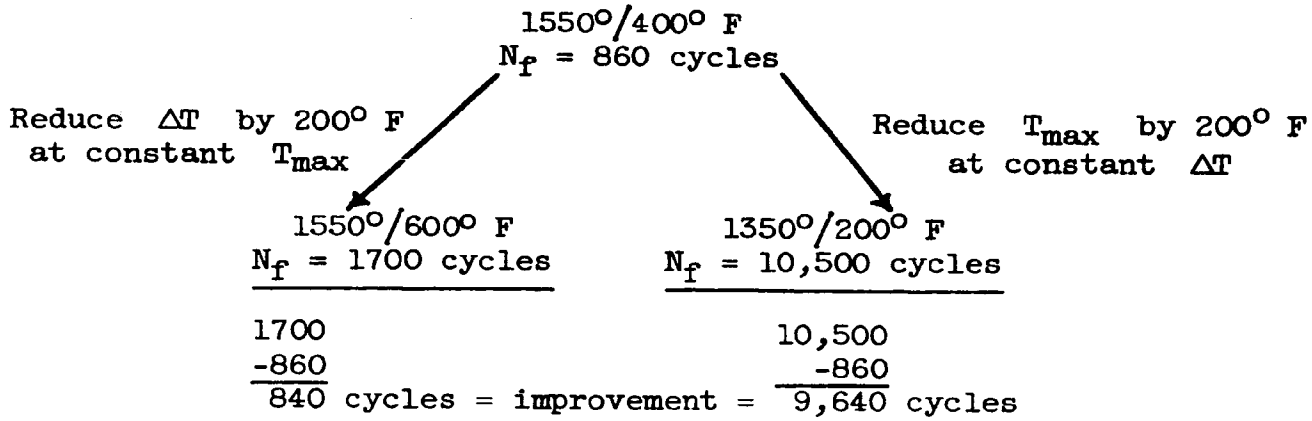
[1]This common point of intersection can be observed in the results for Inconel 550 plotted in figure 15. In the case of S-816, however, the specimens for the two curves were taken from different bars of material, and the one bar was stronger than the other. Hence, the two curves for S-816 in figure 16 are offset from one another. However, despite this offset, the two curves for S-816 show the same relative behavior of decreasing N_f with increasing T_{max} as the curves for Inconel 550. In all subsequent tests where comparisons were made, care was taken to eliminate bar-to-bar variations in material by using specimens from the same bar or from bars that were shown to be equivalent.

increasing T_{max} at a constant ΔT was almost as severe as the decrease in N_f due to increasing both T_{max} and ΔT simultaneously.

Additional tests on Inconel 550 confirmed the strong effect of T_{max} on N_f. Results of these tests are plotted in the solid curve in figure 17, which shows the variation in N_f with ΔT at a constant T_{max} of 1550° F. The dashed curve that is plotted for comparison shows the variation in N_f with ΔT at a constant T_{min} of 200° F. (The dashed curve is the same as that in figure 15; it has been replotted in figure 17 against the ordinate ΔT rather than T_{max}. Note that the point of intersection of the two curves in figure 17 is a common point, T_{max} = 1550° F, T_{min} = 200° F, ΔT = 1350° F.) If T_{max} were completely controlling, the solid curve in figure 17 would be a straight, vertical line. Actually, it is not vertical, and this shows that ΔT also has an effect on N_f. However, as the two curves indicate, increasing or decreasing ΔT and T_{max} simultaneously (dashed curve) had much more effect on N_f than increasing or decreasing ΔT without changing T_{max} (solid curve).

The results can be presented in other ways that indicate numerically the relative importance of T_{max} ΔT for a limited range of conditions. For example, as indicated in the diagram below, Inconel 550 endured about 860 cycles before failing when cycled between 1500° and 400° F. If ΔT were reduced 200° F by raising T_{min} to 600° F while maintaining T_{max} at 1550° F, the life was increased to 1700 cycles; that is, reducing ΔT by 200° F for constant T_{max} approximately doubled N_f. On the other hand, if T_{max} were reduced 200° to 1350° F while maintaining ΔT at 1150° F, the life was increased to 10,500 cycles. Thus, under these conditions, the increase in N_f due to

reducing T_{max} by 200° F was more than 11 times the increase obtained by reducing ΔT by the same amount.



The numerical value calculated above for the relative importance of T_{max} and ΔT is correct only for a particular set of conditions. Other conditions can increase or decrease this relative importance. The concentration of deformation in the center of the test section, due to the manner of heating and cooling, as discussed earlier in this dissertation, has probably emphasized the effect of T_{max} in the experimental results. Under less severe conditions, ΔT could be more important than has been found here. Obviously, no fracture would occur unless there were a ΔT, regardless of how near T_{max} might approach the melting point of the material.

The point emphasized by the results is that T_{max} is an important factor in thermal fatigue, and the life in thermal fatigue is not determined by ΔT alone. The effect of T_{max}, superimposed on that of ΔT, can overshadow the effect of ΔT alone. In view of its importance on life, the effect of T_{max} can hardly be overemphasized in an analysis of thermal fatigue.

Effect of time at T_{max}. - The time of exposure at T_{max} also affected N_f, as shown in figures 18 and 19. This effect was studied by

increasing the hold time at T_{max} from 15 seconds to 1 minute. For both alloys, increasing the hold time at T_{max} by a factor of four increased N_f at high T_{max} and decreased N_f at low T_{max}. The cross-over points were at 1360° F for S-816 and at 1510° F for Inconel 550, and the effect of time appeared more pronounced for S-816 than for Inconel 550.

Although the effect of the time at T_{max} appears small, particularly for Inconel 550, it is significant that it can be observed in relatively short times. Where parts in service are maintained at high temperatures for much longer times than the experimental cycles used here, the effect may be more severe. The disagreement between short-time laboratory thermal shock tests and service lives may be partially due to this effect of time.

Effect of strain change. - As pointed out earlier, Coffin (15 to 18) was successful in correlating the number of cycles to failure in his thermal fatigue studies with the amount of plastic deformation per half-cycle by the equation

$$N_f = K\varepsilon_p^{-n} \tag{3}$$

The question arises as to how general the relation is and under what conditions modifications are required.

In order to evaluate the plastic strain per half-cycle, the elastic strain must be subtracted from the total strain that was measured over the length of the specimen. To do this, the strain change in the shoulders adjacent to the test section was measured on cooling from T_{max} to T_{min} and was multiplied by the modulus of elasticity to give the stress change there. This stress change was multiplied by the ratio of the area of the shoulders to that of the test section to give the stress

change in the test section. Dividing this stress change by the modulus of elasticity gave the elastic strain per half-cycle, which was then subtracted from the total strain in the test section to obtain the average plastic strain per half-cycle.

The calculation of the plastic strain, both in the present tests and in those of Coffin, involves some errors and approximations. The first approximation involves the temperature at which the modulus of elasticity was evaluated for the test section. Coffin gave no details on this point; in the present investigation the modulus has been evaluated at $\frac{1}{2}(T_{max} + T_{min})$. Because the modulus of elasticity of S-816 varies only about 2 percent per 100° F change in temperature (55), the error involved in approximating the modulus of elasticity is small compared to the discrepancies that were noted between the data and equation (3).

A more serious error is encountered in the fact that the strain was not uniform along the test section, due to the temperature gradient and the manner of heating and cooling, as discussed earlier. Ideally, the plastic strain should be evaluated in the narrow section at the center of the test section where fracture occurred. Actually, the higher T_{max}, the more the calculated average plastic strain was concentrated in the area of the fracture.

Subject to these limitations, the data for S-816 showing the variation of N_f with the average plastic strain per half-cycle is plotted in figure 20. According to equation (3), the log-log manner of plotting should reduce the data to a straight line in this figure.

For a single series of tests, such as those at constant T_{min} (open circles, fig. 20), the results can be fitted by a straight line

only for a limited range or for low values of T_{max}. Over a wider range, the curve sweeps upwards at high T_{max} so that N_f is greater than would be predicted by extrapolating the results at low T_{max}. Three data points for tests at a constant ΔT are also plotted in figure 20 (open diamonds). Although there was very little variation in the average plastic strain per half-cycle for these three specimens, N_f was significantly decreased as T_{max} increased.

It appears doubtful that correcting the average plastic strain over the test section to the actual plastic strain in the region of fracture would reduce all of the data points plotted in figure 20 to a single straight line. The test conditions, particularly T_{max}, appear to be important factors in addition to the cyclic strain. Thus one concludes that the number of cycles to failure is not governed solely by the cyclic strain and that equation (3) must be modified by additional terms defining the test conditions in order to have general applicability.

Changes in Material Properties Due to Thermal Fatigue

Whereas the previous section has presented results on the complete failure in thermal fatigue, this section presents results on the changes in the stress-rupture life and ductility that take place as a result of thermal fatigue prior to failure.

Effect of N. - The effect of the number of cycles of thermal fatigue, N, on the subsequent stress-rupture life and ductility varied markedly with the alloy. For S-816, there was an initial increase in the rupture life at 1350° F (fig. 21). This is shown by the lives of the three specimens cycled 500, 100, and 1250 times (approximately 21,

42, and 53 percent of N_f). Beyond 1250 cycles, the data scattered widely. Three specimens (1750, 2200, and 2300 cycles) had lives greater than the average life of the virgin material, and the other two specimens (1500 and 2000 cycles) had lives slightly less than the average life of the virgin material. Even the specimen of lowest life (2000 cycles), however, did not have a life significantly below that of the virgin material. From this, one can conclude that there was no significant loss in the rupture life of S-816 at 1350° F due to prior thermal fatigue for the conditions shown, even though cycling is continued to approximately 98 percent of N_f. Figure 22 shows the same behavior in the rupture life at 1500° F as a function of the number of prior cycles of thermal fatigue.

For Inconel 550, the rupture life dropped off continuously as N was increased (fig. 23). The drop-off was most rapid at first, then slowed down so that the relation between the stress-rupture life and N was approximately linear, and finally suffered an abrupt loss in life. The rupture tests on Inconel 550 ran out to 86.5 percent of the number of cycles required to fracture Inconel 550 by thermal cycling alone. With the exception of the specimen that had been run 5000 cycles, the data showed little scatter.

The ductility of S-816 decreased linearly with N (figs. 24 and 25). After about 98 percent of the number of cycles required to fracture S-816 by thermal cycling alone, the ductility at 1350° F had dropped off to about 1/2 or 2/3 of that for virgin material. There appeared to be no change in the ductility of Inconel 550 during thermal cycling (fig. 26).

For both S-816 and Inconel 550, no changes were observed in the

stress-rupture life or ductility at 1350° F due to temperature cycling in the absence of constraints (figs. 27 to 30).

Effect of time at T_{max}. - The effect of the time at a T_{max} of 1350° F was studied by increasing the time at T_{max} from 15 to 60 seconds. From the results described earlier, this increase had little effect on N_f for S-816 (fig. 19), but caused N_f for Inconel 550 to decrease from 10,500 to 7,400 cycles (fig. 18).

As with the shorter cycle, the rupture life of S-816 increased with the number of cycles (at least up to $N = 1/2\ N_f$), and that of Inconel 550 decreased (figs. 31 and 32). The drop-off in the life of Inconel 550 was more rapid than on the shorter cycle, and failure was reached in fewer cycles. The ductility of Inconel 550 remained constant as N increased (fig. 33). S-816 also retained the same ductility up to 1000 cycles (fig. 34), whereas there was a slight loss in ductility with N on the shorter cycle (fig. 24).

Effect of T_{max}. - The effect of T_{max} was studied by removing specimens for rupture testing after one-half of the number of cycles that would cause failure by thermal fatigue alone. It was found that the effect of T_{max} on the subsequent properties differed considerably between the two alloys.

The stress-rupture life of S-816 after thermal fatigue (fig. 35) was slightly greater than that of the virgin material regardless of T_{max} (for the range of T_{max} from 1250° to 1550° F), provided that cycling was stopped after $1/2\ N_f$. The stress-rupture life of a single specimen of S-816 cycled without constraint between the highest T_{max} (1550° F) and a T_{min} of 200° F (open diamond, fig. 35) was also slightly greater than that of virgin material, although the increase here was less than

that for constrained cycling and could be due to scatter. Inconel 550, on the other hand, suffered a drastic loss in strength as T_{max} was increased (fig. 36). This loss was not due to temperature alone, as shown by the single specimen cycled without constraint between a T_{max} of 1550° F and a T_{min} of 200° F (open diamond, fig. 36), and the loss of strength must therefore be due to the combined effects of the cyclic stresses (or strains) and temperatures. The ductility of both S-816 and Inconel 550 appeared unchanged with T_{max} (fig. 37) for cycling under constraint; however, without constraint, temperature cycling at the high T_{max} of 1550° F increased the ductility slightly.

Specimens Run in Stress-Rupture, Then Failed by Thermal Fatigue

Only a single group of specimens was first run in stress-rupture and then failed by thermal fatigue. The stress-rupture conditions were a temperature of 1350° F and a stress that would cause the virgin material to fail in roughly 100 hours. Specimens were removed from the stress-rupture test after various periods of time less than that for failure, and they were then cycled to failure in thermal fatigue at T_{max} = 1350° F, T_{min} = 200° F. The results for these conditions are plotted in figures 38 and 39. For S-816, N_f decreased as the prior time in stress-rupture increased (fig. 38), and for Inconel 550, N_f appeared to increase slightly with the prior time in stress-rupture (fig. 39).

DISCUSSION

The study of test conditions has demonstrated that the temperature level of thermal cycling exerts an important influence on the thermal fatigue life of ductile alloys. For the materials and test conditions covered in this investigation, the maximum cycle temperature had more effect than the temperature difference on the number of cycles to failure. Increasing the time of exposure at T_{max} during cycling was found either to increase or decrease the number of cycles to failure, depending upon T_{max}. Thus an increase in time at low T_{max} reduced the thermal fatigue life, whereas the same increase in time at high T_{max} increased the thermal fatigue life. No direct correlation was found to exist between the number of cycles to failure and the amount of plastic strain per half-cycle.

Long before a specimen failed in thermal fatigue alone, its mechanical properties could be significantly altered. The stress-rupture strength of one alloy (S-816) was generally increased slightly by prior thermal fatigue, whereas that of the other alloy (Inconel 550) could be drastically reduced. The increase in the stress-rupture life of S-816 was usually accompanied by a loss of ductility. Exposure to stress-rupture conditions decreased the subsequent thermal fatigue life of S-816 and appeared to increase slightly that of Inconel 550.

These observations are discussed in this section in terms of a proposed theory of thermal fatigue. The proposed theory introduces no radically new ideas, but rather it attempts to consolidate the thoughts

of a number of investigators on various behavior, which have been reviewed in the introduction, into a reasonable explanation of what is evidently a very complex phenomenon. In many respects this initial attempt may appear inadequate or incomplete. As further research adds to our knowledge of thermal fatigue, modifications or additions will doubtless become necessary.

In summarizing the theories of simple deformation, creep, and mechanical fatigue reviewed earlier and applying them to thermal fatigue, the fatigue process has been divided into two stages. Each of these stages can proceed at varying rates, depending upon the material and the test conditions. As a first step in presenting the theory, the test conditions are held constant--in the case of the present work, the conditions of cycling are a T_{max} and T_{min} of 1350° and 200° F, respectively, and a 30-15-30-15 cycle, which were the conditions studied most thoroughly.

The two stages into which the process of thermal fatigue is divided are (1) a stage of strain- and/or precipitation-hardening and (2) a stage of the destruction of cohesive bonds and the development and propagation of cracks. During the first stage, the strains are absorbed by the material without cracking, and the strength and hardness increase while the ductility decreases. This was true for S-816 under the conditions stated. Thus, for a large number of cycles, S-816 became harder (fig. 40), stronger in stress-rupture (figs. 21 and 22), and lower in ductility (figs. 24 and 25).

The second stage of fatigue is apparently reached in S-816 only when the number of cycles is near that required for failure by thermal fatigue alone, and then is passed through relatively quickly, as

evidenced by the sharp drop-off in the stress-rupture life and ductility at the ends of the curves in figures 21, 22, 23, and 24. On the other hand, the second stage can be reached very early in the fatigue process, as is apparently the case for Inconel 550. Thus, Inconel 550, which is initially harder and less ductile than S-816, does not harden further during cycling (fig. 41), its stress-rupture life drops off continually during cycling (fig. 23), abruptly at first, then more gradually, and then abruptly again at the end, and its ductility remains the same (fig. 26).

The loss in strength of Inconel 550 during cycling appears to correlate with its microstructural behavior. Thus, thermal cycling the Inconel specimens at $1350^{o}/200^{o}$ caused the grain boundaries to fragment, as shown in figures 42, 43, and 44. Figure 42 shows a grain boundary running from the junction of three grains. The original boundary appears to be broken into smaller segments that are offset from one another. The axis of the specimen was approximately as indicated, and this specimen was removed after only 1000 cycles, or about 1/10 of its expected life. Figure 43 shows the same area as figure 42 but at a lower magnification. Figure 44 is another example of grain boundary fragmentation. This specimen was removed after 7000 cycles, or 7/10 of its expected life. Note the amount by which the grain boundary was displaced near the right side of the photomicrograph.

An example of deformation by twinning is shown in figure 45. The twin lines run at a slight angle to the axis of the specimen, and what appear to be small cracks are seen at the ends of those twin lines that are more nearly perpendicular to the axis. This specimen was removed after 2000 cycles (approximately 2/10 of N_f). Several other examples

of deformation within the grains are shown in figures 46 and 47. The specimen is the same for these last two figures and was removed after 7000 cycles (7/10 N_f).

Microstructural damage (e.g., cracks) starts in Inconel 550 after fewer cycles than in S-816, but it apparently propagates more slowly in Inconel 550. As a result, Inconel 550 endures more cycles of thermal fatigue under these conditions than does S-816.

Several hypotheses can be advanced for the onset of the second stage of fatigue and for the differences in the behavior of S-816 and Inconel 550. One is that the second stage begins when the ductility of the material is too low to absorb the cyclic strains without cracking. S-816 reaches this stage only after extensive strain- and/or precipitation-hardening in the first stage, while Inconel 550, which is fully-hardened by the prior heat treatment and is much less ductile then S-816, seems to be in the second stage of fatigue from the start. This reasoning is supported by the hardness behavior during cycling (figs. 40 and 41), and by the variation in the subsequent stress-rupture behavior of the two alloys (figs. 21 through 26). On the other hand, Inconel 550 is a ductile alloy, undergoing a reduction of area of about $7\frac{1}{2}$ percent in the stress-rupture test, and S-816 still has considerable ductility--more than 30 percent reduction of area--even when the number of cycles is close to that required for failure by thermal fatigue alone. These values would seem to insure sufficient ductility so that the alloys could absorb the cyclic strains without cracking; however, the deformation and cracking responsible for fatigue failures occur in highly localized regions, as discussed earlier, whereas the measurement of ductility by the reduction in area is a gross measurement. Thus it may

be possible to have or develop brittle areas where cracks form even though the major portion of the material is still quite ductile.

Another point to be considered is the tendency of Inconel 550 to deform in thermal fatigue by twinning, in contrast to simple slip in the case of S-816. As noted previously, twinning is considered by some to be related to cleavage and brittle fracture. Thus the early incidence of cracking in Inconel 550, as evidenced primarily by the drop-off in stress-rupture life, might be due to its particular mode of deformation under cyclic strains. Although this answers the objection to the strain- or precipitation-hardening mechanism raised above in the case of Inconel 550, it does not explain the failure of S-816 when the gross ductility is still high.

A third factor to be considered is the effect of the particles of precipitate in the alloys (or, more exactly, the effect of the coherency stresses surrounding the particles). Most of the precipitates are formed during processing and heat treatment prior to thermal fatigue, but additional precipitation during thermal fatigue is possible. Precipitation-hardening can be removed at high temperatures by overaging, much as strain-hardening can be removed by annealing. Both precipitation and overaging during thermal fatigue will, of course, be influenced by the cyclic strains as well as the cyclic temperatures. The tendencies of different materials to overage will depend upon the stability of the precipitates; however, as figures 40 and 41 indicate, neither S-816 nor Inconel 550 overages or anneals during cycling to a T_{max} of 1350° F. Overaging and annealing at higher temperatures will be considered later. The significant points here are that the precipitates can act as barriers to the movement of dislocations and can serve as the sites at which

vacancies cluster together to form voids. In this action, the precipitates would promote cracking. On the other hand, if the precipitates overage and the material softens, some of these damaging effects might be alleviated.

If the separation of the fatigue process into the two stages described is accepted, the behavior of specimens that were first run in stress-rupture at 1350° F for varying times short of fracture and then failed in thermal fatigue between 1350° and 200° F (figs. 38 and 39) can be interpreted as follows: Specimens of S-816 removed from stress-rupture at 1350° F will have used up an appreciable amount of their ductility due to creep, and the remaining ductility will be less as the time in stress-rupture increases. When the specimens are then cycled in thermal fatigue, the first stage will be shorter as the prior time in stress-rupture is longer--that is, as the remaining ductility for absorbing the cyclic strains is decreased. As a result, the number of cycles to failure in thermal fatigue should fall off as the prior time in stress-rupture is made longer, and this is the effect shown in figure 38. Note that this effect for S-816 is exactly opposite to that for the reverse order of testing, where prior thermal fatigue is found to increase the subsequent stress-rupture life (figs. 21 and 22).

In contrast to S-816, Inconel 550 creeps very little in a 100-hour stress-rupture test at 1350° F; hence its available ductility for subsequent thermal fatigue is not markedly diminished. Moreover, Inconel 550 does not show a significant first stage of thermal fatigue. Therefore, the number of cycles to failure in thermal fatigue should not fall off markedly as the prior time in stress-rupture increases. Figure 39 shows that, in accordance with the concepts proposed, the thermal

fatigue life of Inconel 550 does not decrease; in fact, there appears to be a slight increase, due perhaps to secondary effects. Again, the effect is opposite to that for the reverse order of testing (fig. 23).

The next step in understanding thermal fatigue is to consider how this behavior under fixed conditions is modified by changing the test conditions. The two test conditions that were studied in this investigation were T_{max} and the time at T_{max}.

T_{max} can be important in a number of ways: (1) by its effect on strength, (2) by its effect, with ΔT, on the thermal strains that must be absorbed, (3) by its effect on failure mechanisms, and (4) by its effect on structural changes. Since some of these effects are also time-dependent, the time at T_{max} can also be important. The strain changes are also important, since deformation can produce vacancies that increase diffusion rates and promote certain reactions that would normally take place only at much higher temperatures, and also because deformation can provide nucleation sites for certain reactions. Because of the importance of strain, the changes noted earlier in stress-rupture life and ductility after constrained cycling did not occur after cycling without constraint.

The time-temperature-strain dependent structural changes can have opposite effects. On the one hand, strain- and/or precipitation-hardening can reduce the ductility of the material and promote failure by thermal fatigue, although the strength in stress-rupture is increased (e.g., S-816 cycled to a T_{max} of 1350° F). On the other hand, annealing or overaging can occur at high T_{max} and restore the ductility lost by strain- and/or precipitation hardening, and this can prolong the thermal fatigue life. As an example, consider the behavior of S-816

cycled from various T_{max} to a T_{min} of 200° F. Figure 48 shows that as T_{max} increased from 1150° to about 1450° F, the decrease in N_f could be represented by a straight line on a semi-log plot. At about 1450° F the curve swung upwards, so that at higher values of T_{max} the thermal fatigue life was greater than predicted by extrapolating the straight line portion at the lower temperatures. Hardness measurements made on the fractured specimens of S-816 are summarized in figure 49. These measurements showed that all specimens of S-816 underwent strain- and/or precipitation-hardening at their fracture. The maximum hardening was reached at a T_{max} of 1450° F, and at higher T_{max} the specimens were softer. The upswing in the curve for S-816 in figure 48 can now be interpreted as being due to annealing and/or overaging effects that soften the material. This softening would increase or renew the ductility so that the material could absorb more cyclic straining than would otherwise be expected.

Note that the behavior of Inconel 550 was distinctly different from that of S-816. As the curves for Inconel 550 in figure 48 and 49 show, there was no upward swing in the thermal fatigue life at high T_{max}, nor was there an appreciable softening. Because of these behaviors, the curves of $\log N_f$ versus T_{max} for the two alloys cross at a T_{max} of about 1525° F. Although S-816 had a greater life than Inconel 550 above this temperature, both materials underwent considerable upsetting at the high cycling temperatures. The amount of upsetting was measured as the increase in area at the time of fracture, and was found to increase with T_{max} in the manner shown in figure 14. S-816 upset more at fracture than Inconel 550, in accordance with its lower yield and creep strength. Thus, while S-816 was better than Inconel 550 in

the number of cycles to failure at maximum cycle temperatures above 1525° F, it suffered more deformation.

The annealing process can also cause recrystallization. Thus, the microstructure of Inconel 550 frequently showed small, recrystallized grains along the fractured edges and in regions of intense deformation. Figures 50 through 54 provide several examples of this. Note particularly the photograph at high magnification in figure 51. This photograph shows small recrystallized grains at either side of a crack below the main fracture; it furnishes good evidence of the intense concentration of deformation in the regions where cracks develop. (Fractured specimens of S-816 did not show recrystallization; see, for example, figs. 55 and 56.)

Another aspect of structural changes is the production of voids and cracks. As discussed earlier, the vacancy theory of the creep-rupture process points out that vacancies can be produced in the crystal lattice and can diffuse together to form voids and cracks. Several examples of voids are shown in the fractured specimens of Inconel 550 shown in figures 52 through 54. Cracks and grain boundary fragmentation in specimens of Inconel 550 that had not yet failed in thermal fatigue have already been mentioned in connection with figures 42 through 47. Such damage could account for the decrease in the stress-rupture life of Inconel 550 as a result of thermal cycling.

One thus concludes that structural changes are important factors in the thermal fatigue process and that these changes can have a variety of forms and effects, depending upon the material and the test conditions.

The effect of raising T_{max} on the subsequent stress-rupture life

after about 50 percent N_f (figs. 35 and 36) is now interpreted as follows: For S-816 cycling at 1350°/200° F, the second stage of fatigue is apparently not entered until very near the end of the thermal fatigue process. Since subsequent loss of stress-rupture life depends upon entering the second stage of fatigue, there should be no direct loss if the cycling is stopped while still in the first stage. Thus, if cycling at 1350°/200° F is stopped when $N = 1/2\ N_f$, fatigue of S-816 is still far from the second stage. Using this conservative fraction of N_f, one might expect that if a number of specimens of S-816 are cycled between various T_{max} and 200° F and if cycling is stopped when $N = 1/2\ N_f$, fatigue will not have reached the second stage so long as the T_{max} is not excessively high. Figure 49 shows that S-816 undergoes a net hardening during thermal fatigue up to T_{max} as high as 1600° F. On this basis, then, one might expect that the stress-rupture life of S-816 after $1/2\ N_f$ should not drop-off as the T_{max} of cycling is raised, and this is shown to be the case in figure 35. In fact, the strengthening action of strain- and/or precipitation-hardening was preserved up to a T_{max} of 1550° F, which was the highest T_{max} studied.

Inconel 550, in contrast to S-816, has been shown to enter the second stage of fatigue very early in the process. The higher strains, as well as the increased rate of vacancy diffusion and the occurrence of recrystallization which accompany an increase in T_{max}, should aggravate the cracking. As a result, the stress-rupture life after one-half the number of cycles to failure should fall off with T_{max}, and this behavior is shown in figure 36. Note that this effect of T_{max} was very pronounced; when T_{max} equalled 1550° F, the stress-rupture life was only about 2 percent that of the virgin material.

Further information on the effect of T_{max} is gained from considering the effect of the time at T_{max} on the subsequent stress-rupture life. This effect was studied for a T_{max} of 1350° F and a T_{min} of 200° F. For S-816, increasing the time of exposure at T_{max} from 15 to 60 seconds had little effect on N_f (see fig. 19; at most, there was a very slight reduction). Comparison of figures 21 and 31 shows that this increase in time at T_{max} did not affect the general trend in the variation of the stress-rupture life with the number of cycles. For both times of exposure, there was an initial increase, and the increase appeared greater for the longer cycle. This last observation might indicate that an appreciable part of the strengthening was due to precipitation-hardening as well as strain-hardening, with the amount of precipitation-hardening increasing with the time of exposure, as was actually observed in the microstructures of S-816.

For Inconel 550, the increase in the time of exposure at a T_{max} of 1350° F reduced N_f from 10,500 to 7,400 cycles (fig. 18). Apparently, the damaging effects are time dependent and have more time to operate and decrease N_f on the longer cycle. The time-dependency of this damaging effect is also clearly shown in stress-rupture tests on specimens removed before failure. Thus there was a greater reduction in the stress-rupture life for a given number of cycles when the time at T_{max} was increased (compare figs. 23 and 32). This effect might mean that the vacancies created by plastic deformation are allowed more time to diffuse together to form cracks.

Additional evidence in support of the theory advanced is given by the effect of time at various T_{max} on N_f (figs. 18 and 19). The time-dependence of the damaging effects, which has just been considered for

Inconel 550, can explain the decrease in N_f with increasing time at low T_{max}. The occurrence of structural changes which partially offset these damaging effects is supported by the opposite effect at high T_{max}. The facts that the effect of time is more pronounced for S-816 than for Inconel 550 and that the cross-over points in figures 18 and 19 occur at a lower temperature for S-816 than for Inconel 550 are consistent with the hardness behavior of the two alloys (figs. 40, 41, and 49) and with the variation in N_f with T_{max} of the two alloys (fig. 48) and add further proof of the importance of structural changes in thermal fatigue.

CONCLUSIONS

A study has been made of the behavior of ductile alloys in thermal fatigue. The following conclusions are drawn for the materials and test conditions studied:

1. The maximum cycle temperature had more effect than the temperature difference on the number of cycles to failure.

2. Increasing the time of exposure at high maximum cycle temperatures increased the number of cycles to failure, whereas the same increase in time at low maximum cycle temperatures decreased the number of cycles to failure.

3. The number of cycles to failure could not be directly related to the cyclic plastic strain.

4. Exposure to thermal fatigue conditions strengthened one alloy (S-816) and weakened the other (Inconel 550). Under the most damaging conditions studied, Inconel 550 lost 98 percent of its original stress-rupture life as a result of prior thermal fatigue, even though the number of cycles was only one-half of that required for failure by thermal fatigue alone.

5. A theory has been tentatively proposed that divides the process of thermal fatigue into two stages: First, a stage of strain- and/or precipitation-hardening, during which the ductility is reduced and the strength is increased, and second, a stage of the destruction of the cohesive bonds and the development and propagation of cracks. Structural changes that occur during thermal fatigue are an important part of this theory.

REFERENCES

1. W. C. Stewart and W. G. Schreitz, "Thermal-Shock and Other Comparison Tests of Austenitic and Ferritic Steels for Main Steam Piping," Trans. ASME, 72, 1043-1055 (1950).

2. W. C. Stewart and W. G. Schreitz, "Thermal-Shock and Other Comparison Tests of Austenitic and Ferritic Steels for Main Steam Piping - A Summary Report," Trans. ASME, 75, 1051-1067 (1953).

3. E. S. Dixon, "Needs of the Oil Industry for Metals at High Temperatures," Symposium on Effect of Temperature on the Properties of Metals, published jointly by the American Society for Testing Materials, Philadelphia, Pa., and the American Society of Mechanical Engineers, New York, N. Y., 1932, pp. 66-84.

4. M. E. Holmberg, "Experience with Austenitic Steels in High-Temperature Service in the Petroleum Industry," Trans. ASME, 73, 733-742 (1951).

5. John J. B. Rutherford, "Some Experience in Service (Power, Oil and Chemical Plants)," High Temperature Properties of Metals, American Society for Metals, Cleveland, Ohio, 1951, pp. 133-170.

6. John W. Weeton, "Mechanisms of Failure of High Nickel-Alloy Turbojet Combustion Liners," N.A.C.A. Technical Note 1938 (Oct. 1949).

7. Floyd B. Garrett and Charles Yaker, "Turbojet-Engine Evaluation of AISI 321 and AISI 347 Stainless Steels as Nozzle-Blade Materials," N.A.C.A. Research Memo E9K17 (Feb. 27, 1950).

8. Morton B. Millenson and Samuel S. Manson, "Investigation of Rim Cracking in Turbine Wheels with Welded Blades," N.A.C.A. Research Memo E6L17 (1947).

9. P. I. Wilterdink, "Experimental Investigation of Rim Cracking in Disks Subjected to High Temperature Gradients," N.A.C.A. Research Memo E9F16 (1949).

10. P. I. Wilterdink, A. G. Holms, and S. S. Manson, "A Theoretical and Experimental Investigation of the Influence of Temperature Gradients on the Deformation and Burst Speeds of Rotating Discs," N.A.C.A. Technical Note 2803 (1952).

11. A. S. Thompson, "Thermal Stress in Power-Producing Elements," J. Aero. Sci., 19, 476-480 (July 1952).

12. M. Bentele and C. S. Lowthian, "Thermal Shock Tests on Gas Turbine Materials," Aircraft Engineering, 24, 32-38 (Feb. 1952).

13. M. J. Whitman, R. W. Hall, and C. Yaker, "Resistance of Six Cast High-Temperature Alloys to Cracking Caused by Thermal Shock, " N.A.C.A. Tech. Note 2037 (Feb. 1950).

14. Anon., "Thermal Shock Properties of High Temperature Alloys," Research Laboratories, Allegheny Ludlum Steel Corp., Watervliet, N. Y., Nov. 24, 1954.

15. L. F. Coffin, Jr. and R. P. Wesley, "Apparatus for the Study of Effects of Cyclic Thermal Stresses on Ductile Materials," Trans. ASME, 76, 923-930 (1954).

16. L. F. Coffin, Jr., "A Study of the Effects of Cyclic Thermal Stresses on a Ductile Material," Trans. ASME, 76, 931-950 (1954).

17. L. F. Coffin, Jr., "The Problem of Thermal Stress Fatigue in Austenitic Steels at Elevated Temperature," paper from Symposium on Effect of Cyclic Heating and Stressing on Metals at Elevated Temperatures, American Society for Testing Materials Special Technical Publication No. 165, pp. 31-50, disc. pp. 51-52 (June 17, 1954).

18. L. F. Coffin, Jr., "Design Aspects of High Temperature Fatigue with Particular Reference to Thermal Stresses," Trans. ASME, 78, 527-531 (April 1956).

19. W. H. Bruckner, "The Micro-Mechanism of Fracture in Ferrite," Letters to the Editor, Acta Met., 2, 168-169 (Jan. 1954).

20. C. Zener, Elasticity and Anelasticity of Metals, Chicago: University of Chicago Press, 1948, p. 146.

21. T. M. Elsesser, O. M. Sidebottom, and H. T. Corten, "The Influence of Aging on the Buaschinger Effect in Inelastically Strained Beams," Trans. ASME, 74, 1291-1296 (November 1952).

22. H. J. Corten and T. M. Elsesser, "The Effect of Slightly Elevated Temperature Treatment Upon Microscopic and Submicroscopic Residual Stresses Induced by Small Elastic Strains in Metals," Trans. ASME, 74, 1297-1302 (November 1952).

23. E. Orowan, "The Creep of Metals," J. West of Scotland Iron and Steel Inst., 54, 45-96 (Feb. 1947).

24. Oleg D. Sherby, Raymond L. Orr, and John E. Dorn, "Creep Correlations of Metals at Elevated Temperatures," Trans. AIME, 200, 71-80 (1954).

25. F. Seitz, "On the Generation of Vacancies by Moving Dislocations," Advances in Physics, 1, 43-90 (January 1952).

26. F. S. Buffington and M. Cohen, "Self-Diffusion in Alpha Iron under Uniaxial Compressive Stress," Trans. AIME, 194, 859-860 (1952).

27. F. Seitz, "On the Porosity Observed in the Kirkendall Effect," Acta Met., 1, 355-369 (May 1953).

28. C. F. Baes, Jr. and H. H. Kellog, "Effect of Dissolved Sulfur on the Surface Tension of Liquid Copper," Trans. AIME, 197, 643-648 (1953).

29. R. Balluffi and L. Seigle, "Effect of Grain Boundaries upon Pore Formation and Dimensional Changes during Diffusion," Acta Met., 3, 170 (1955).

30. R. W. Balluffi, "The Supersaturation and Precipitation of Vacancies during Diffusion," Acta Met., 2, 194-202 (March 1954).

31. L. Seigle and R. Resnick, "On Pore Formation During Diffusion," Letters to the Editor, Acta Met., 3, 605-606 (November 1955).

32. E. S. Machlin, "Creep-Rupture by Vacancy Condensation," Trans. AIME, 206, 106-111 (1956).

33. Frances D. Coffin and Andrew L. Weiman, "The Influence of the Atmosphere on the Stress-Rupture Life of Inconel," NACA TN to be published.

34. J. A. Brinkman, "Mechanism of Pore Formation Associated with the Kirkendall Effect," Acta Met., 3, 140-145 (March 1955).

35. J. A. Brinkman, "On the Mechanism of Pore Formation during Diffusion," Letters to the Editor, Acta Met., 3, 606-607 (November 1955).

36. L. Seigle and R. Resnick, "On Pore Formation during Diffusion," Letters to the Editor, Acta Met., 3, 605-606 (November 1955).

37. C. H. M. Jenkins, E. H. Bucknall, and E. A. Jenkinson, "The Inter-Relation of Age-Hardening and Creep Performance. Part II - The Behavior in Creep of an Alloy Containing 3 Per Cent Nickel and Silicon in Copper," J. Inst. Met., 70, 57-79 (1944).

38. M. Whitaker, E. Voce, and A. R. Bailey, "Intercrystalline Failure of Brasses and Aluminum Brasses in Air, Ammonia, and Certain Aqueous Solutions and Molten Metals," Metallurgia, 39, 21-29, 66-70 (1948).

39. N. D. Benson, J. McKeown, and D. N. Mends, "The Creep and Softening Properties of Copper for Alternator Rotor Windings," J. Inst. Met., 80, 131-143 (1951).

40. J. Neill Greenwood, D. R. Miller, and J. W. Suiter, "Intergranular Cavitation in Stressed Metals," Acta Met., 2, 250-258 (March 1954).

41. A. G. Guy, Digest of "Fracture of Metals during Creep," by V. S. Iranova, Metallovedenie I Obrabotka Metallov., No. 1, 1955, pp. 19-26 26, and by I. A. Oding and V. S. Ivanova, Doklady Akademii Nauk S.S.S.R., 103, 77-80 (1955) in Metal Progress, March 1956, pp. 158, 160, and 162.

42. John F. Eckel, "The Influence of Frequency on the Repeated Bending Life of Acid Lead," Proc. ASTM, 51, 745-756 (1951).

43. J. A. Ewing and J. C. W. Hunfrey, "The Fracture of Metals under Repeated Alternations of Stress," Phil. Trans. Roy. Soc., 200, 241 (1903).

44. G. T. Beilby, "The Hard and Soft States in Ductile Metals," Proc. Roy. Soc., 79A, 463 (1907).

45. G. T. Beilby, "The Hard and Soft States in Metals," J. Inst. Metals, 6, 5 (1911).

46. H. J. Gough, "Crystalline Structure in Relation to Failure of Metals, Especially by Fatigue," Proc. ASTM, 33, part 2, 3-114 (1933).

47. H. J. Gough and W. A. Wood, "A New Attack upon the Problem of Fatigue of Metals, using X-Ray Methods of Precision," Proc. Roy. Soc., 154A, 510-539 (1936).

48. E. Orowan, "Theory of the Fatigue of Metals," Proc. Roy. Soc., 171A, 79 (1939).

49. W. A. Wood and R. B. Davis, "Effects of Alternating Strain on the Structure of a Metal," Proc. Roy. Soc., 220A, 255-266 (1953).

50. T. Broom, J. H. Molineux, and V. N. Whittaker, "Structural Changes During the Fatigue of Some Aluminum Alloys," J. Inst. Metals, 84, 357-363 (June 1956).

51. R. F. Hanstock, "Fatigue Phenomena in High-Strength Aluminum Alloys," J. Inst. Metals, 83, 11-15 (1954-55).

52. A. M. Freudenthal, "The Statistical Aspect of the Fatigue of Materials," Proc. Roy. Soc., 187A, 416-429 (1946).

53. S. S. Manson, "Behavior of Materials Under Conditions of Thermal Stress," N.A.C.A. Report 1170 (1954).

54. S. I. Liu, J. J. Lynch, E. J. Ripling, and G. Sachs, "Low Cycle Fatigue of the Aluminum Alloy 24ST in Direct Stress," Trans. AIME, 175, 469 (1948).

55. Anon., "Technical Data on Allegheny Ludlum Alloy S-816," Allegheny Ludlum Steel Corp., Watervliet, N. Y., Jan. 30, 1950.

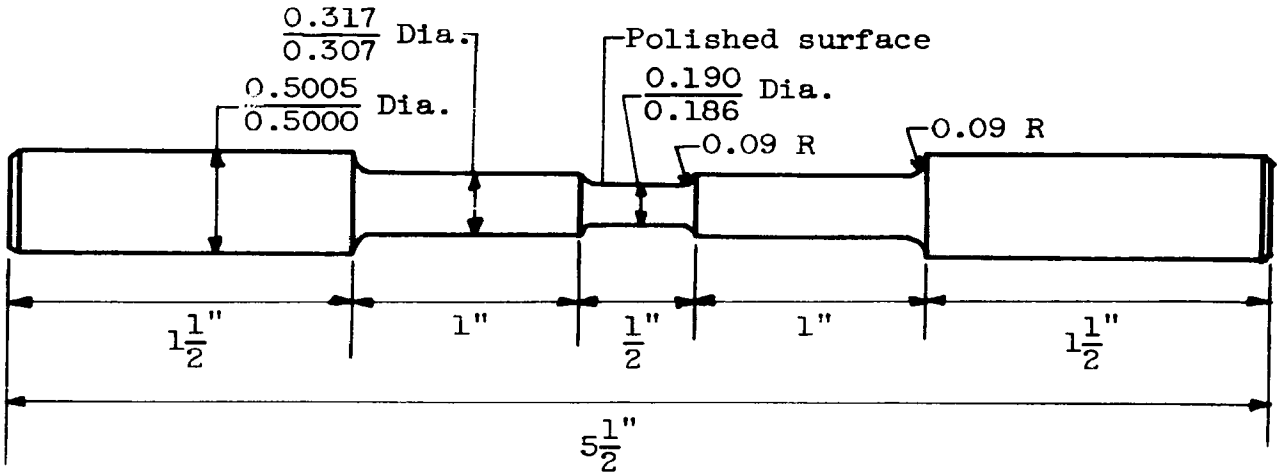


Fig. 1. - Test specimen.

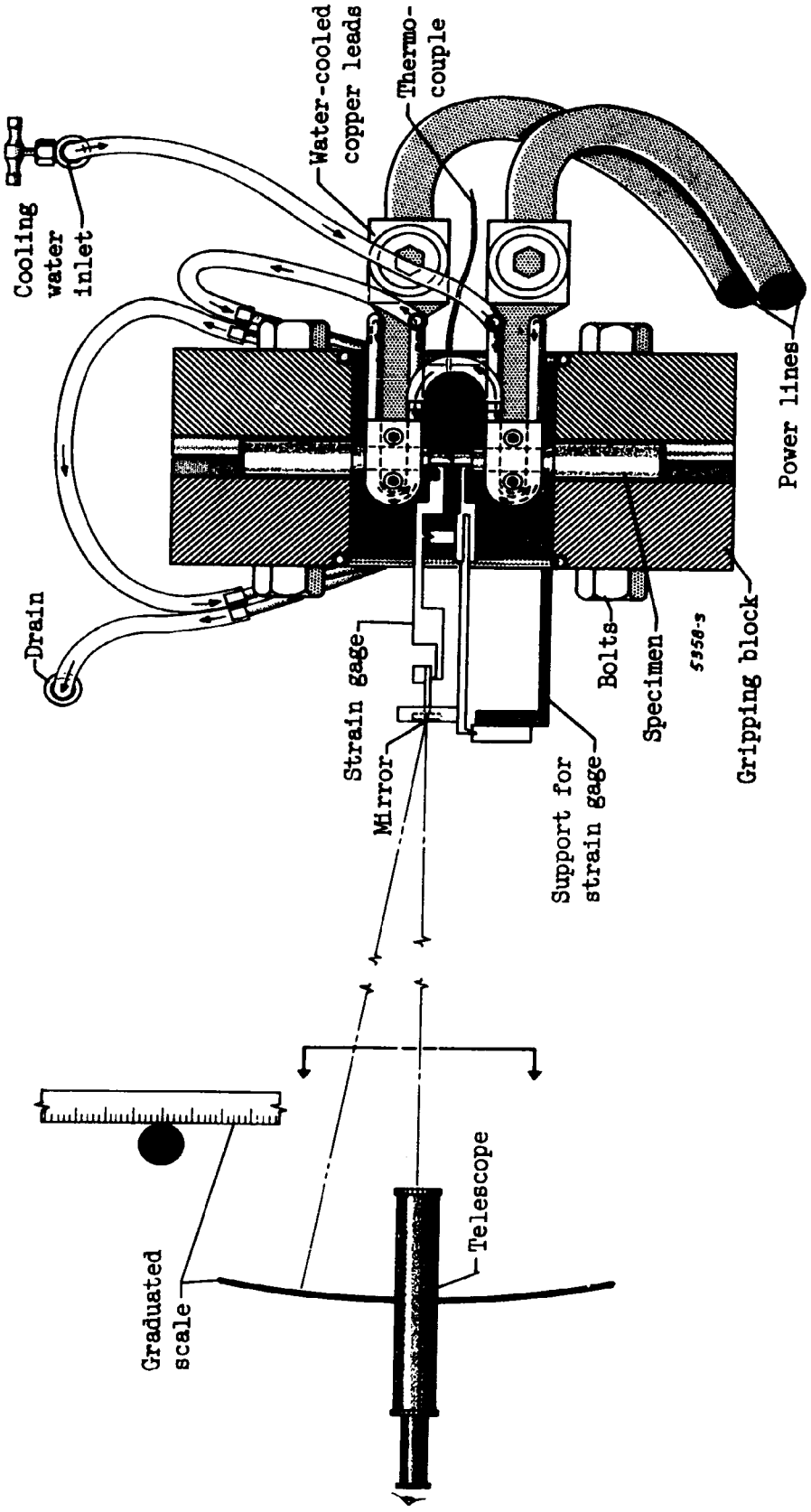


Fig. 2. - Diagram of equipment.



Magnification: 250X
Electrolytically etched in a dilute solution of nitric and hydrochloric acids

Fig. 3. - Thermocouple wires spot-welded to S-816 specimen (specimen had been cycled 200 times between 1350° and 200°F).

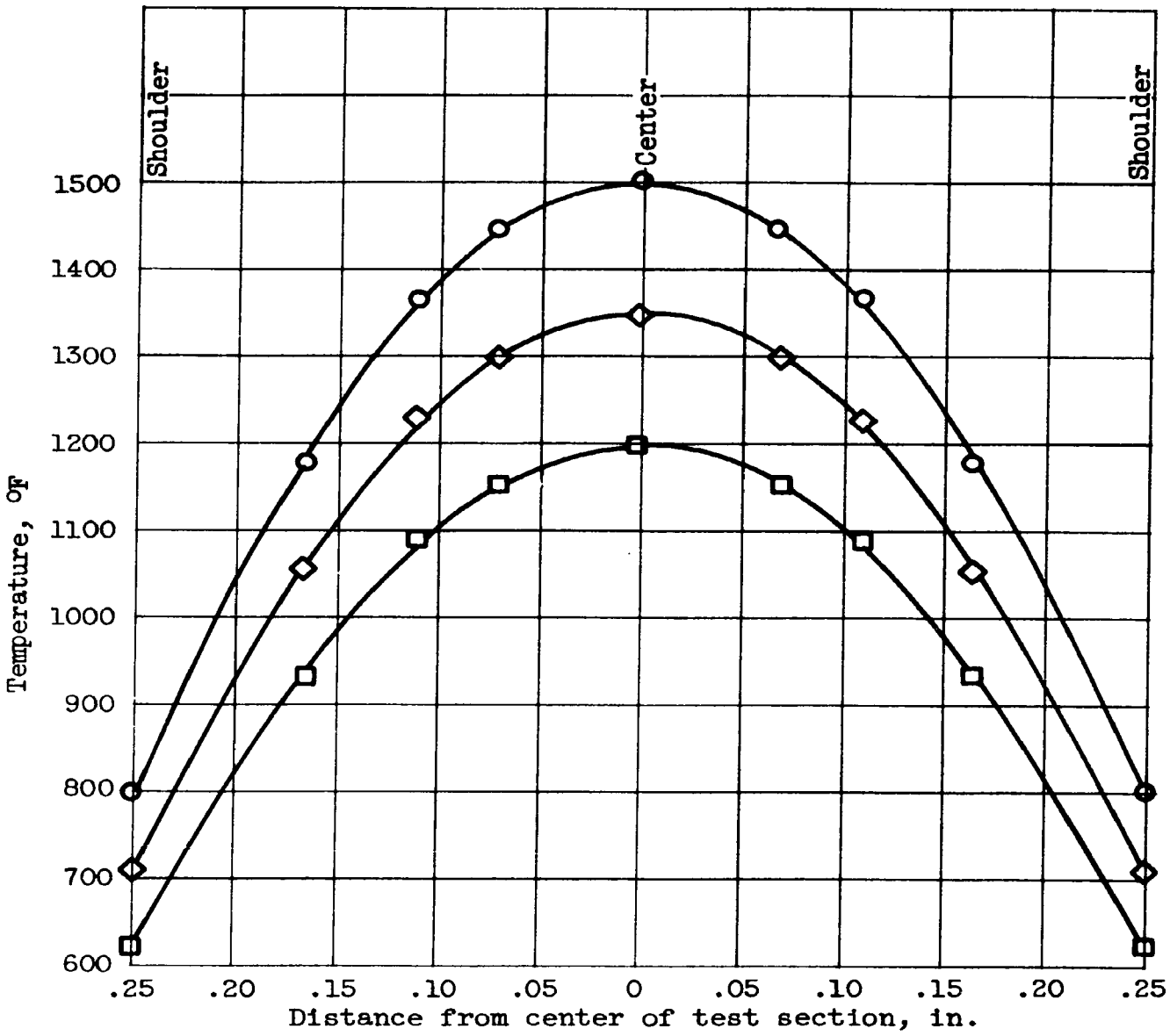


Fig. 4. - Temperature profiles of test specimens.

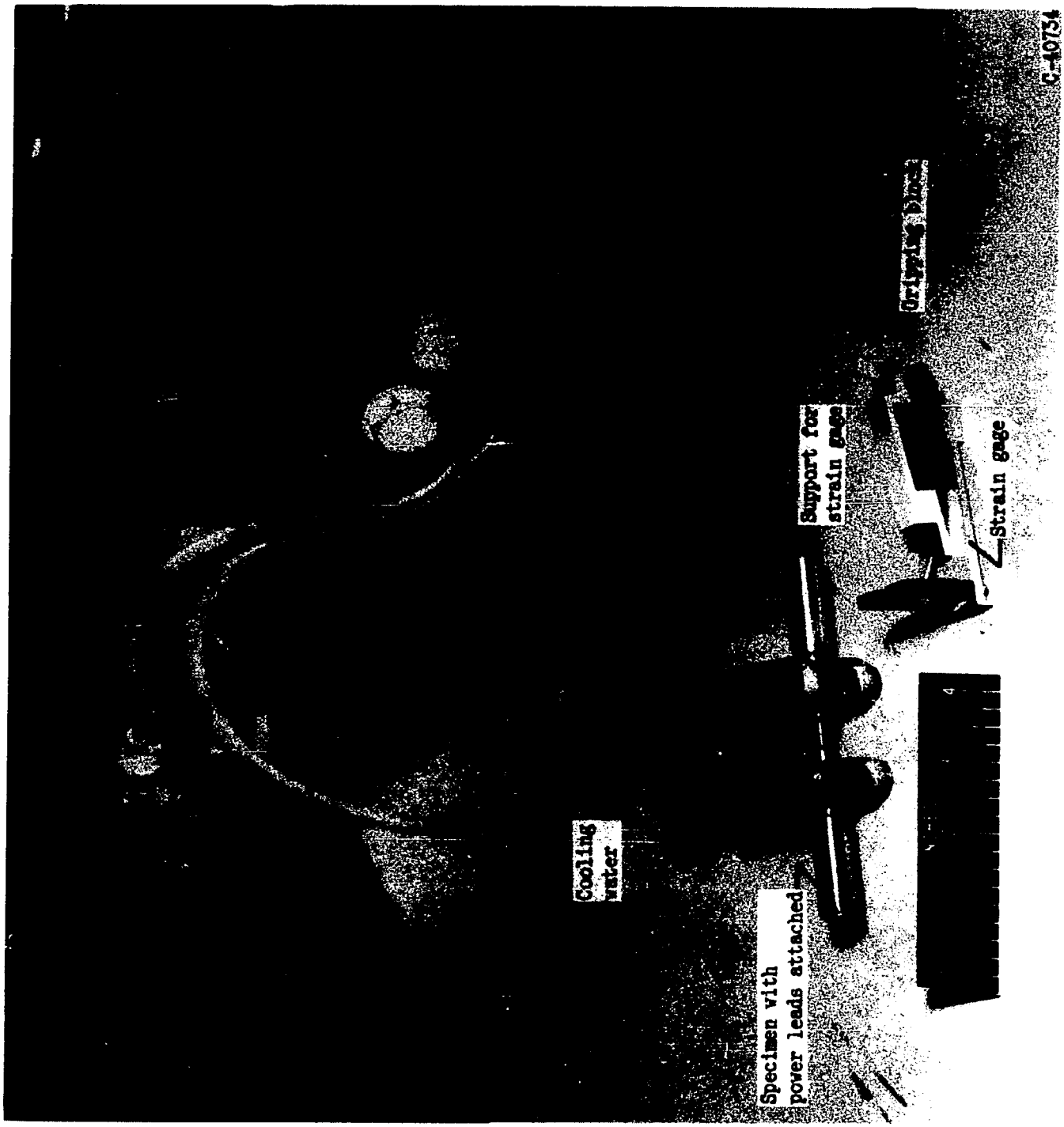


Fig. 5. - Photograph of equipment.

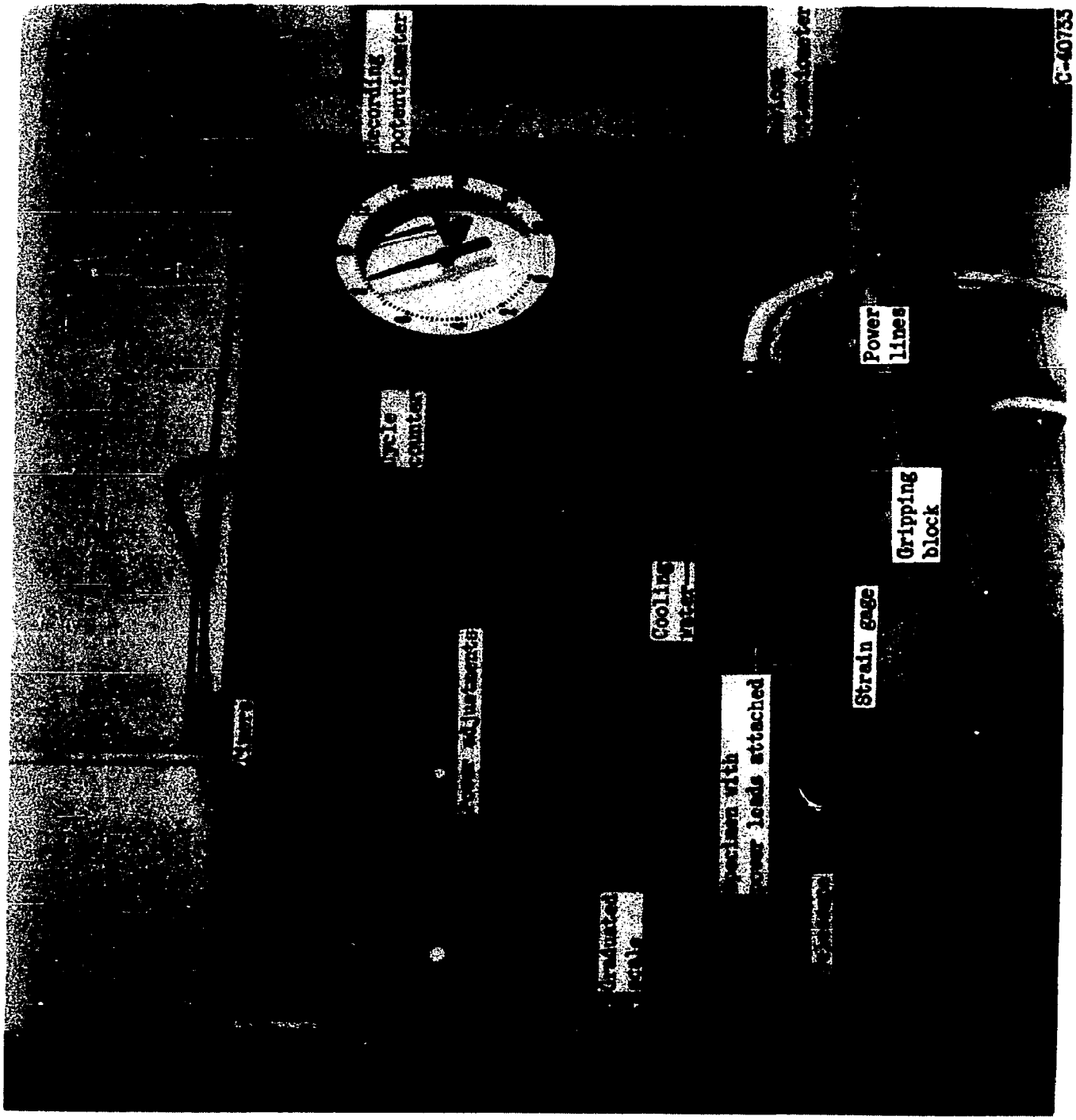
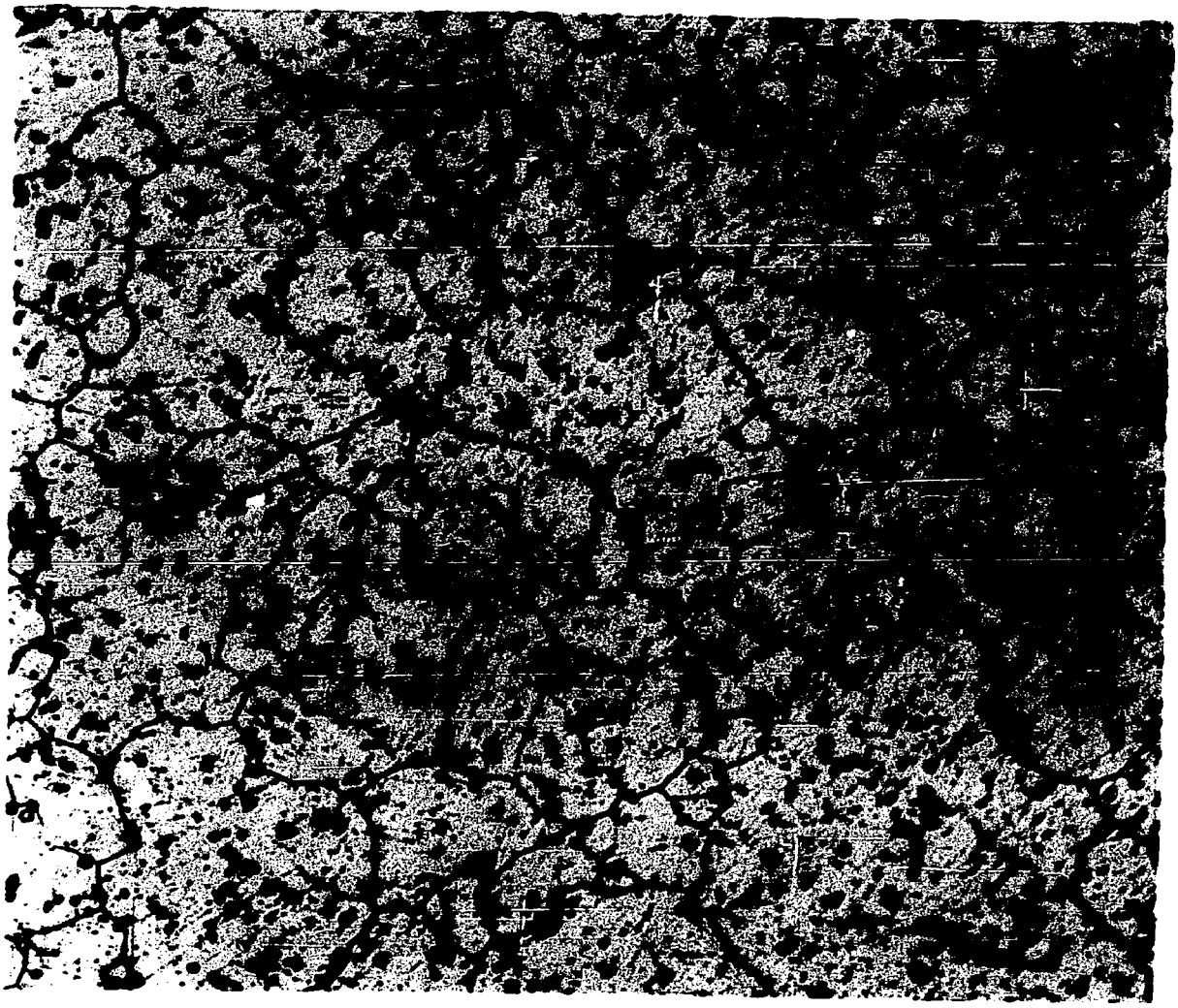
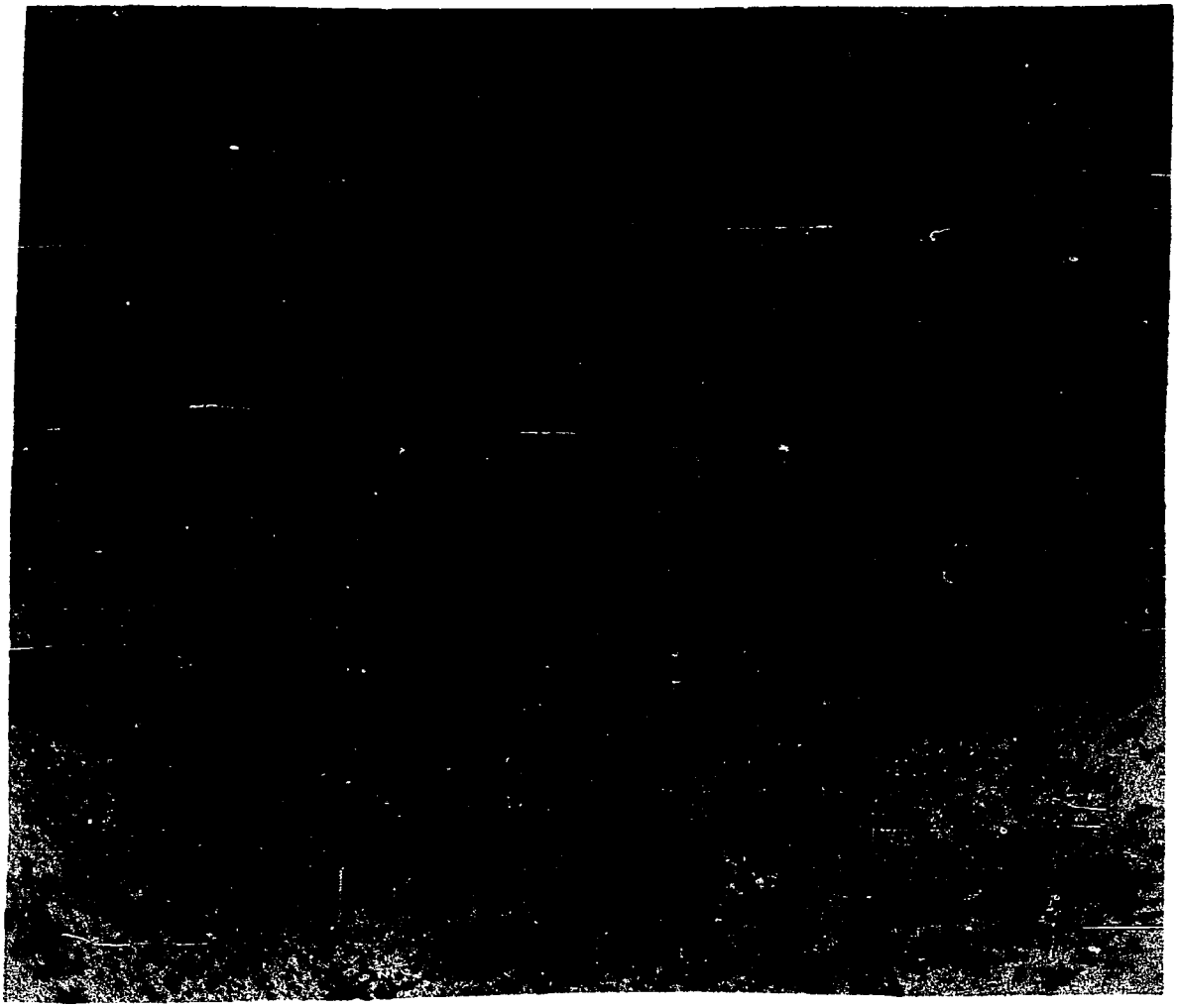


Fig. 6. - Photograph of equipment.



Magnification: 250X
Electrolytically etched in a dilute solution of sulfuric and boric acids

Fig. 7. - Microstructure of heat-treated S-816



Magnification: 250X
Electrolytically etched in a dilute solution of hydrofluoric acid and glycerol in water

Fig. 8. - Microstructure of heat-treated Inconel 550

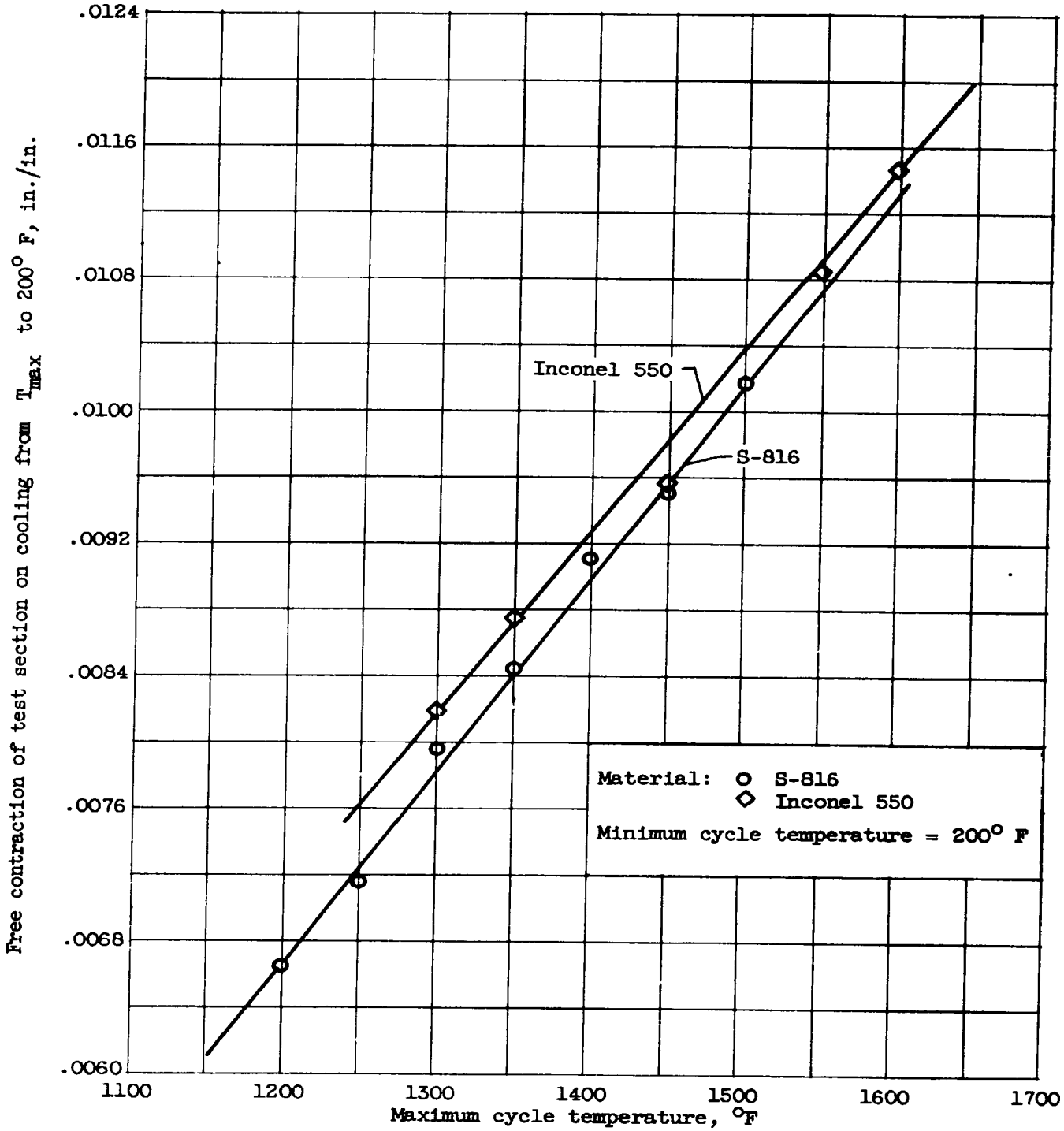


Fig. 9. - Free contraction of test section during cooling from various maximum temperatures to a minimum temperature of 200° F.

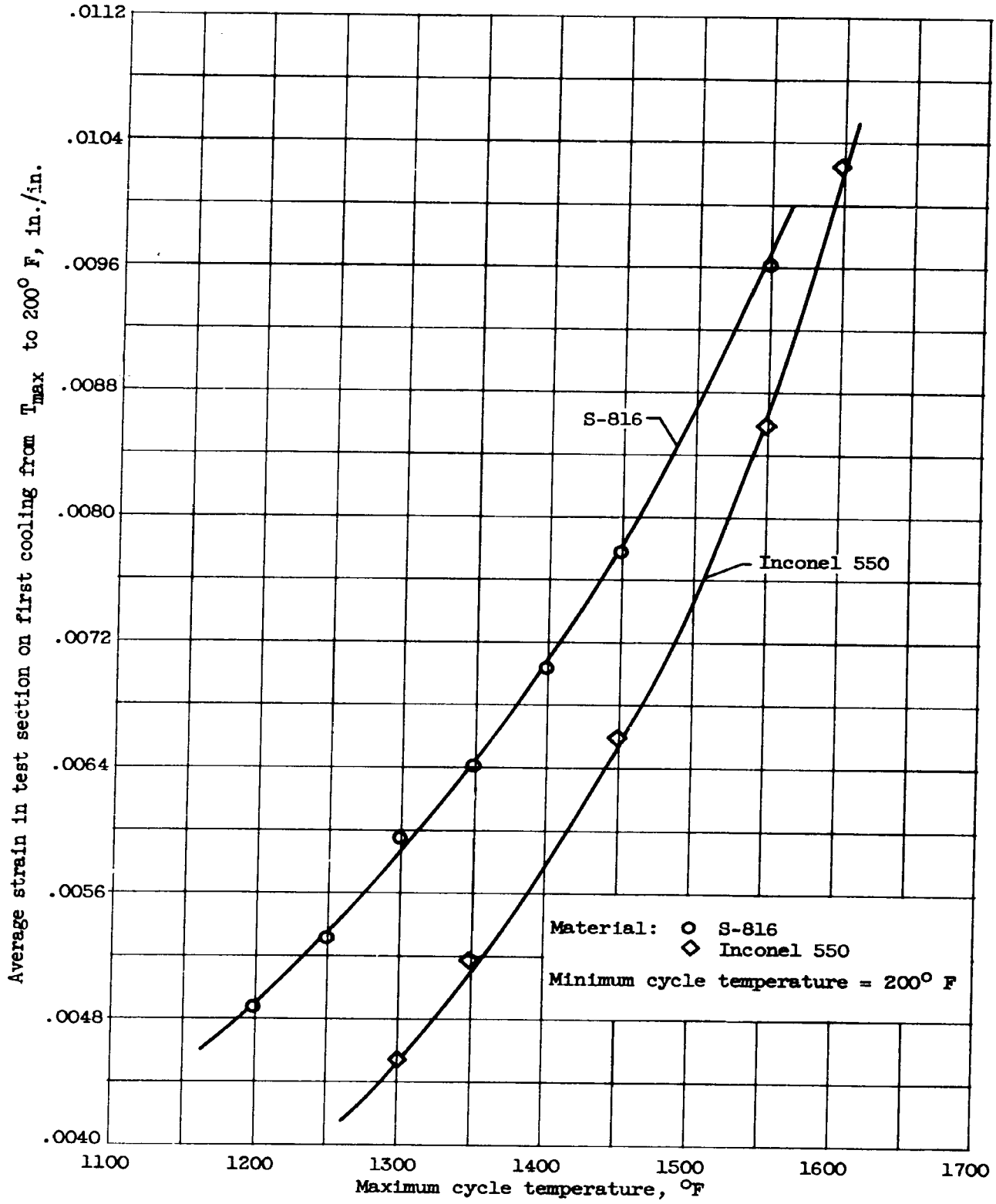


Fig. 10. - Average strain in test section during first cycle of constrained cooling from various maximum temperatures to a minimum temperature of 200° F.

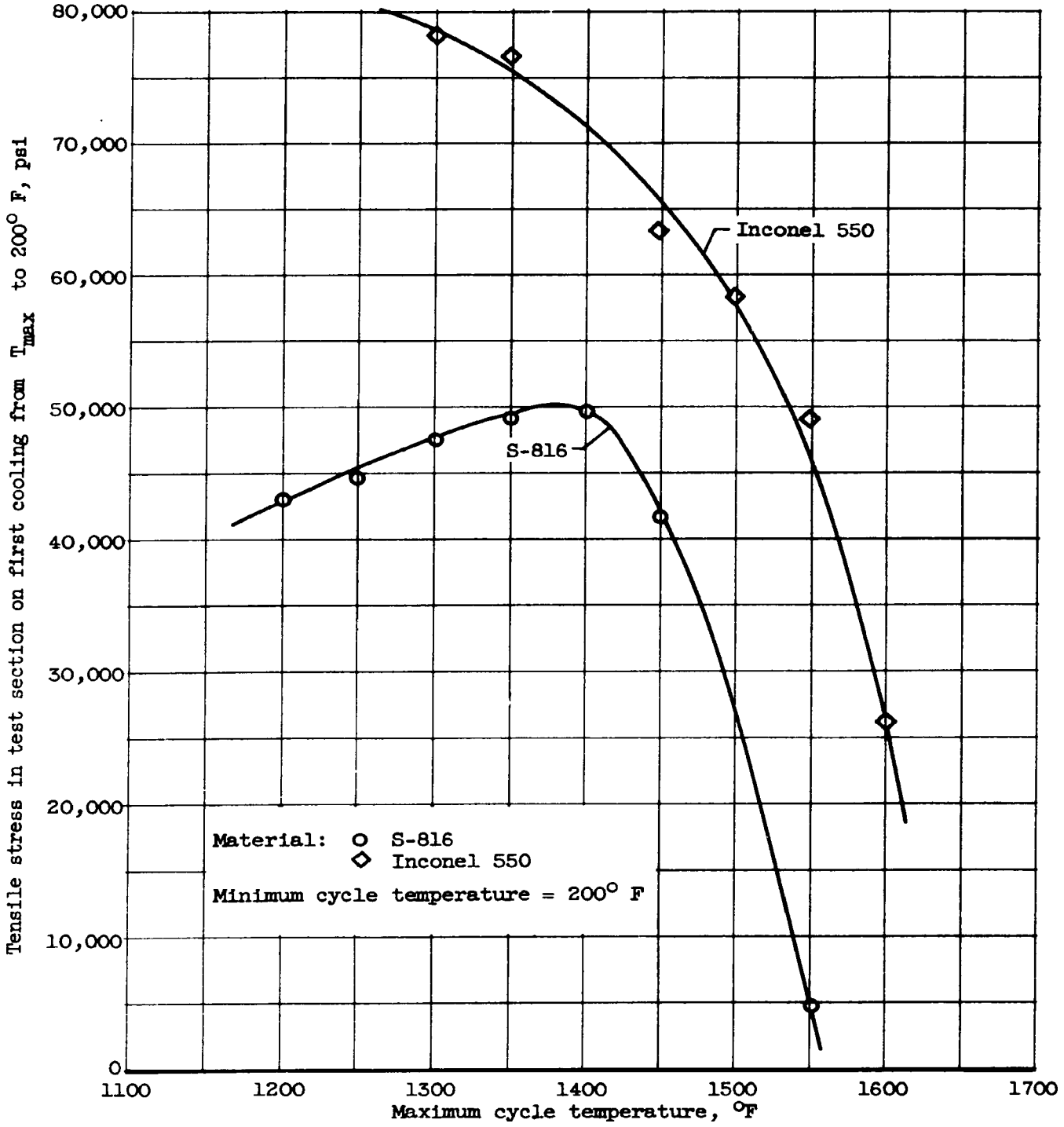
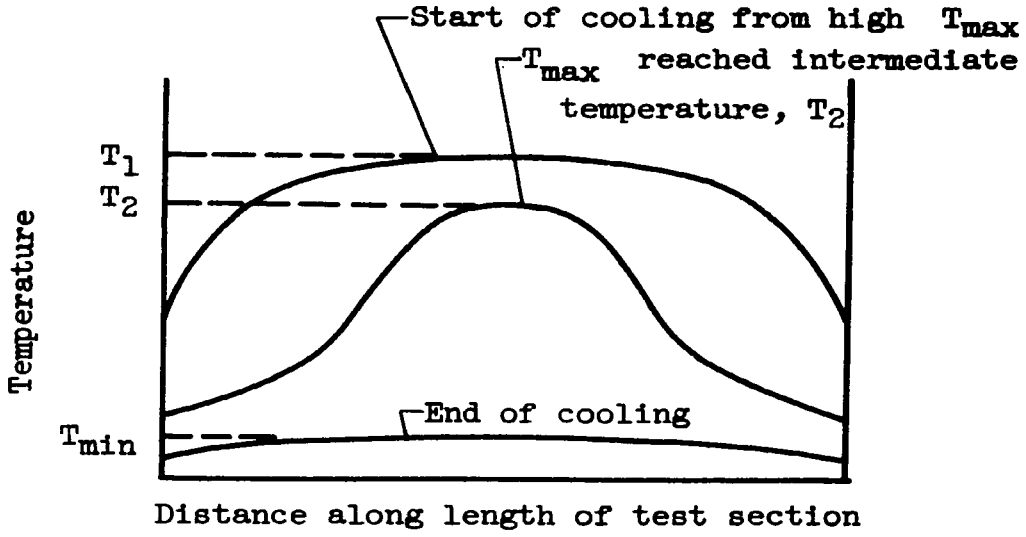
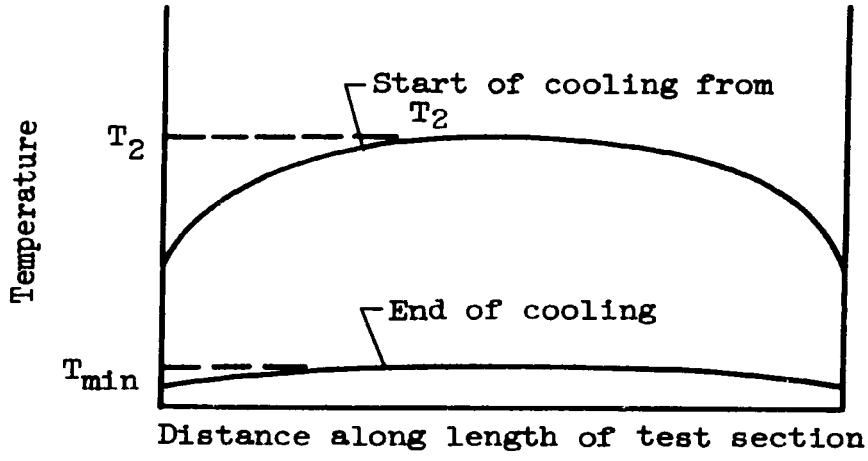


Fig. 11. - Tensile stress in test section during first cycle of constrained cooling from various maximum temperatures to a minimum temperature of 200° F.



(a) Cooling from $T_{max} = T_1$.



(b) Cooling from $T_{max} = T_2 < T_1$.

Fig. 12. - Temperature conditions during cooling.

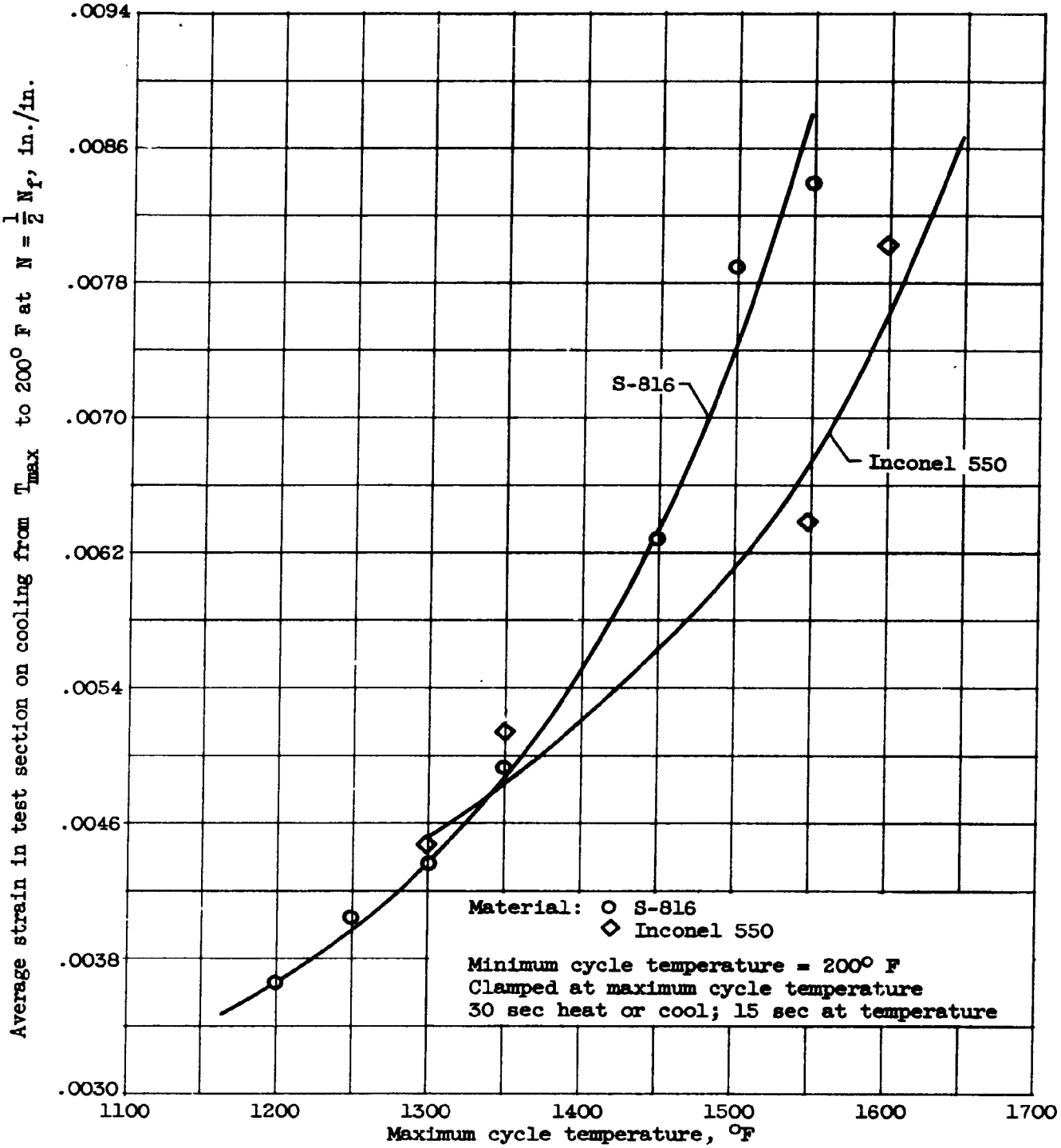


Fig. 13. - Average strain in test section during constrained cooling from various maximum cycle temperatures to a minimum cycle temperature of 200° F at $N = \frac{1}{2} N_f$.

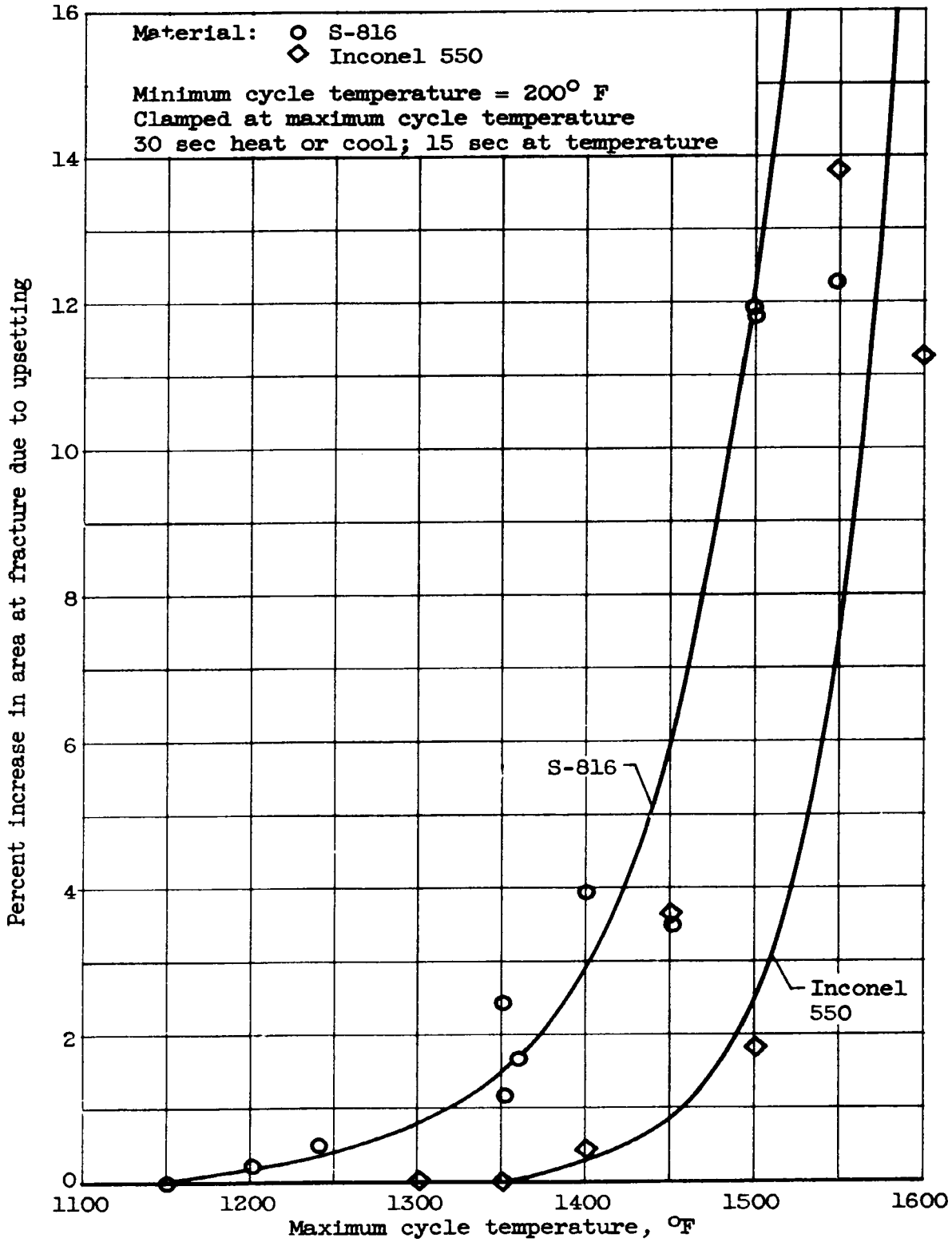


Fig. 14. - Amount of bulging in specimens that had failed in thermal fatigue at various T_{max}.

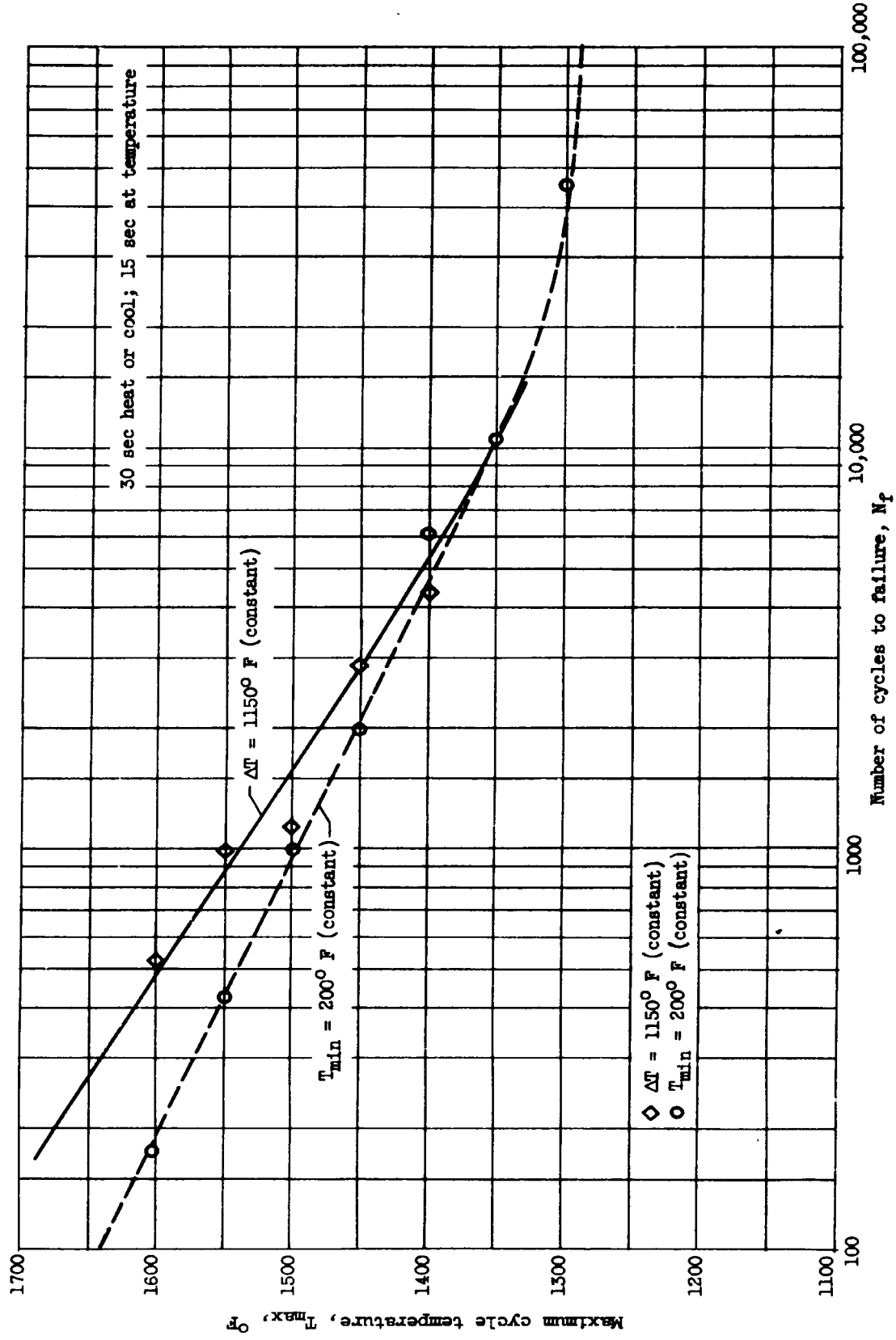


Fig. 15. - Effect of T_{max} on N_f for Inconel 550 specimens thermally cycled at a constant ΔT and at a constant T_{min}.

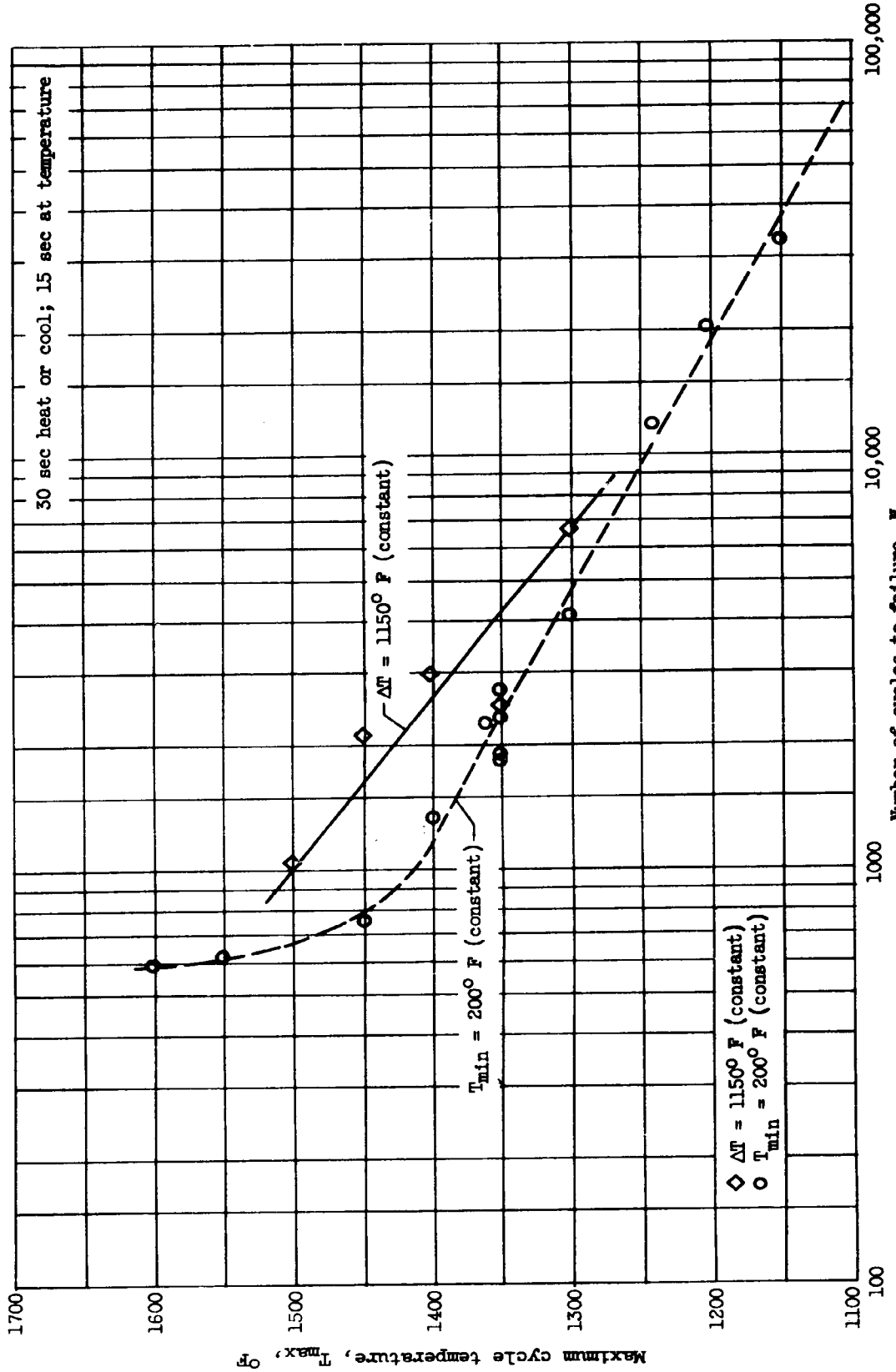


Fig. 16. - Effect of T_{max} on N_f for S-816 specimens thermally cycled at a constant ΔT and at a constant T_{min}.

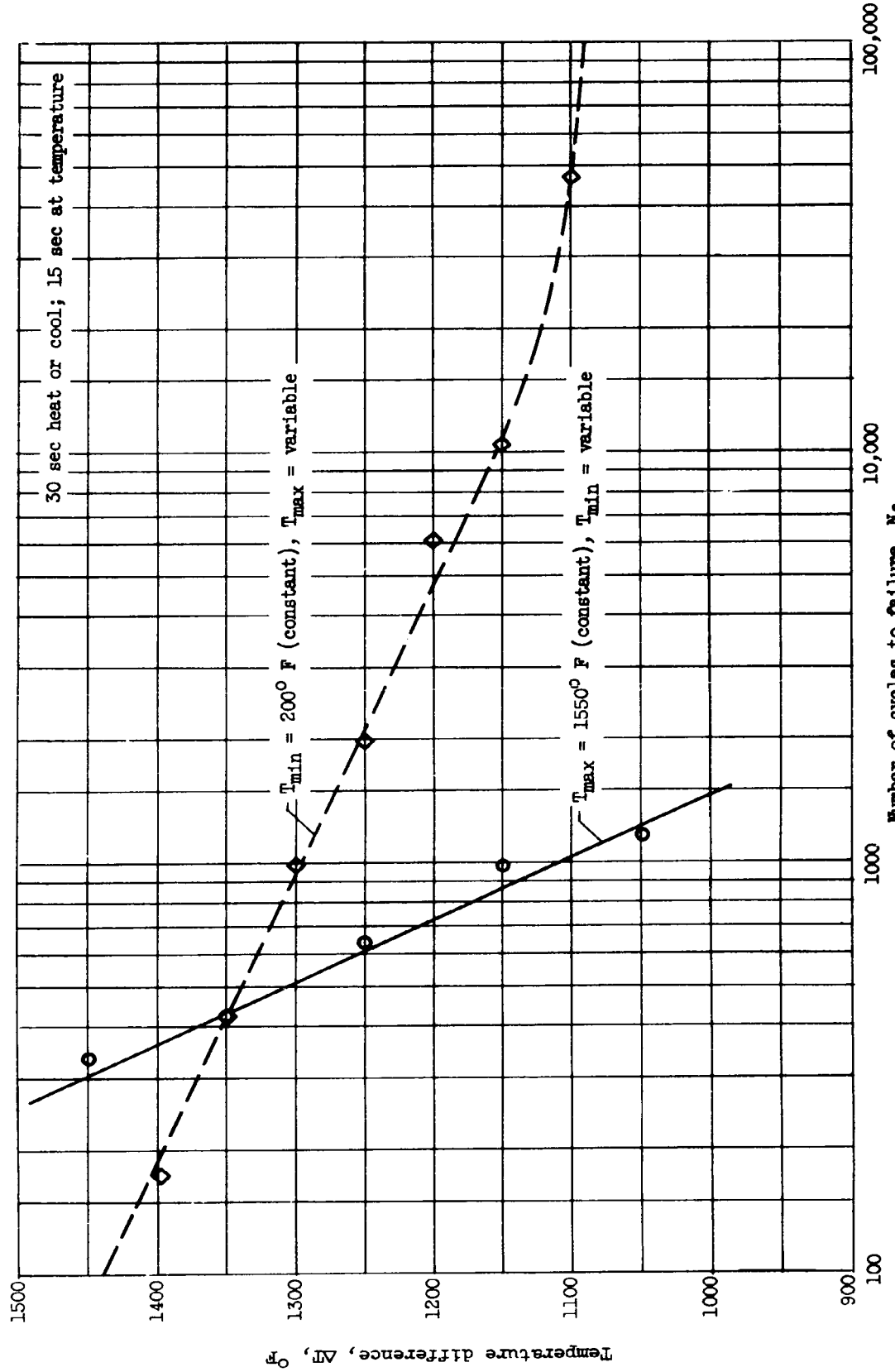


Fig. 17. - Effect of ΔT on N_f for Inconel 550 specimens thermally cycled at a constant T_{max} and at a constant T_{min}.

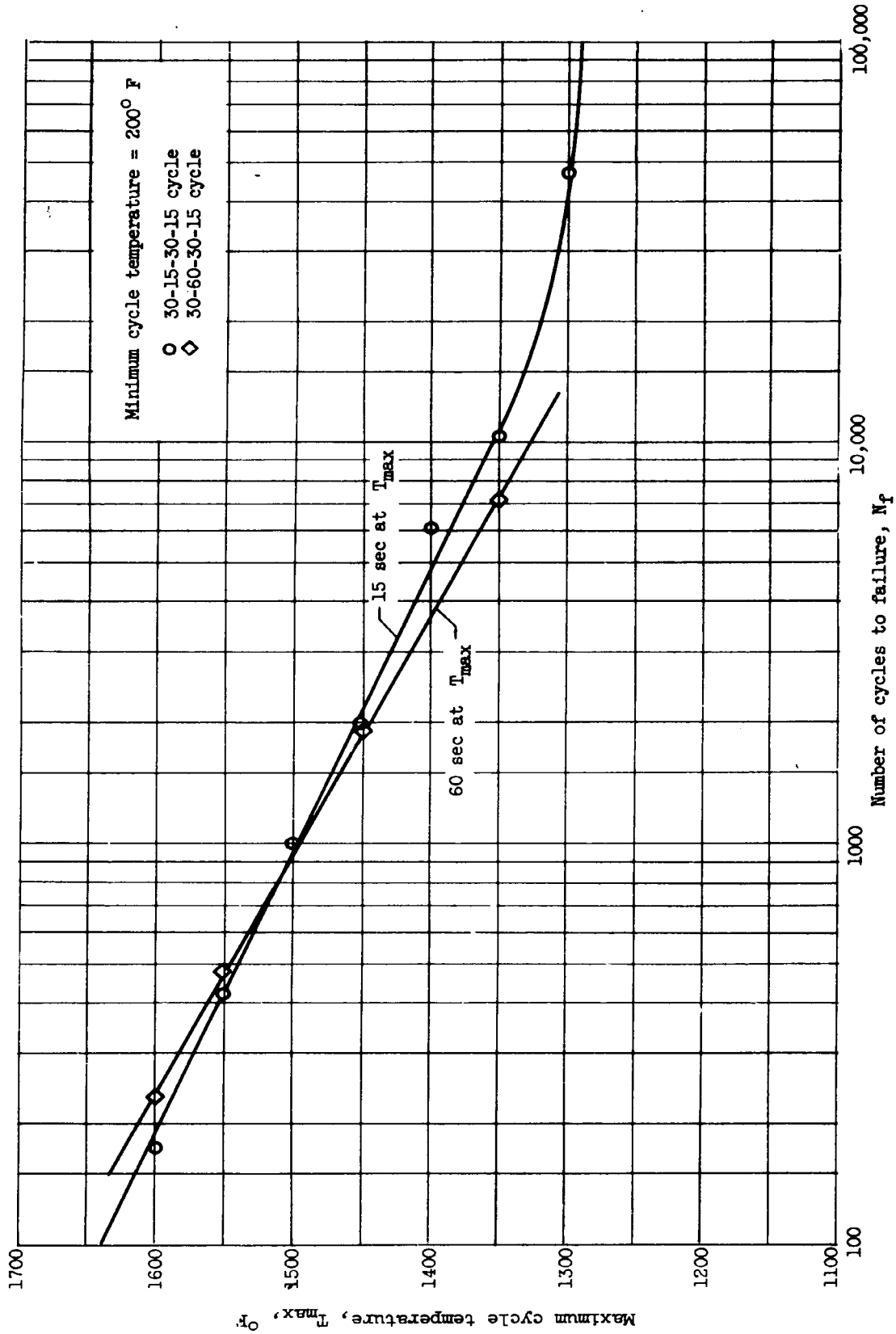


Fig. 18. - Effect of time of exposure at T_{max} on N_f for Inconel 550 specimens thermally cycled at various T_{max}.

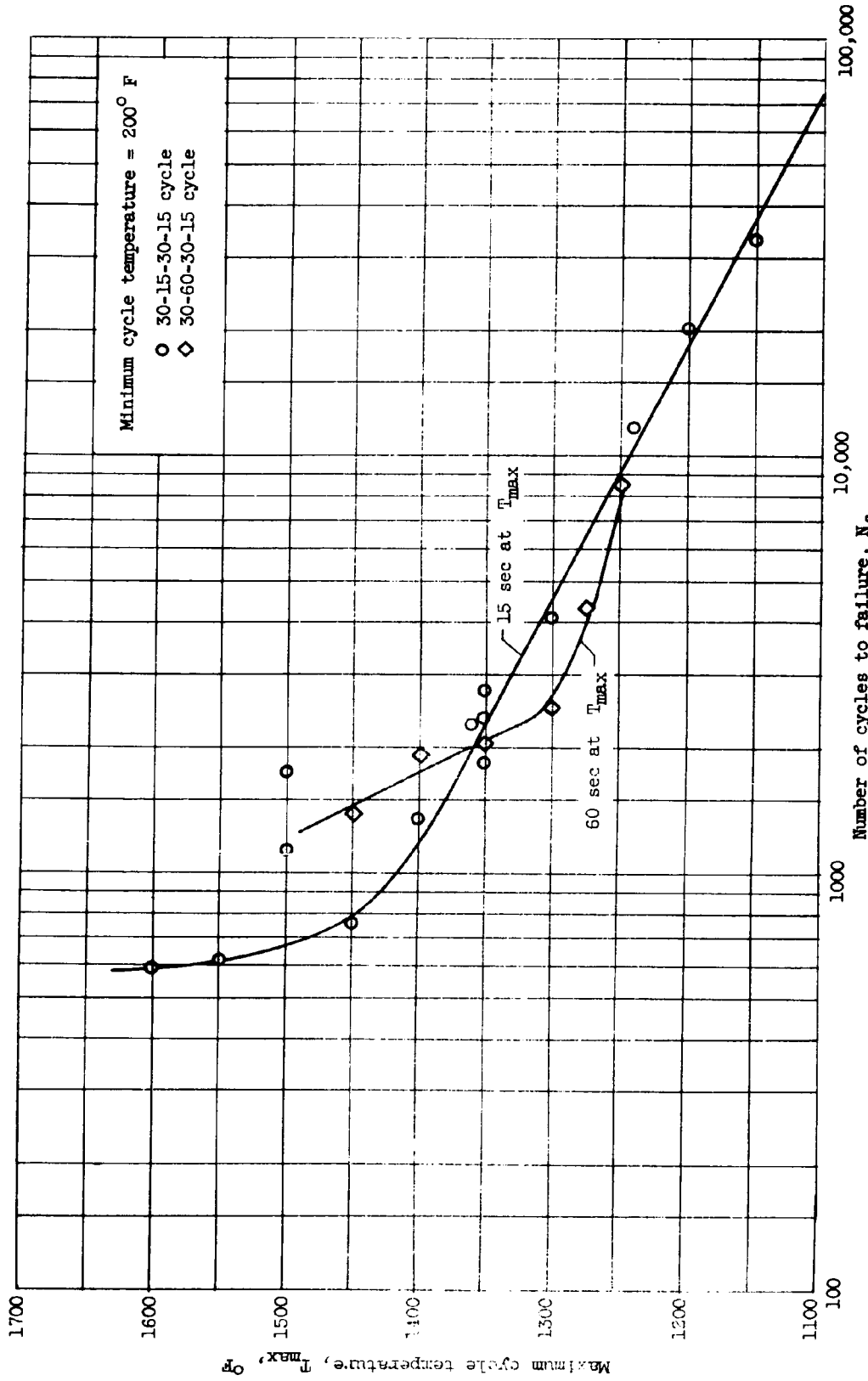


Fig. 19. - Effect of time of exposure at T_{max} on N_f for S-816 specimens thermally cycled at various T_{max}.

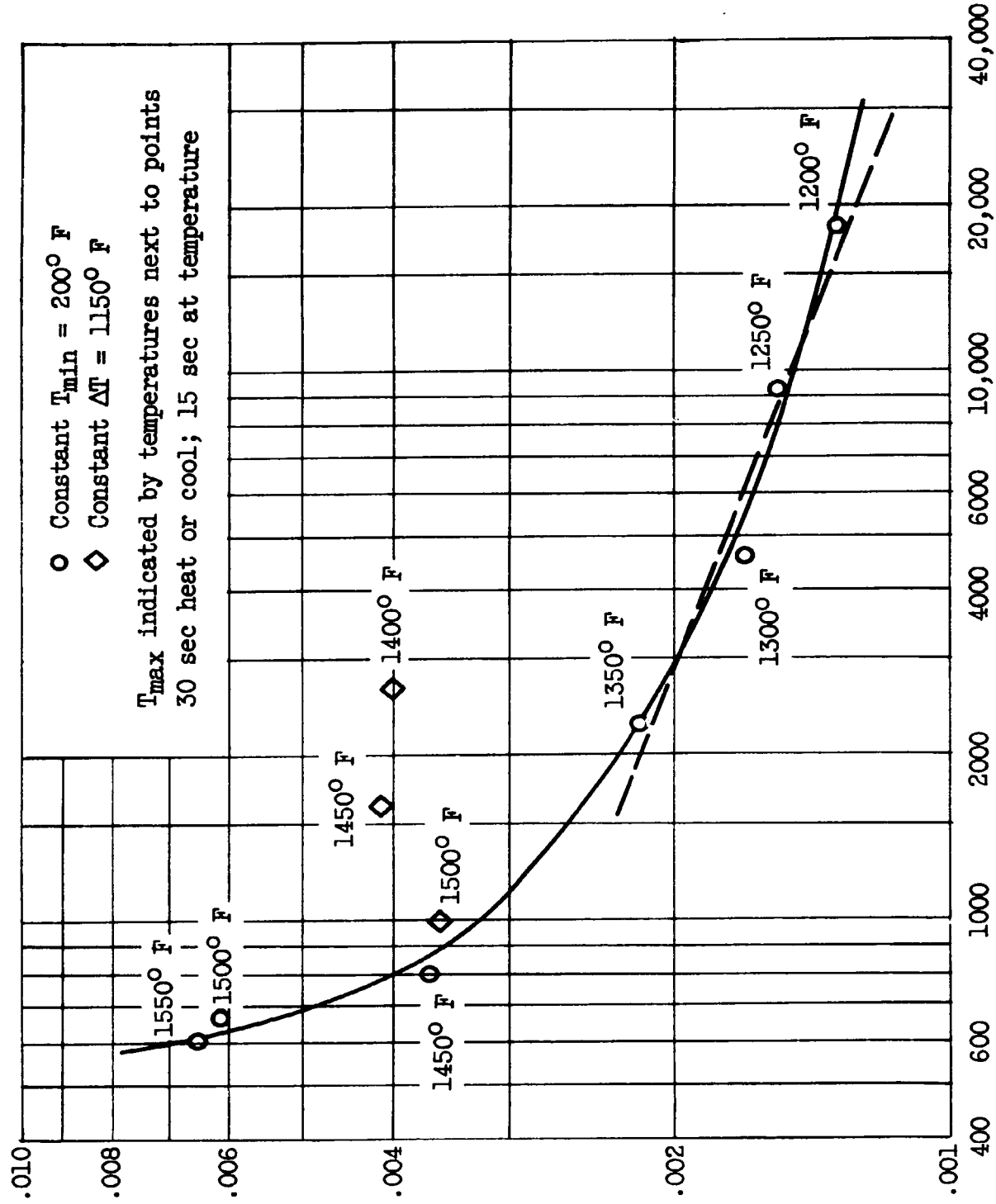


Fig. 20. - Variation of the number of cycles to failure of S-816 specimens with the average plastic strain per half-cycle.

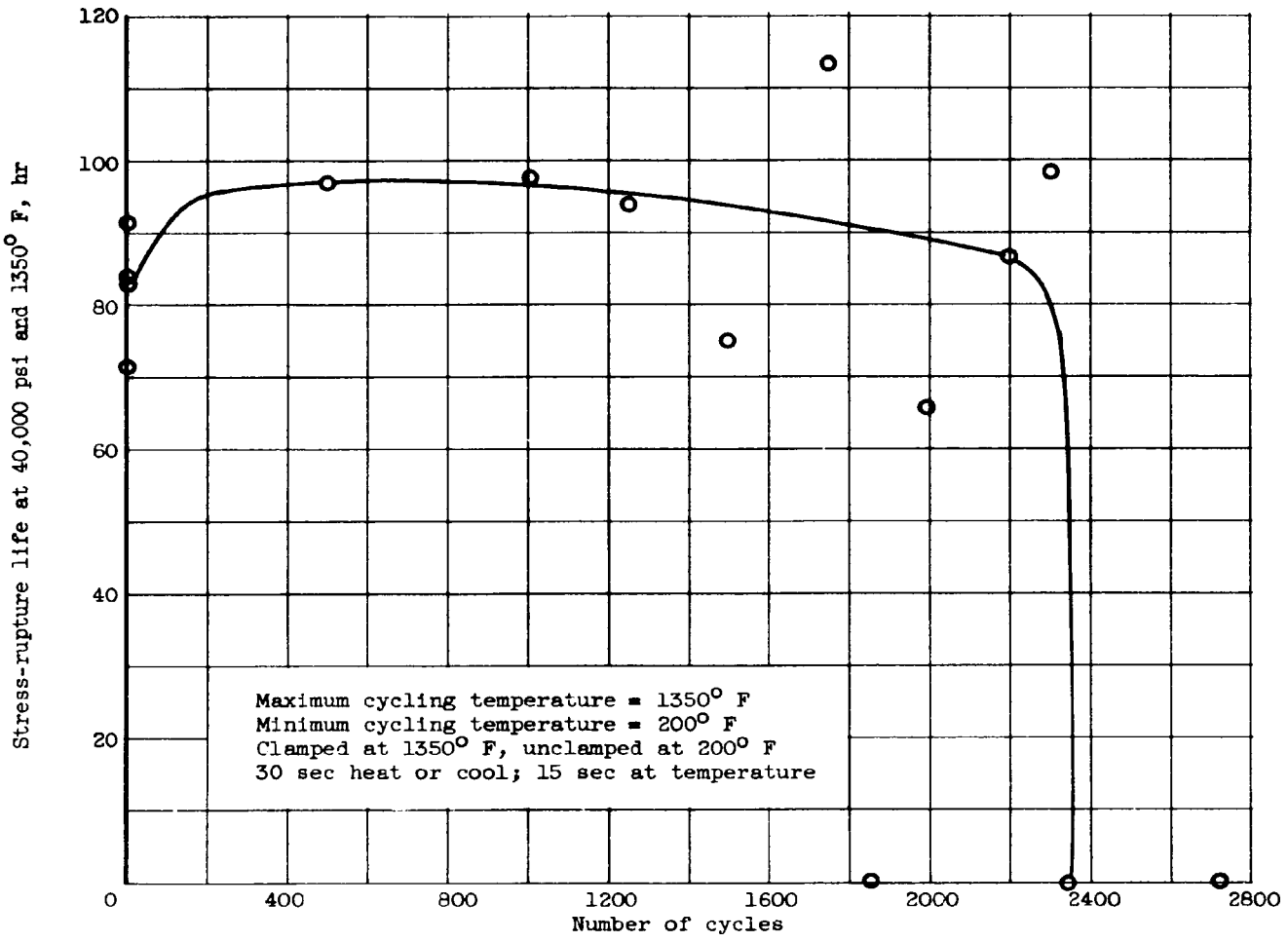


Fig. 21. - Effect of prior thermal cycling on the stress-rupture life of S-816 at 1350° F.

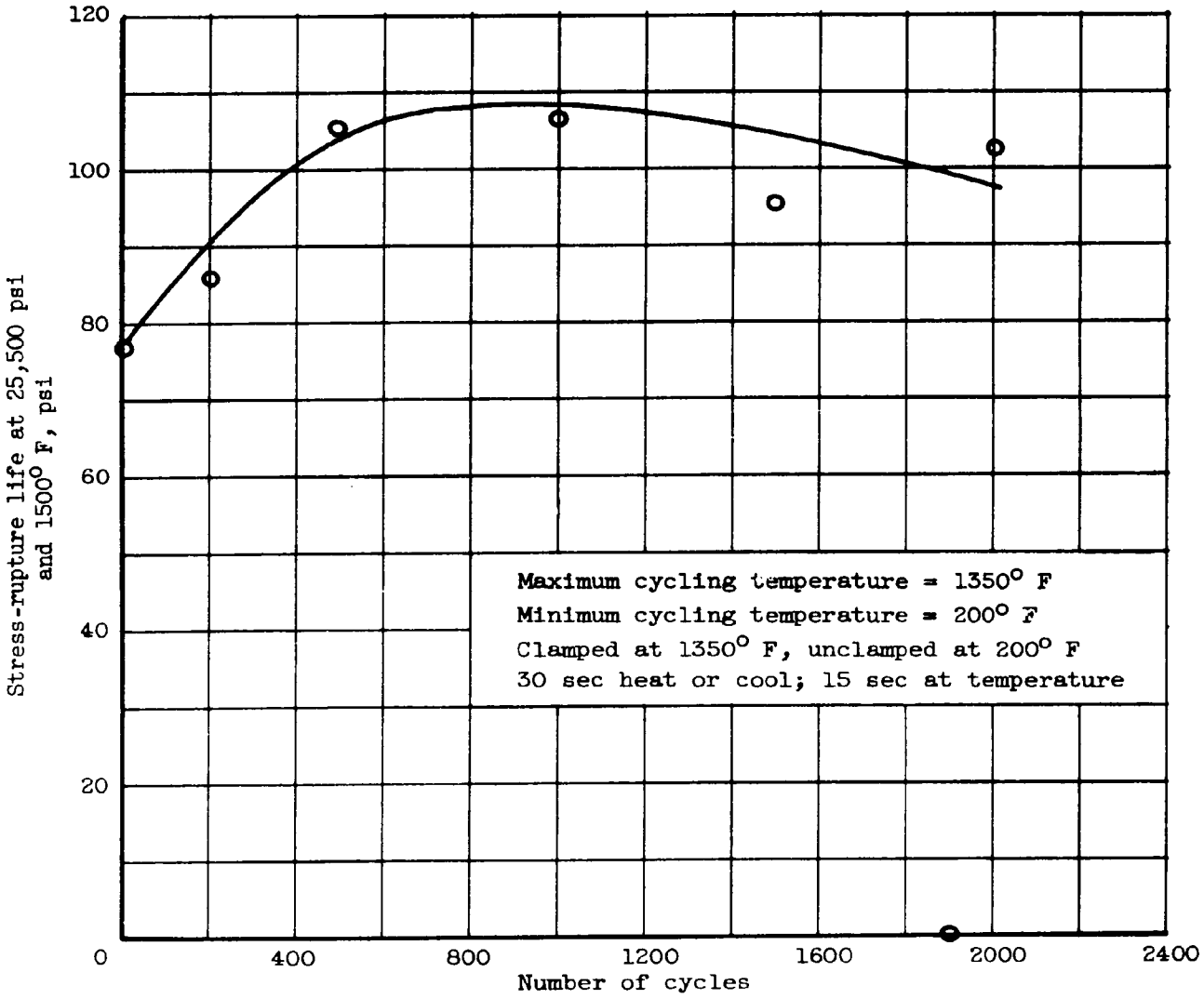


Fig. 22. - Effect of prior thermal cycling on the stress-rupture life of S-816 at 1500° F.

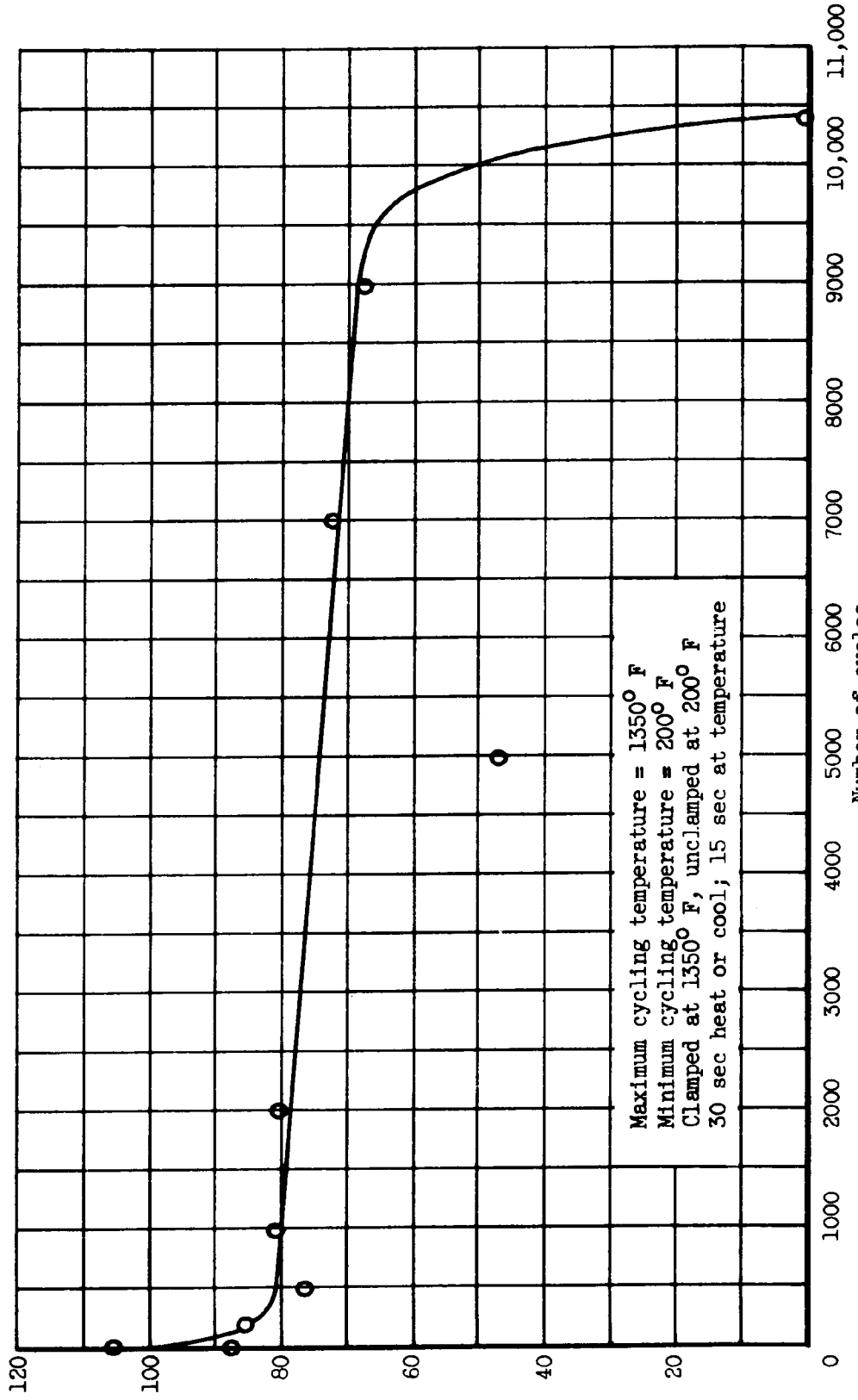


Fig. 23. - Effect of prior thermal cycling on the stress-rupture life of Inconel 550 at 1350° F.

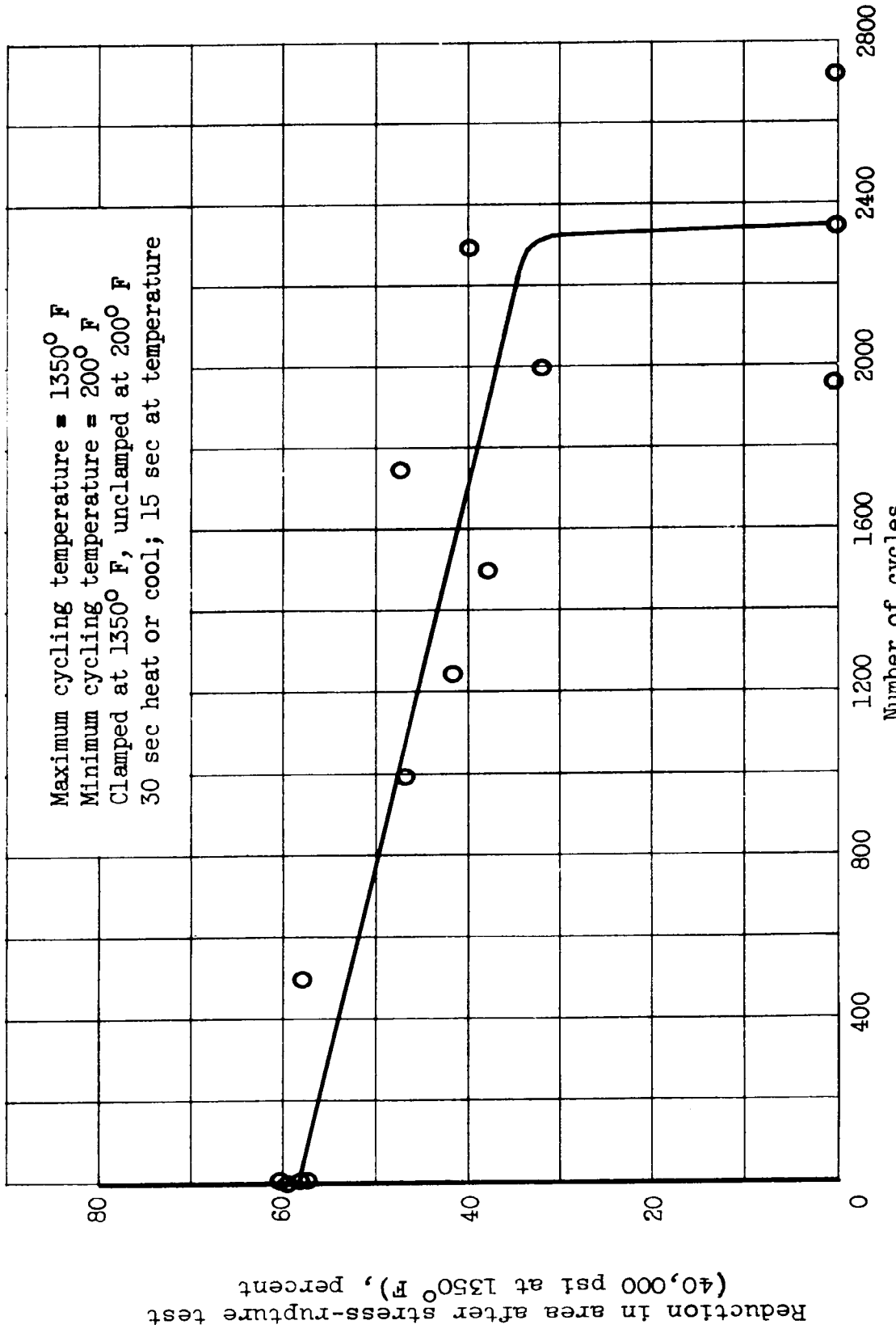


Fig. 24. - Effect of prior thermal cycling on the stress-rupture ductility of S-816 at 1350° F.

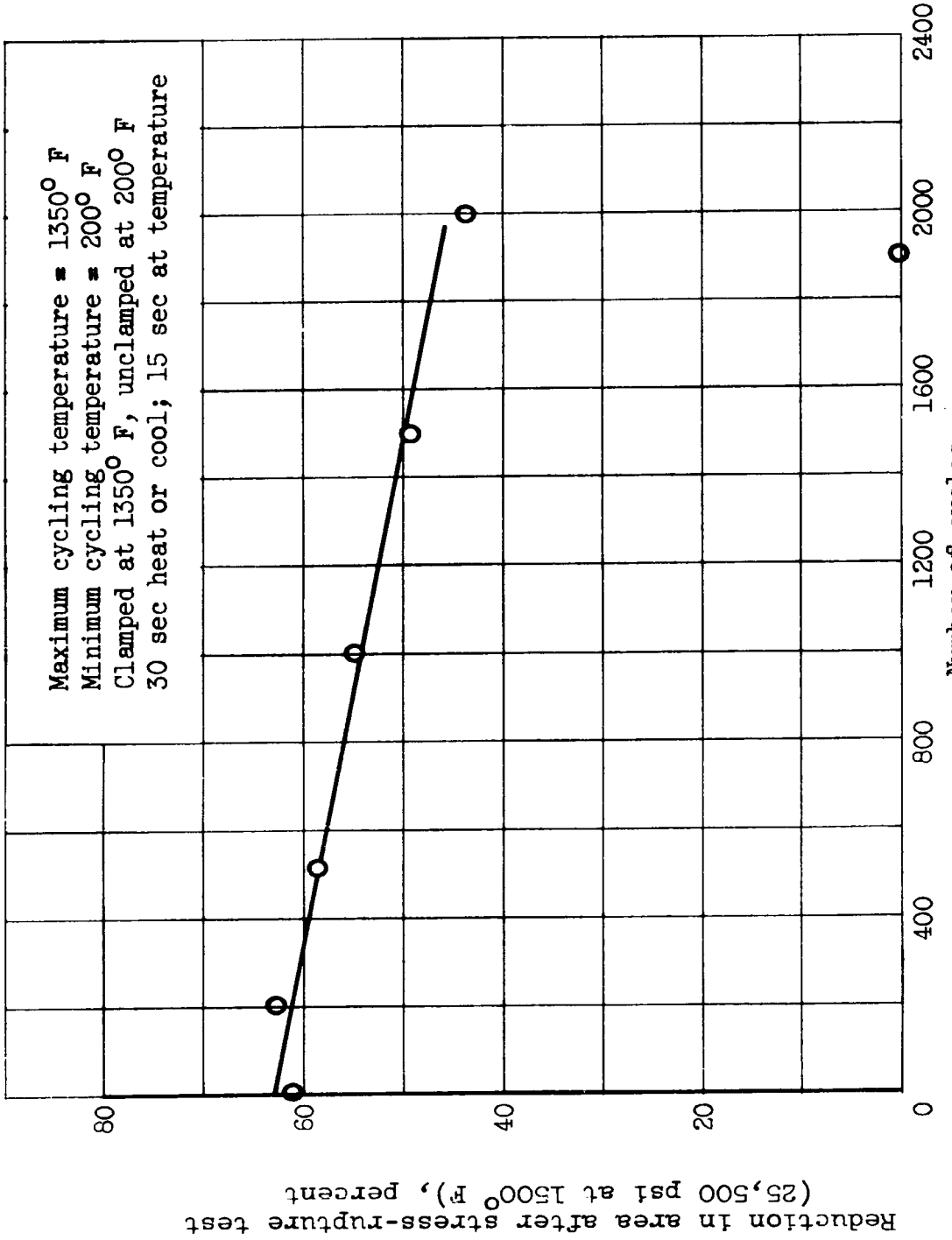


Fig. 25. - Effect of prior thermal cycling on the stress-rupture ductility of S-816 at 1500° F.

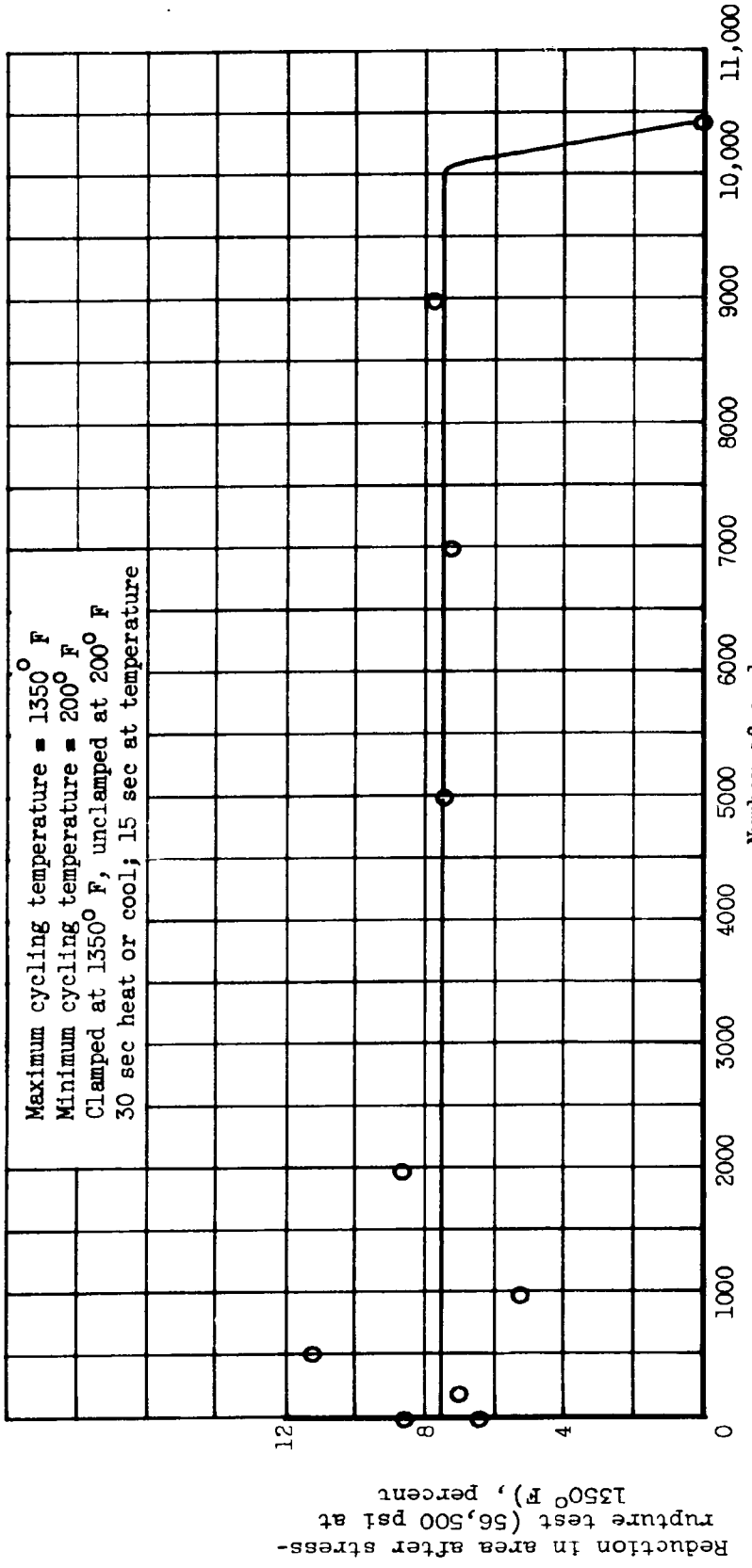


Fig. 26. - Effect of prior thermal cycling on the stress-rupture ductility of Inconel 550 at 1350° F.

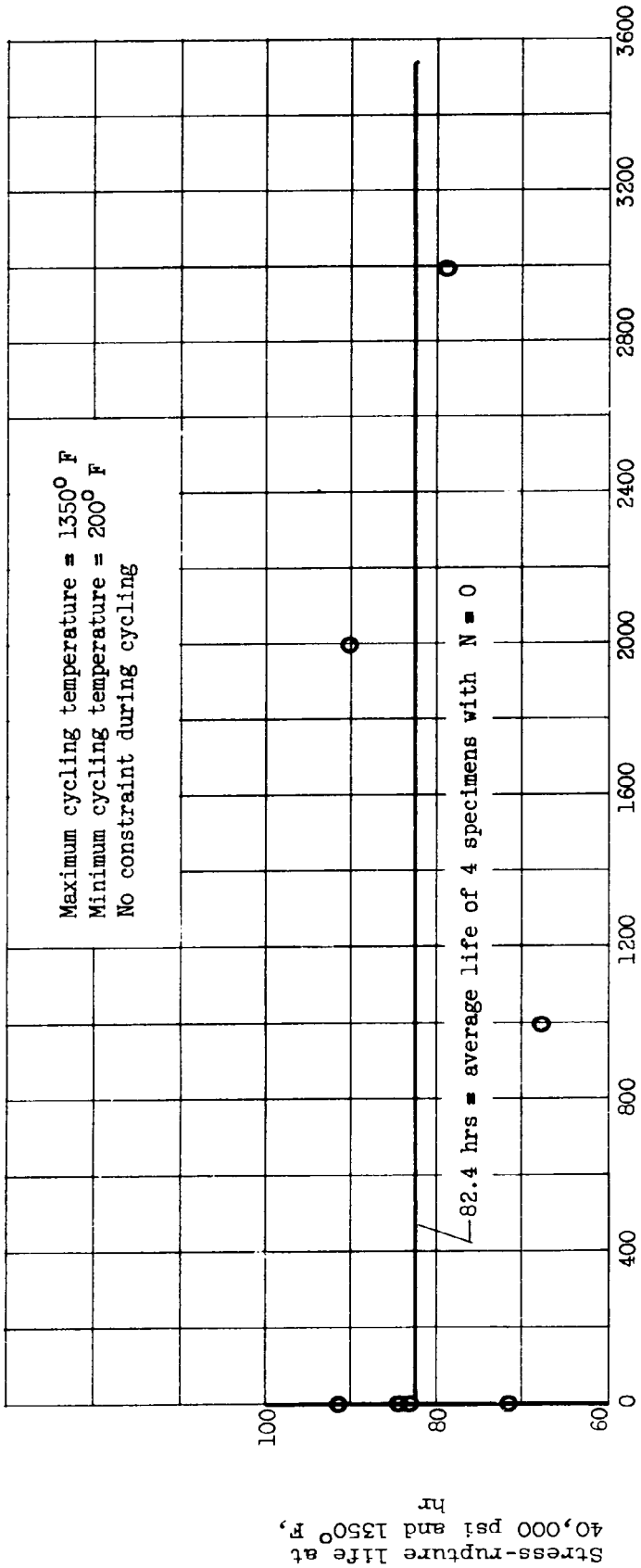


Fig. 27. - Effect of prior thermal cycling without constraint on the stress-rupture life of S-816 at 1350° F.

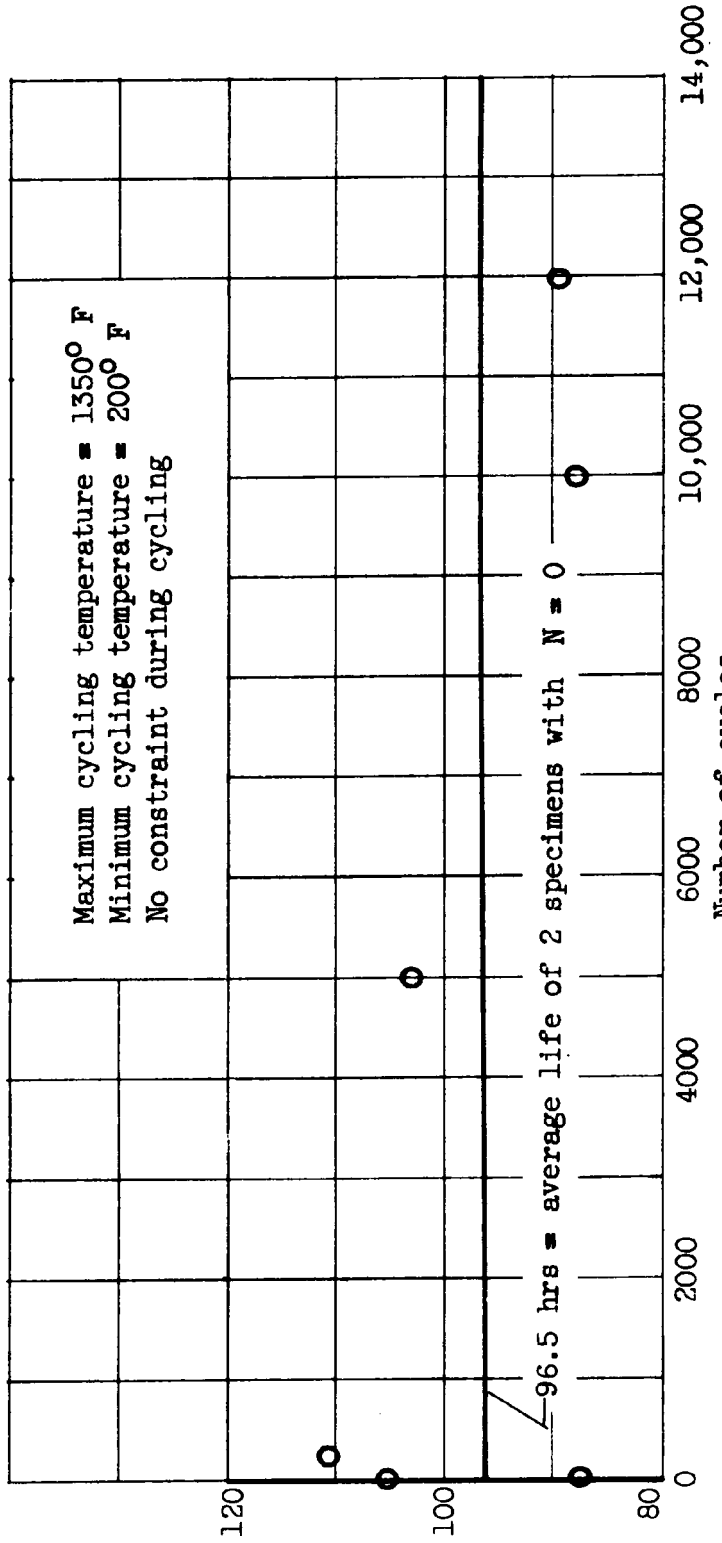


Fig. 28. - Effect of prior thermal cycling without constraint on the stress-rupture life of Inconel 550 at 1350° F.

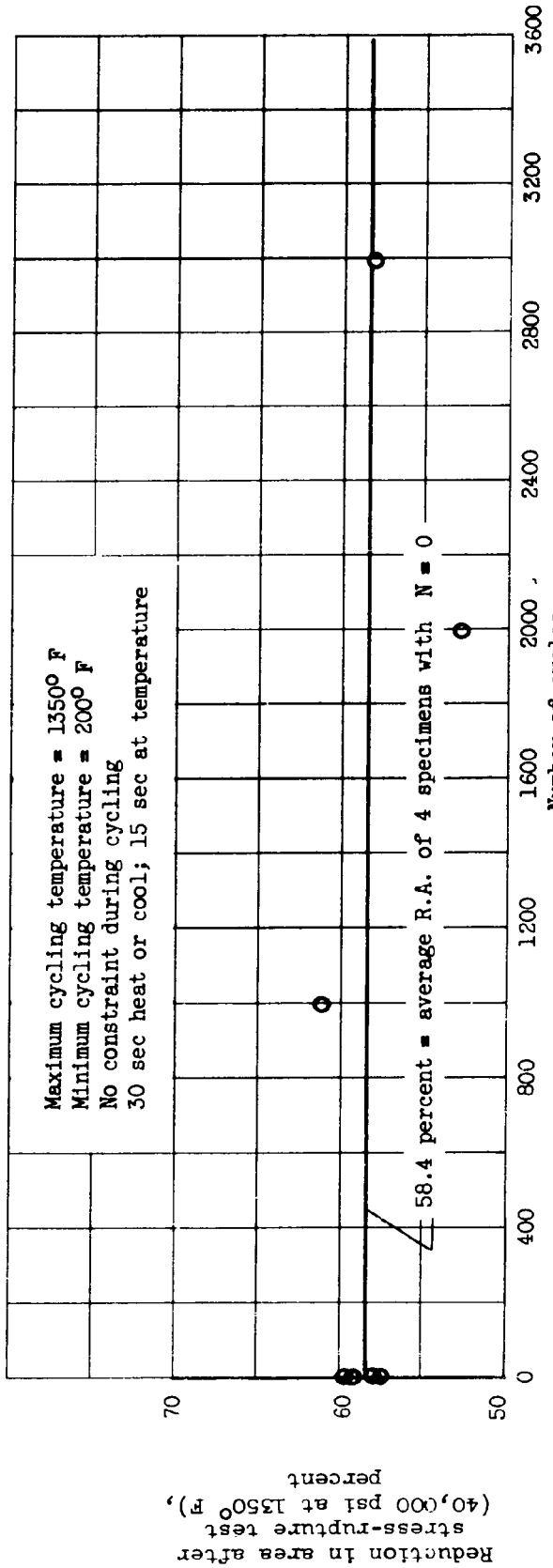


Fig. 29. - Effect of prior thermal cycling without constraint on the stress-rupture ductility of S-816 at 1350° F.

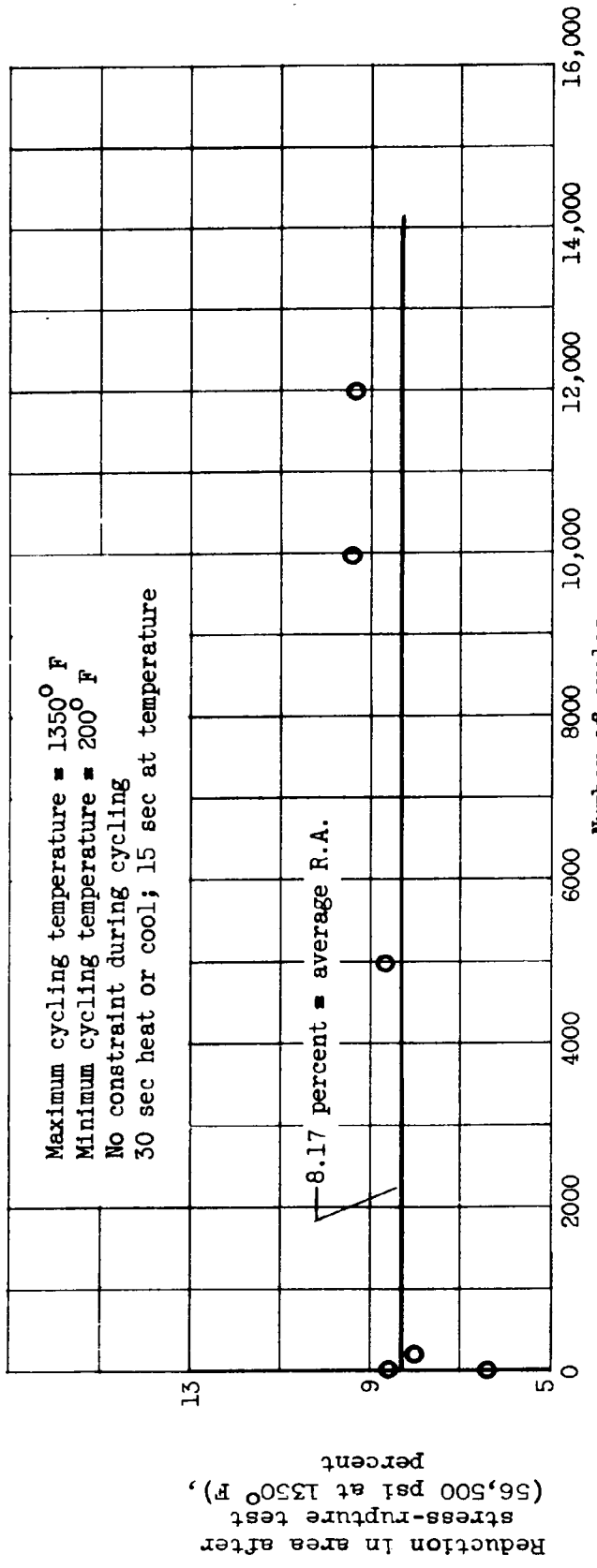


Fig. 30. - Effect of prior thermal cycling without constraint on the stress-rupture ductility of Inconel 550 at 1350° F.

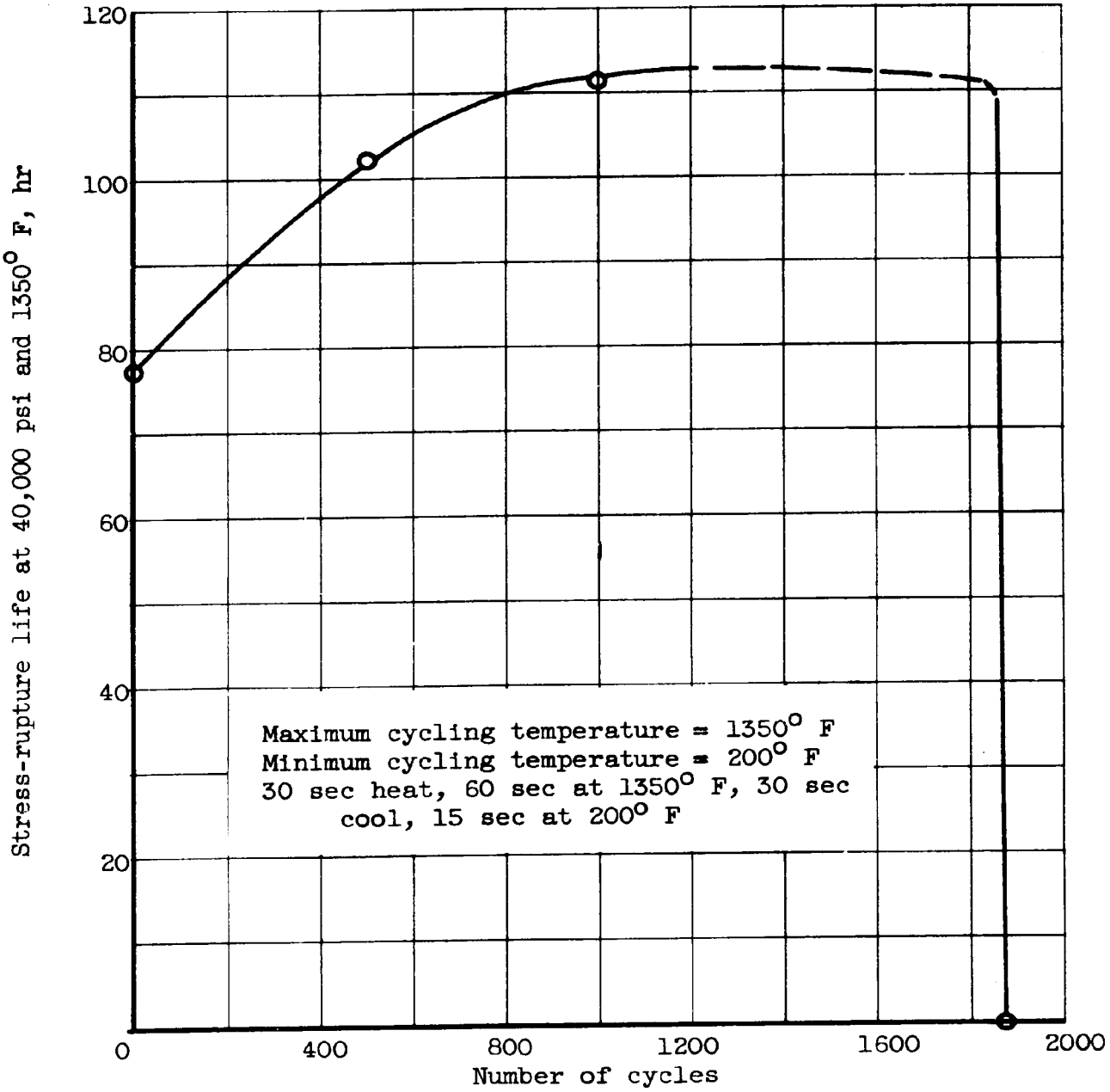


Fig. 31. - Effect of prior thermal cycling on the stress-rupture life of S-816 at 1350° F (60 seconds exposure at T_{max}).

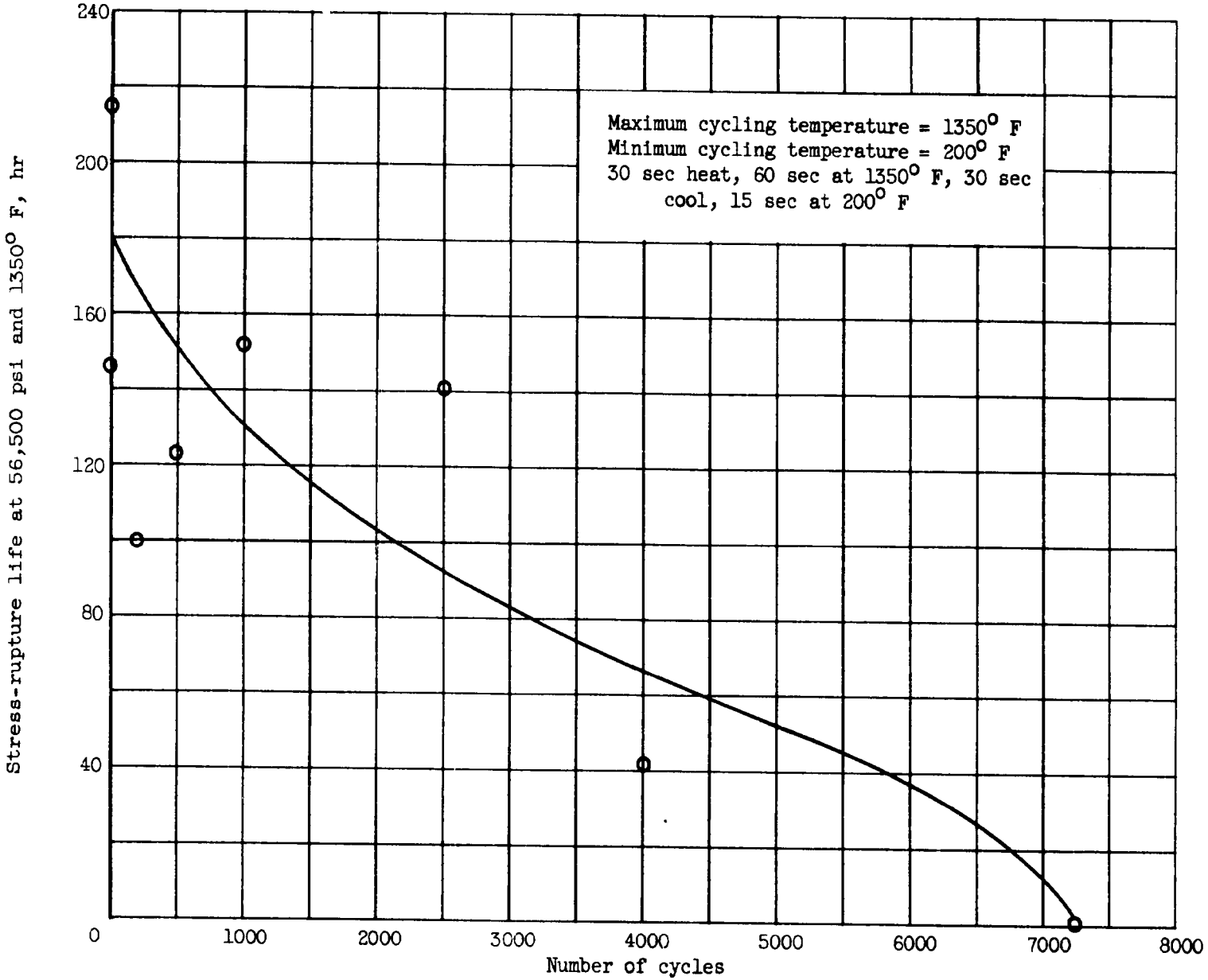


Fig. 32. - Effect of prior thermal cycling on the stress-rupture life of Inconel 550 at 1350° F (60 seconds exposure at T_{max}).

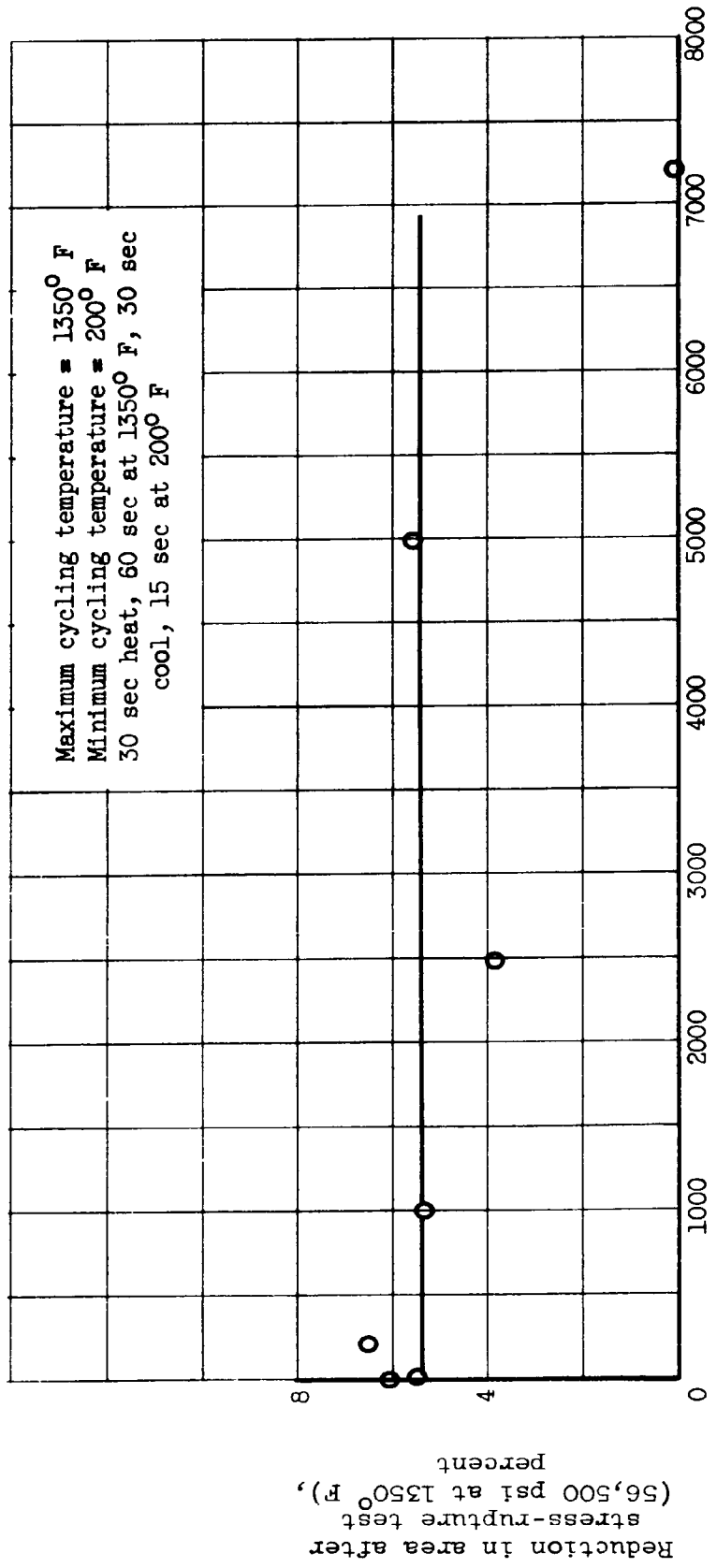


Fig. 33. - Effect of prior thermal cycling on the stress-rupture ductility of Inconel 550 at 1350° F (60 seconds exposure at T_{max}).

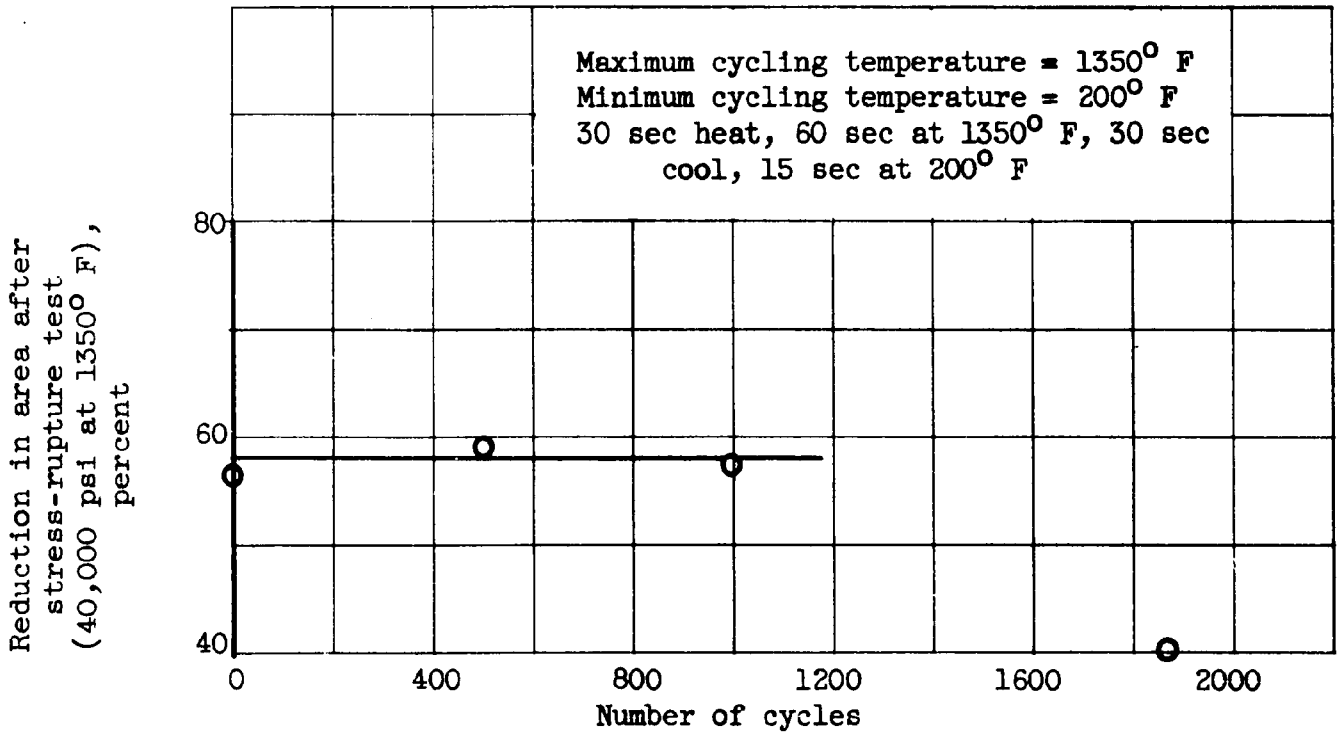


Fig. 34. - Effect of prior thermal cycling on the stress-rupture ductility of S-816 at 1350° F (60 seconds exposure at T_{max}).

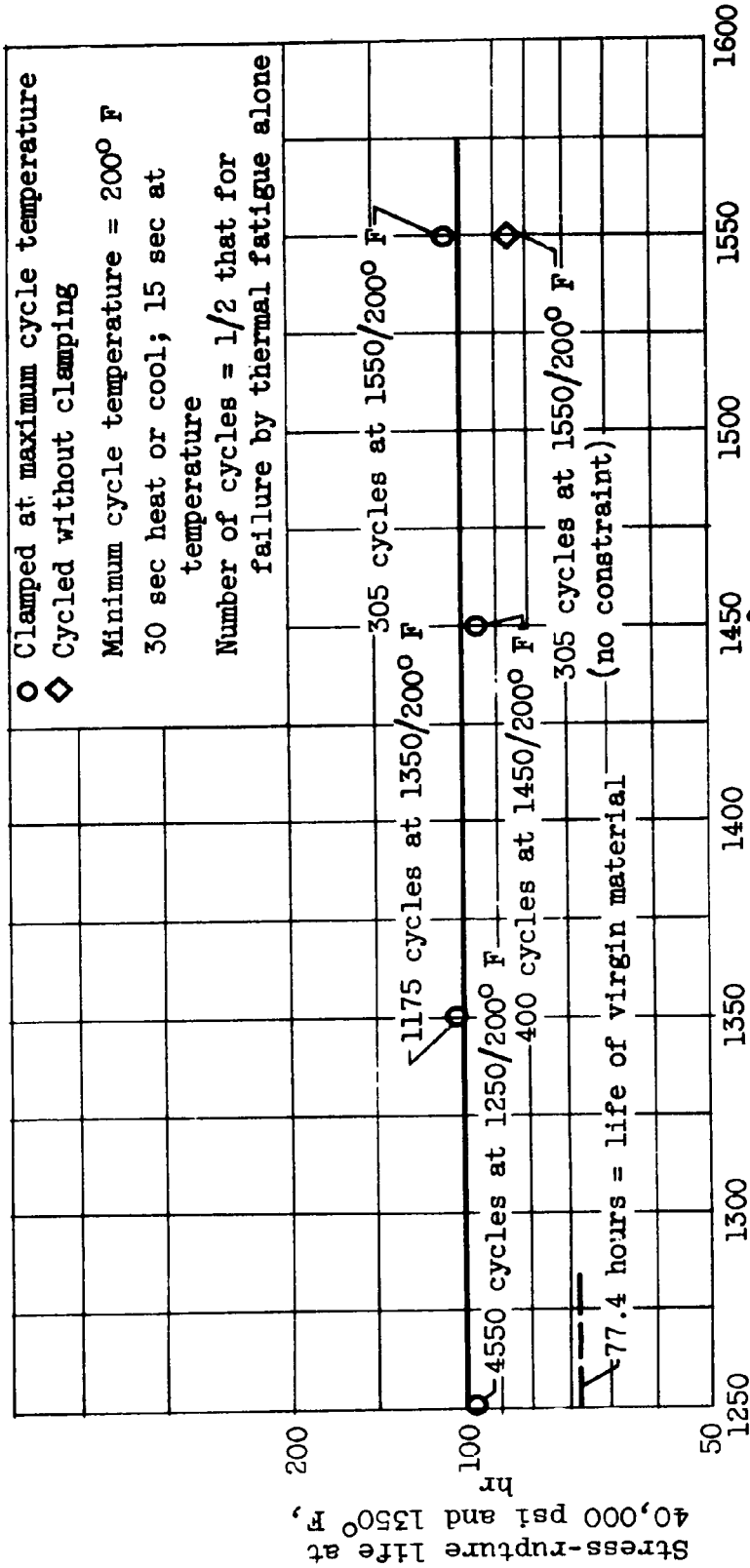


Fig. 35. - Effect of the T_{max} of thermal cycling on the stress-rupture life of S-816 at 1350° F ($N = \frac{1}{2} N_f$).

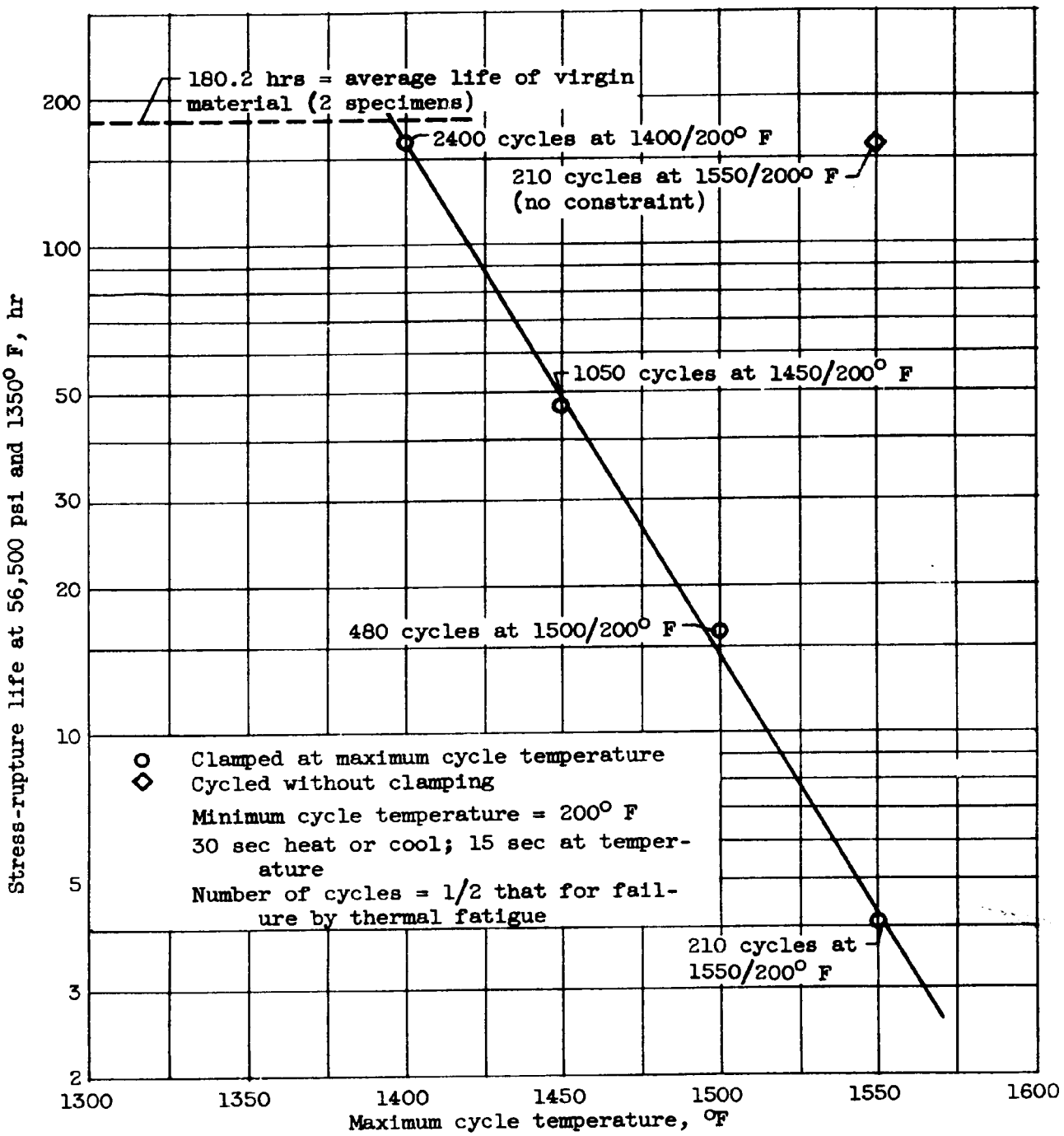


Fig. 36. - Effect of the T_{max} of thermal cycling on the stress-rupture life of Inconel 550 at 1350° F ($N = \frac{1}{2} N_f$).

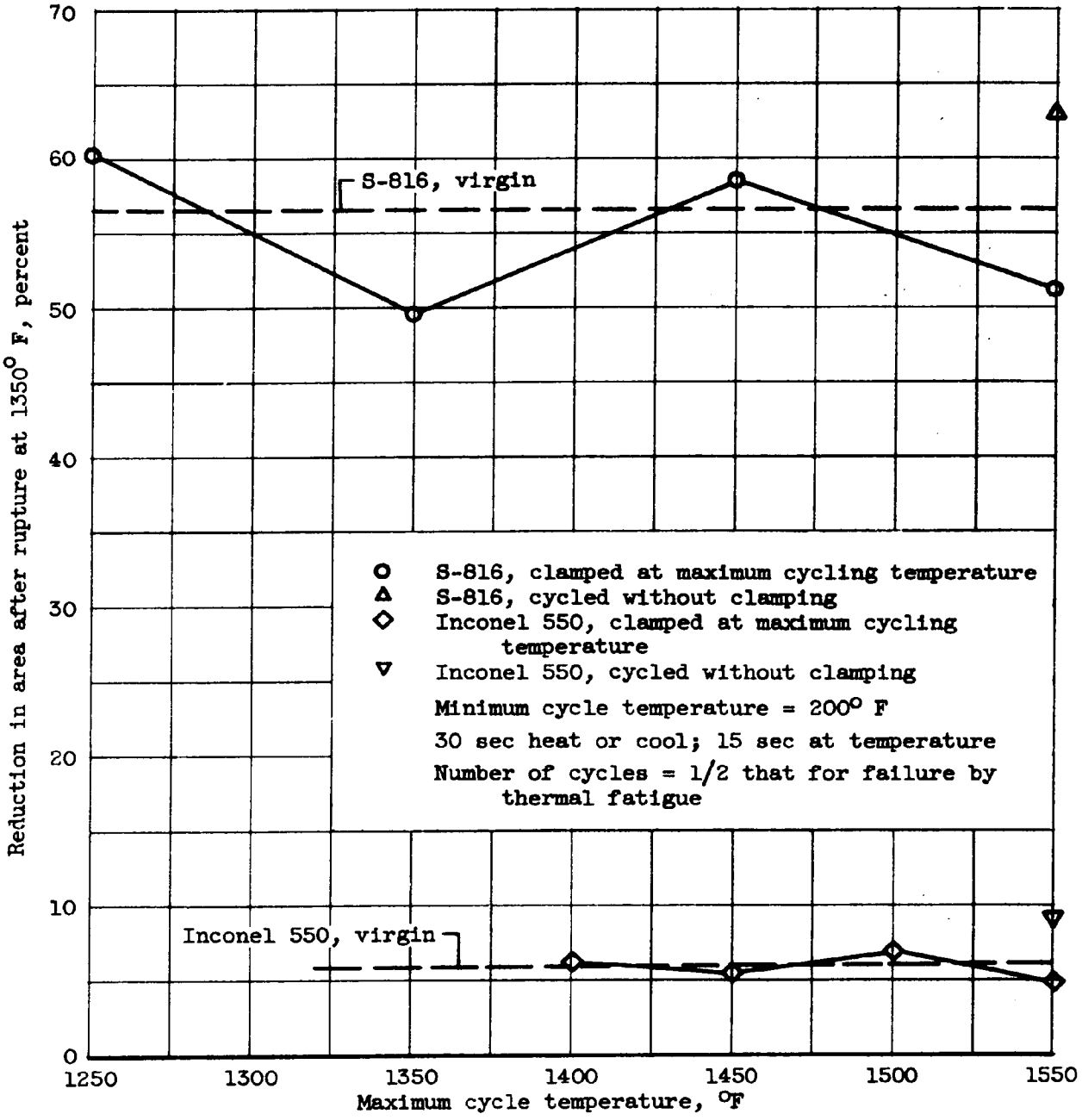


Fig. 37. - Effect of the T_{max} of thermal cycling on the stress-rupture ductility of S-816 and Inconel 550 at 1350° F ($N = \frac{1}{2} N_f$).

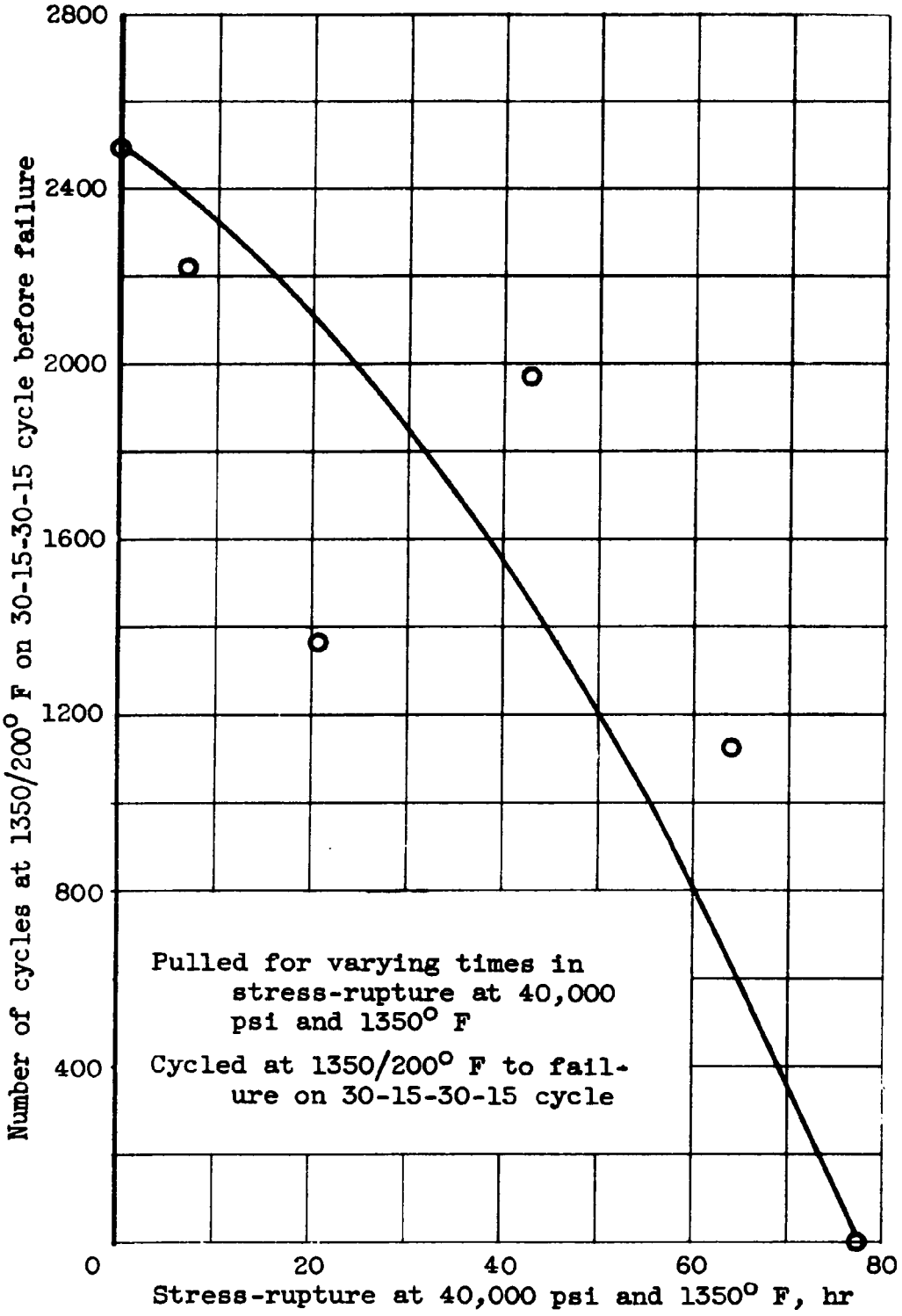


Fig. 38. - Effect of exposure to stress-rupture conditions on the thermal fatigue life of S-816.

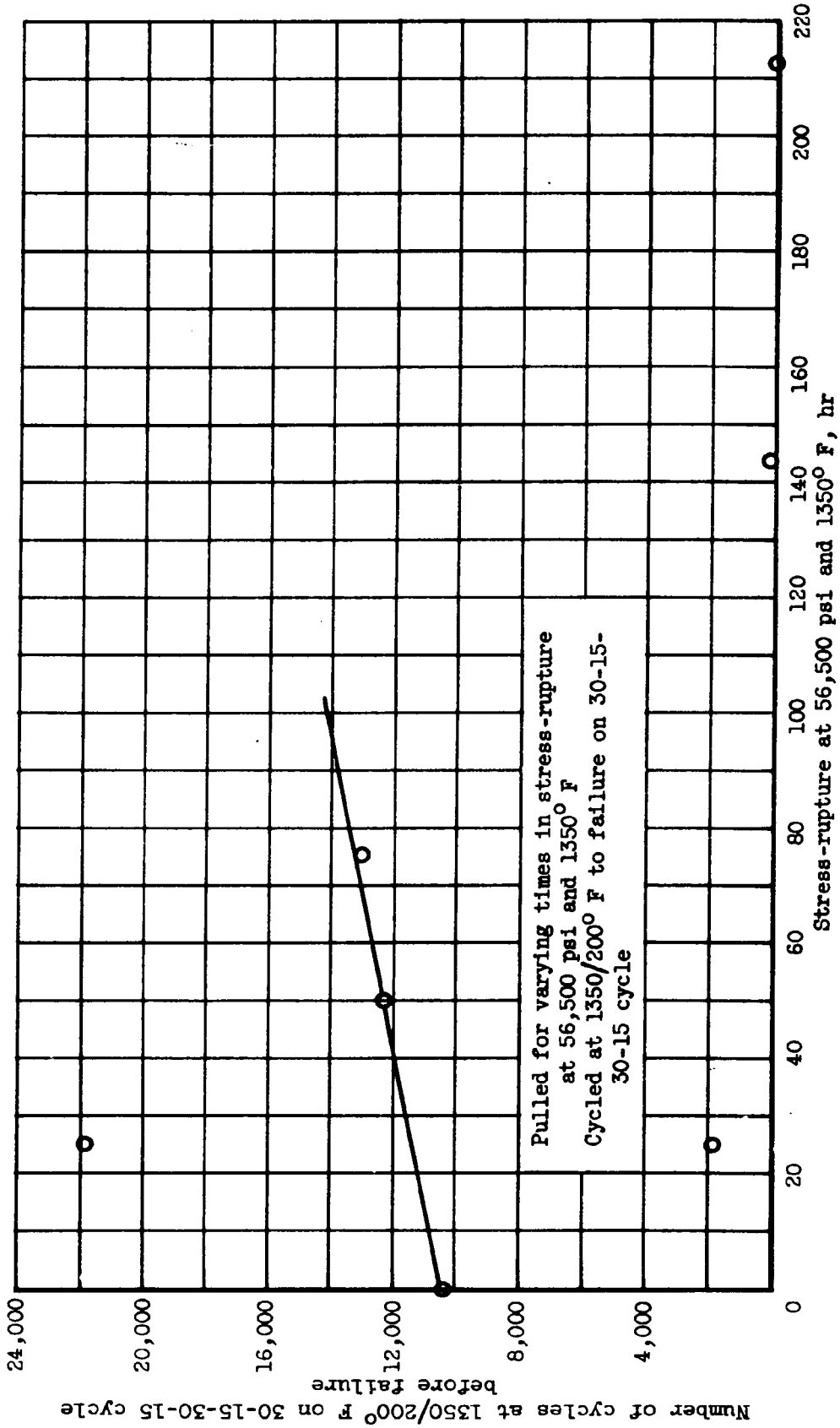


Fig. 39. - Effect of exposure to stress-rupture conditions on the thermal fatigue life of Inconel 550.

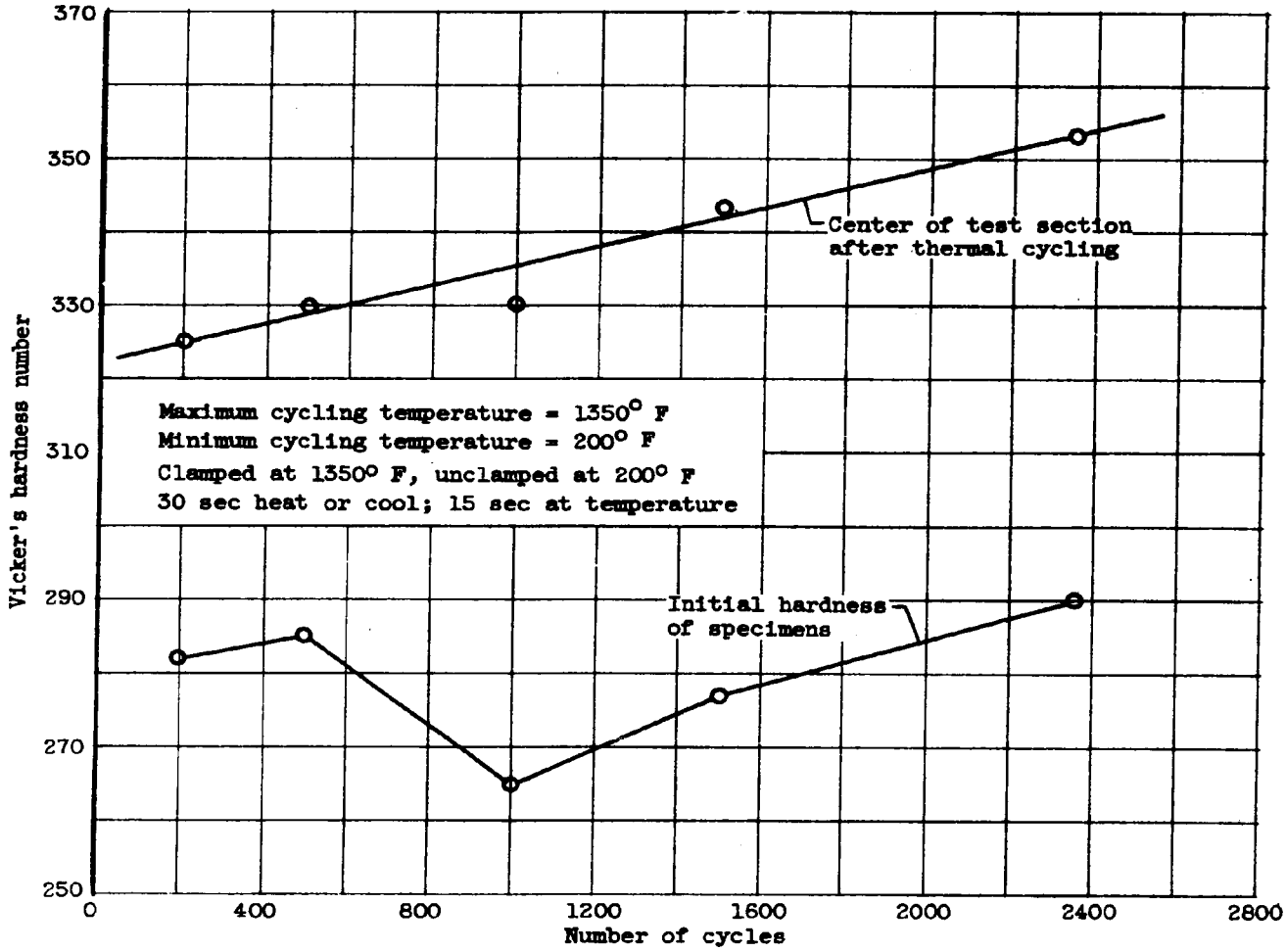


Fig. 40. - Effect of thermal cycling on the hardness of S-816.

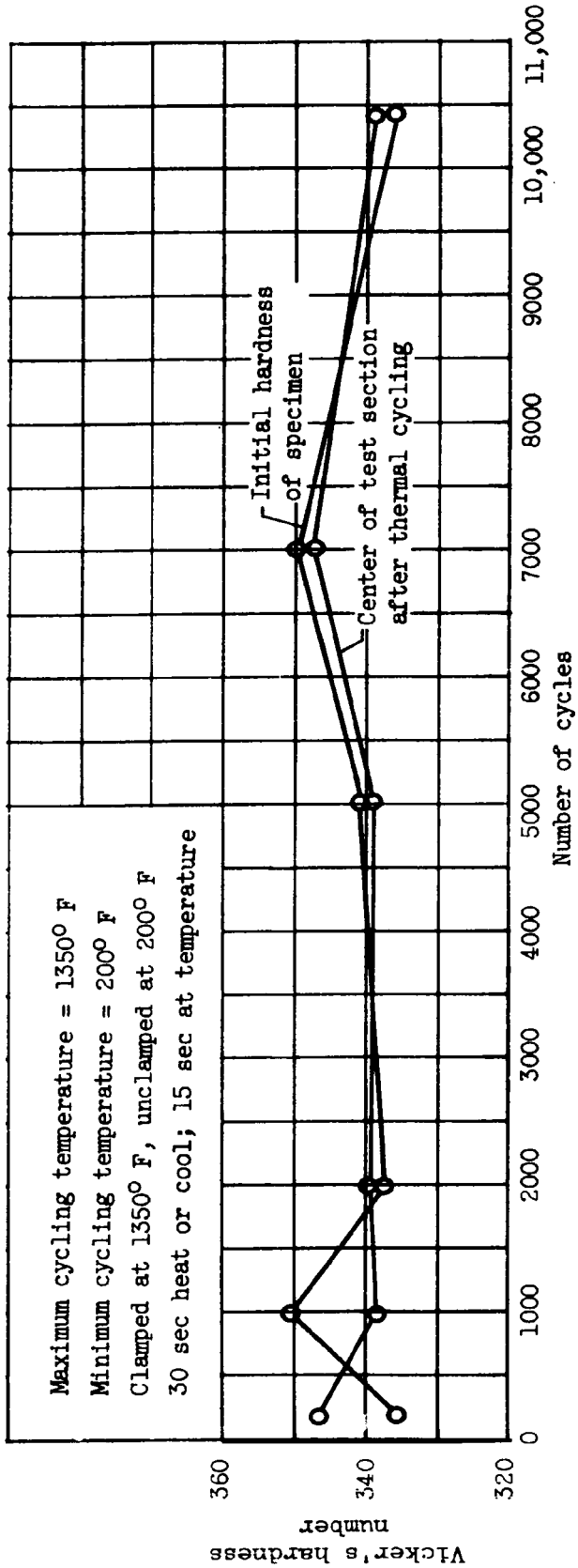
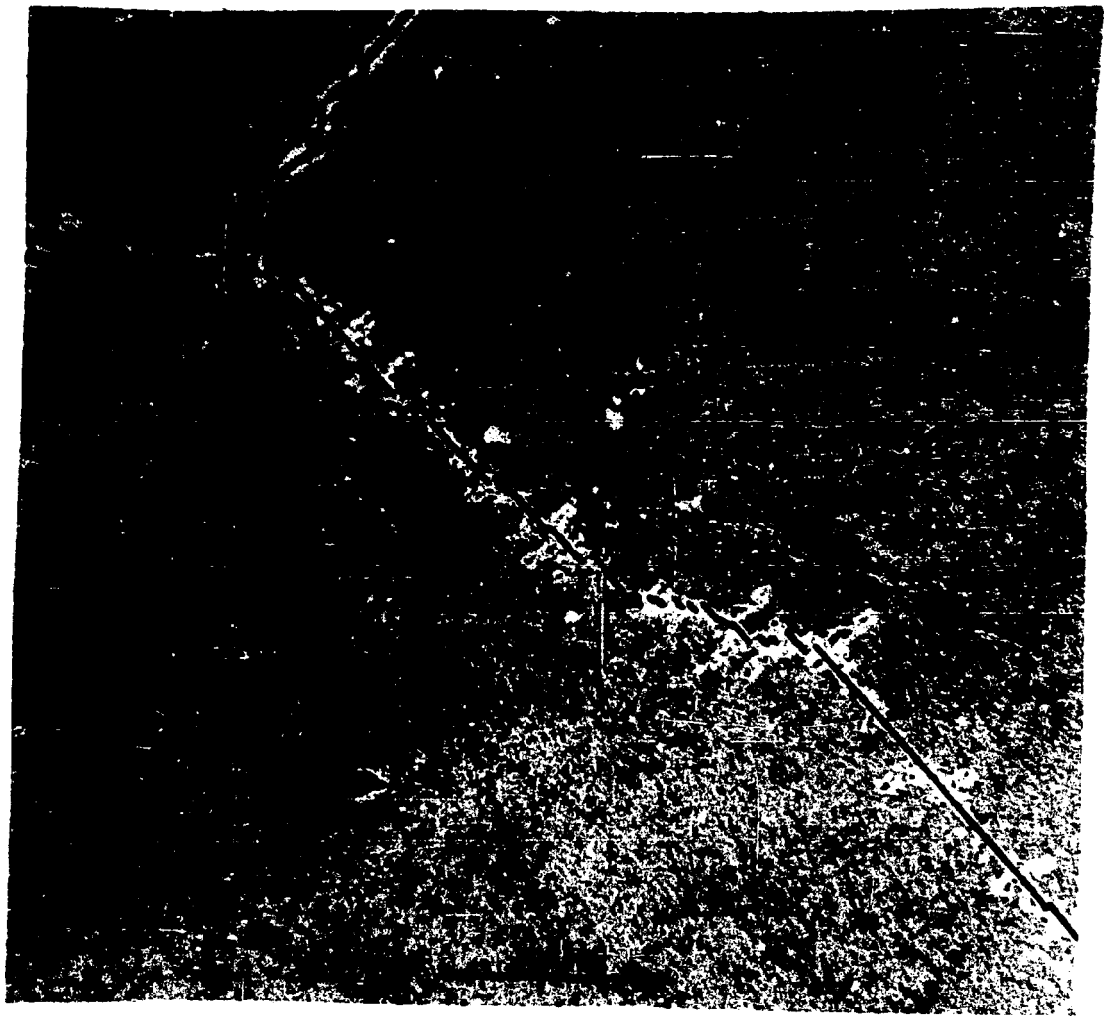
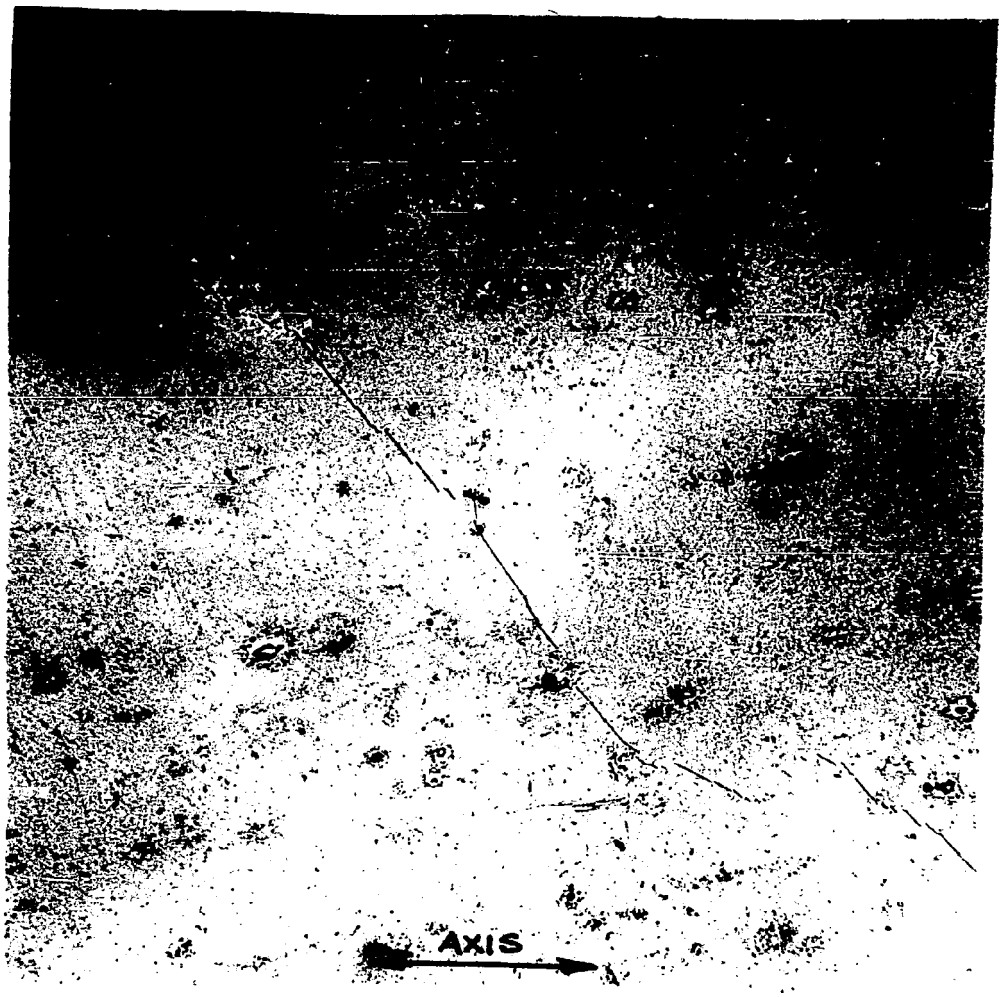


Fig. 41. - Effect of thermal cycling on the hardness of Inconel 550.



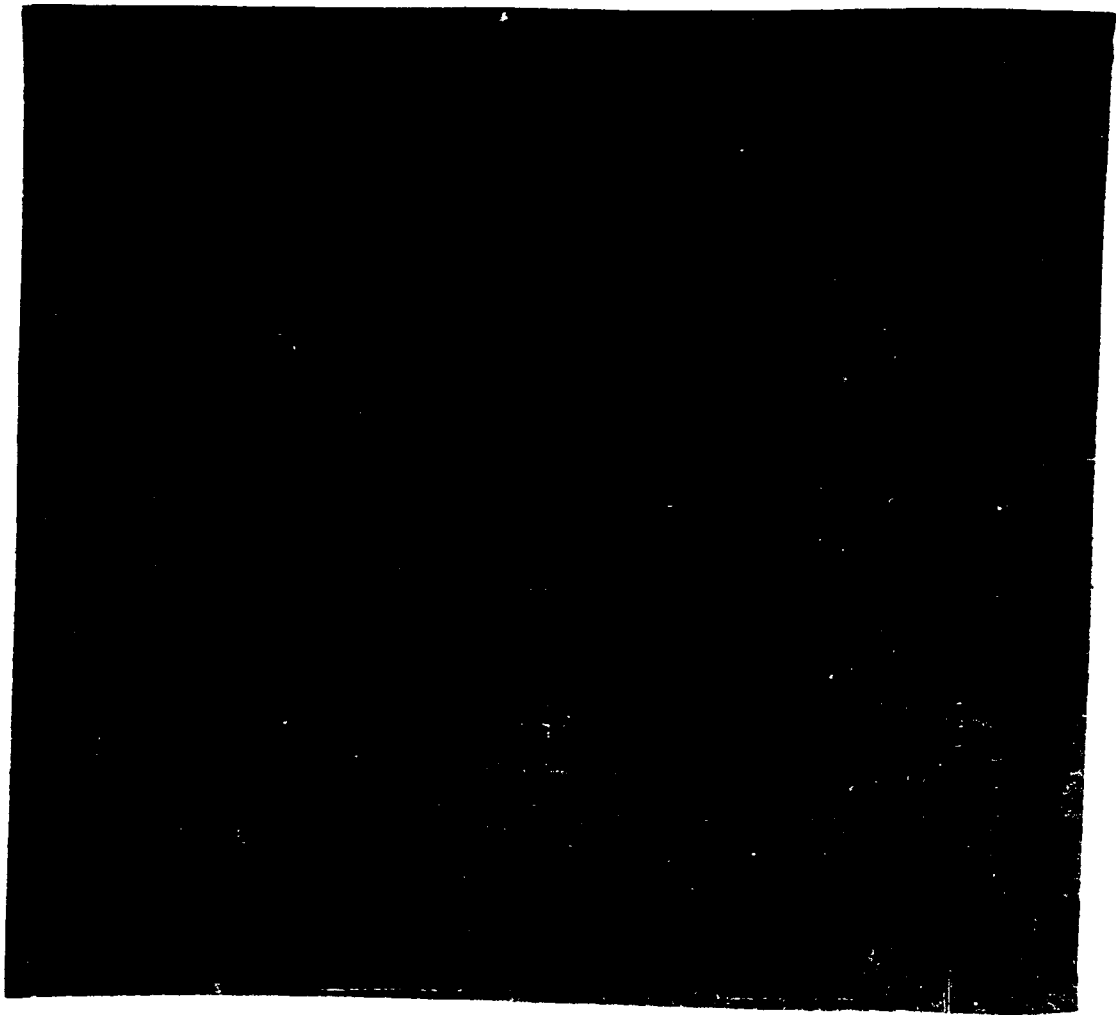
Magnification: 750X
Electrolytically etched in a dilute solution of hydrofluoric acid and glycerol in water

Fig. 42. - Microstructure of Inconel 550 after 1000 cycles at 1350/200°F.



Magnification: 220X
Electrolytically etched in a dilute solution of hydrofluoric acid and glycerol in water

Fig. 43. - Microstructure of Inconel 550 after 1000 cycles at 1350/200°F.



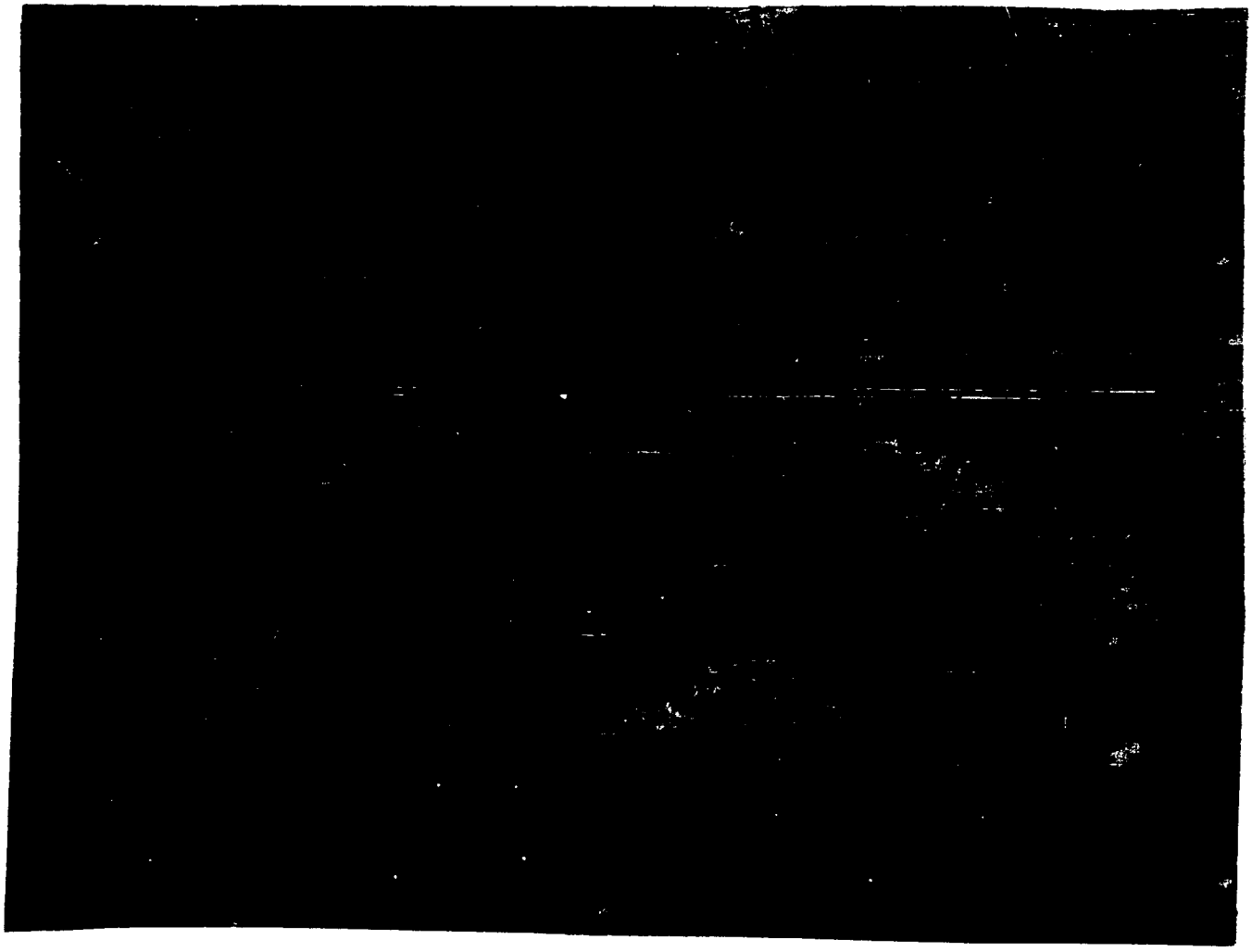
Magnification: 750X
Electrolytically etched in a dilute solution of hydrofluoric acid and glycerol in water

Fig. 44. - Microstructure of Inconel 550 after 7000 cycles at 1350/200°F.



Magnification: 250X
Electrolytically etched in a dilute solution of hydrofluoric acid and glycerol in water

Fig. 45. - Microstructure of Inconel 550 after 2000 cycles at 1350/200°F.



Magnification: 750X
Electrolytically etched in a dilute solution of hydrofluoric acid and glycerol in water

Fig. 46. - Microstructure of Inconel 550 after 7000 cycles at 1350/200°F.



Magnification: 500X
Electrolytically etched in a dilute solution of hydrofluoric acid and glycerol in water

Fig. 47. - Microstructure of Inconel 550 after 7000 cycles at 1350/200°F.

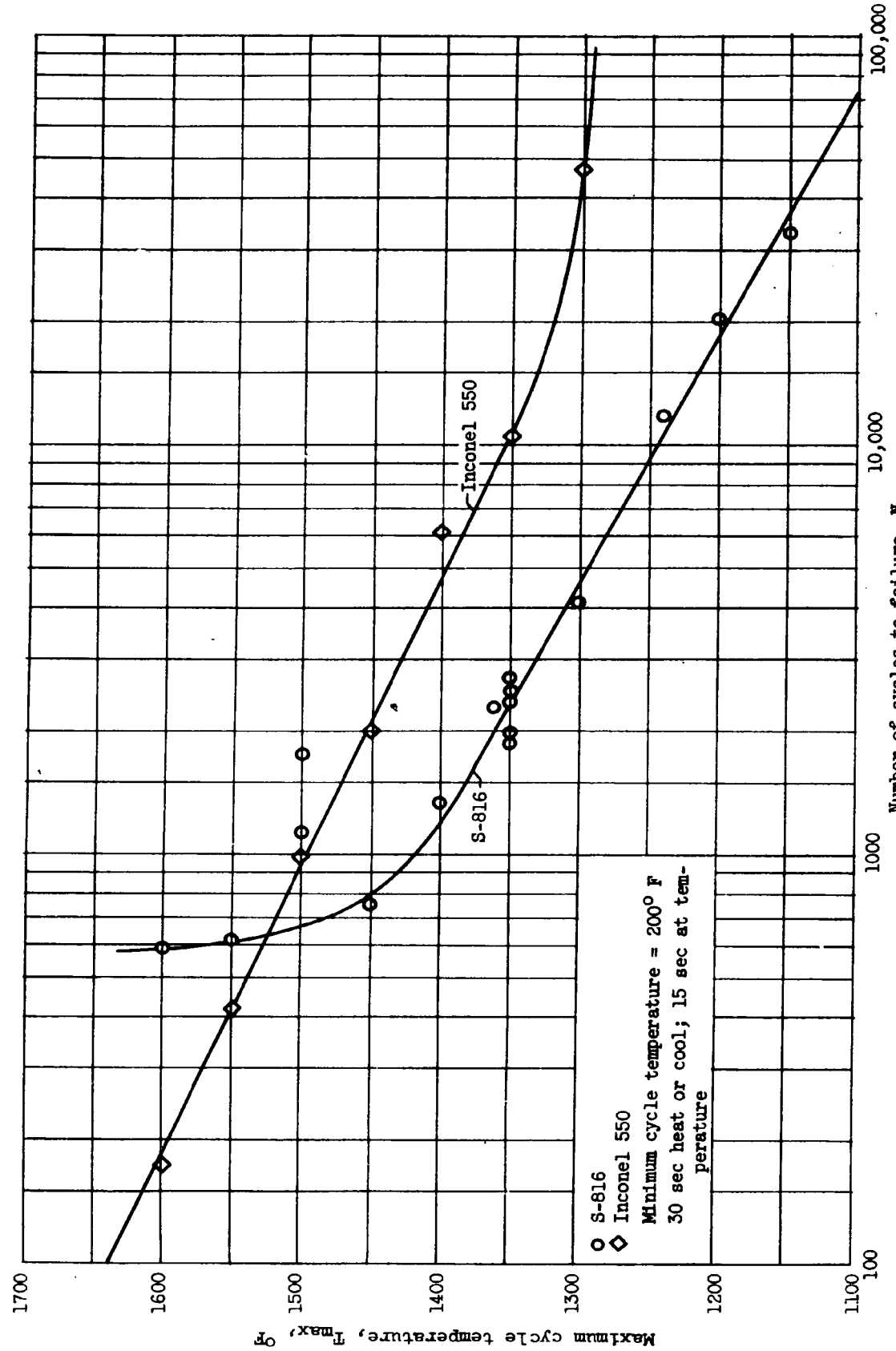


Fig. 48. - Effect of T_{max} on N_f for S-816 and Inconel 550 specimens thermally cycled at a constant T_{min}.

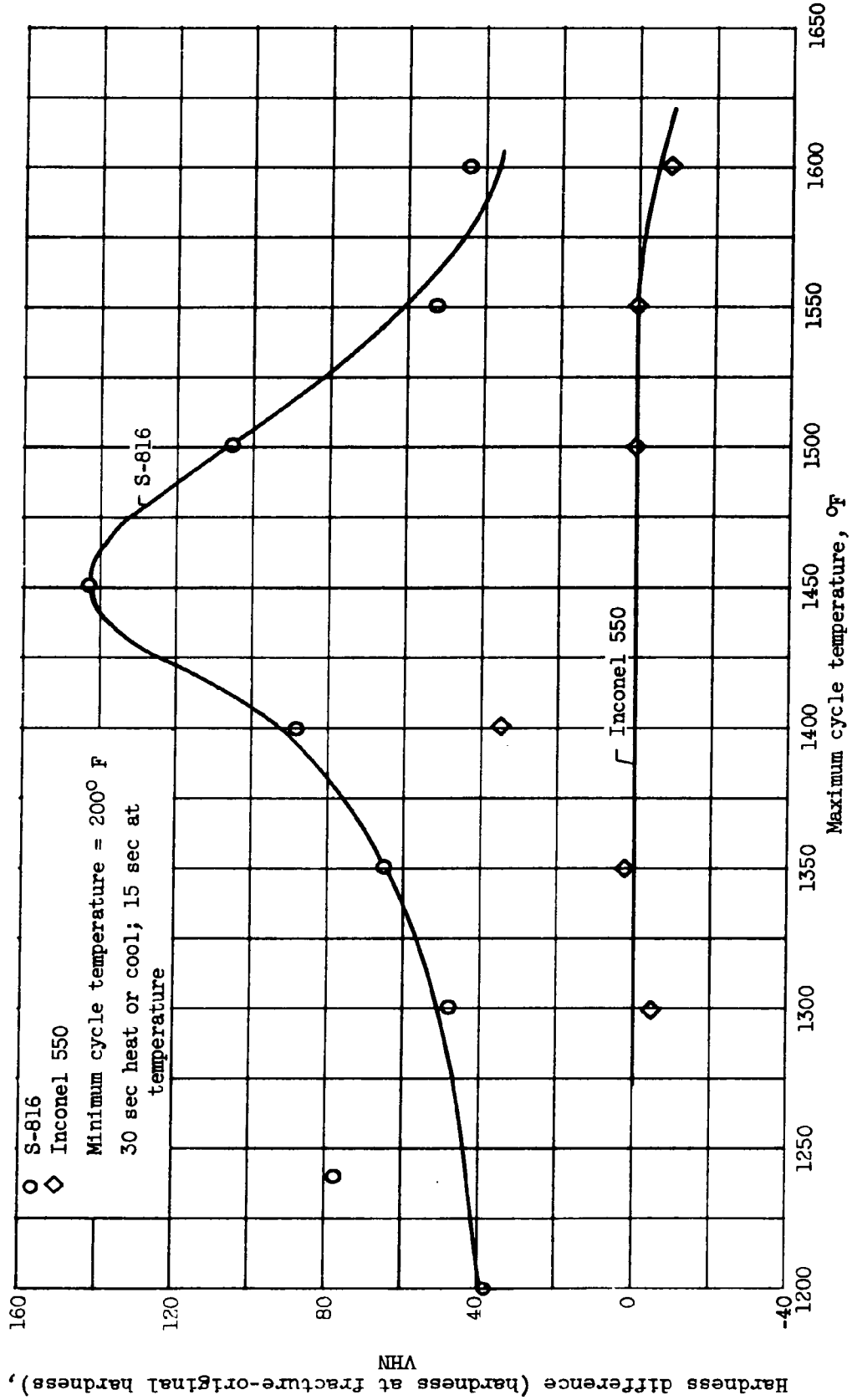
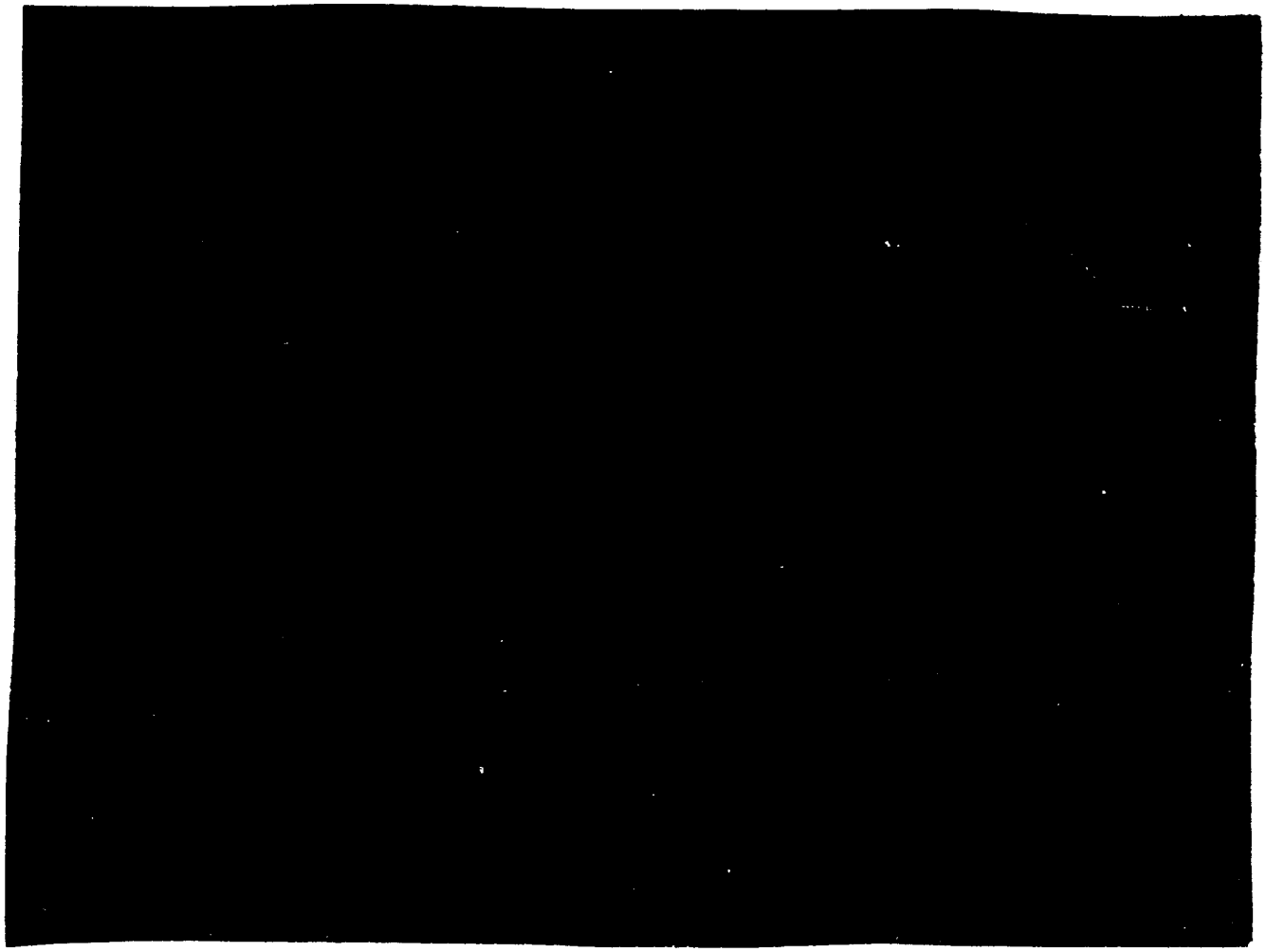


Fig. 49. - Effect of T_{max} on the amount of hardness change of S-816 and Inconel 550 specimens that had been fractured as a result of thermal fatigue.



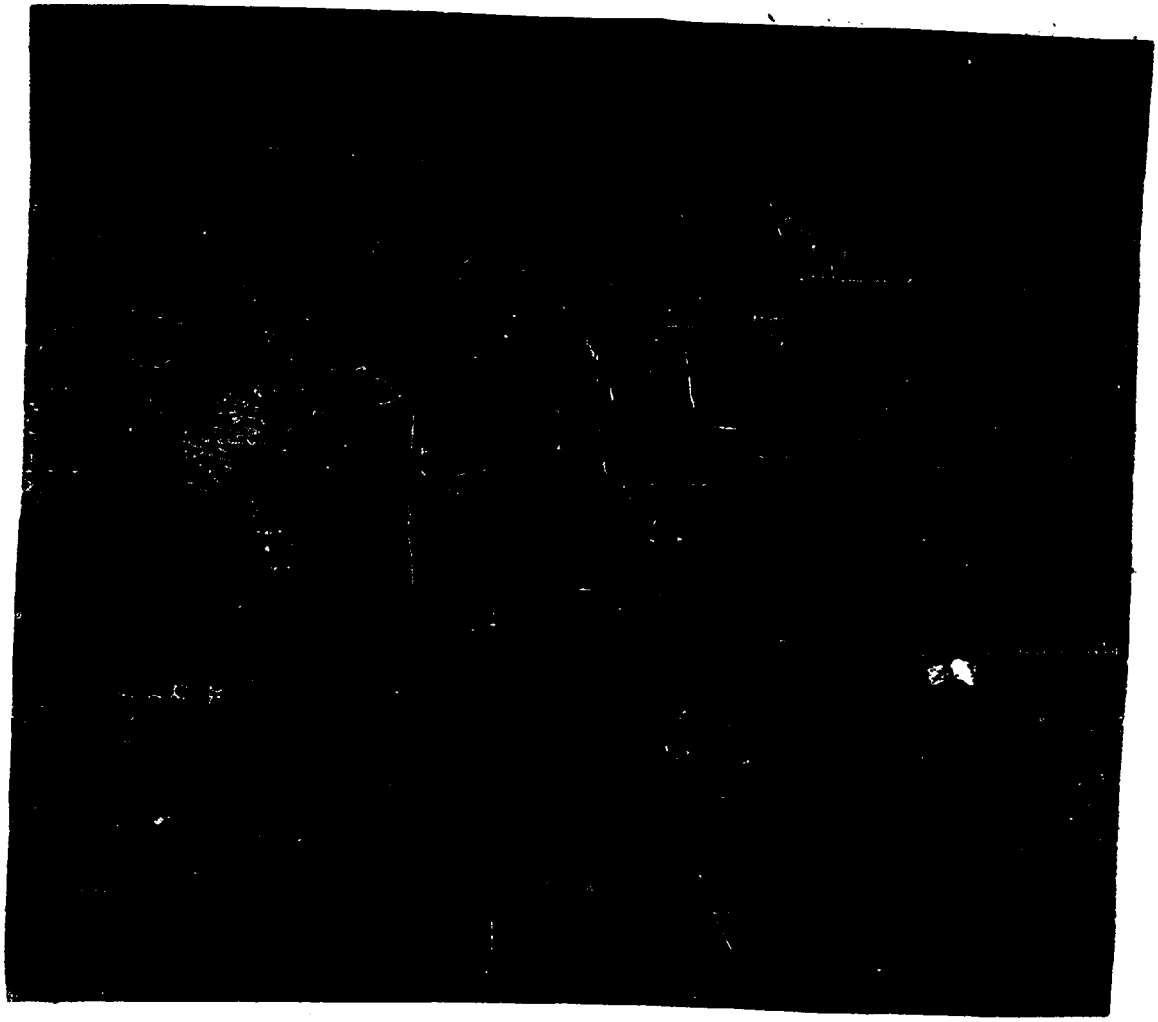
Magnification: 100X
Electrolytically etched in a dilute solution of hydrofluoric acid and glycerol in water

Fig. 50. - Microstructure of Inconel 550 specimen that had been fractured by thermal fatigue at 1600/200°F.



Magnification: 750X
Electrolytically etched in a dilute solution of hydrofluoric acid and glycerol in water

Fig. 51. - Microstructure of Inconel 550 specimen that had been fractured by thermal fatigue at 1600/200°F.



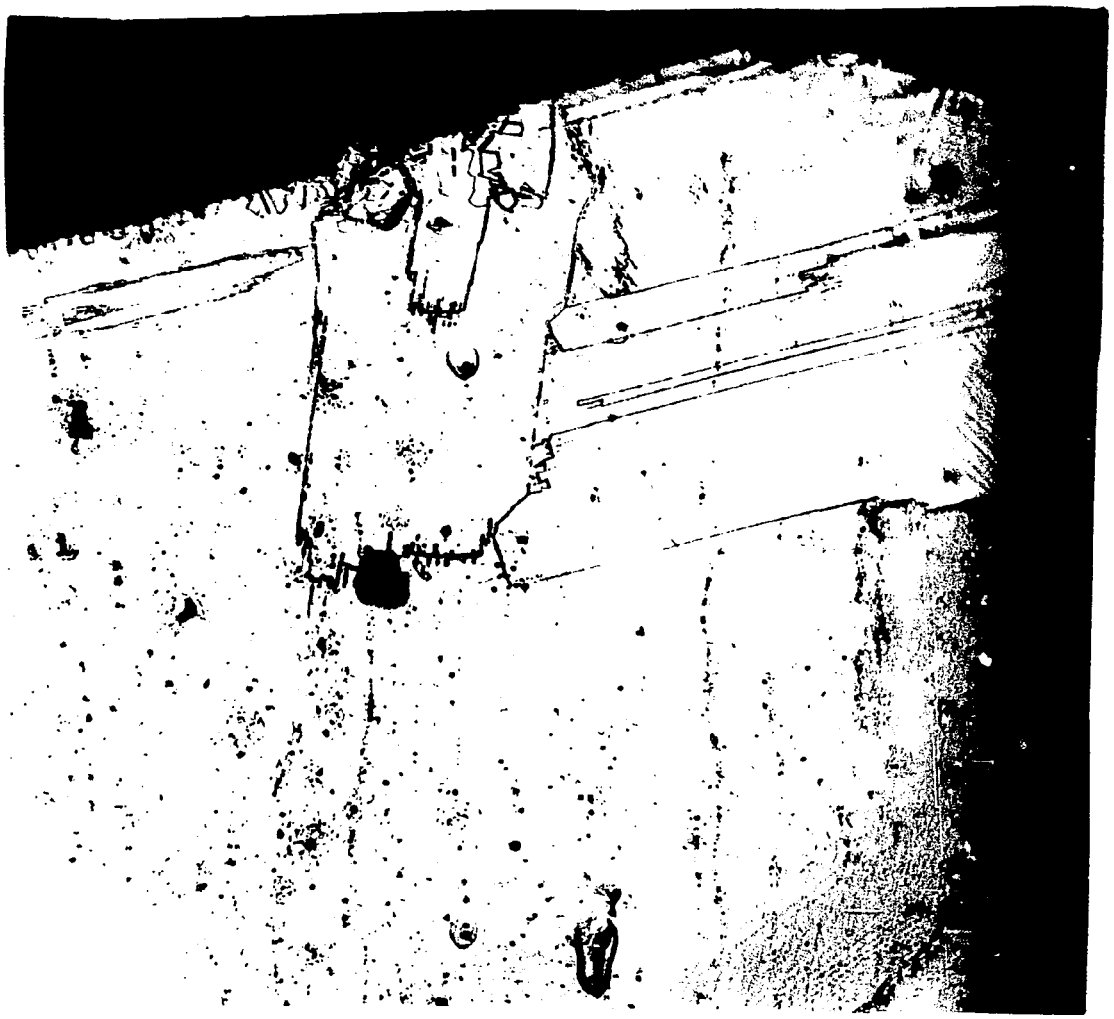
Magnification: 250X
Electrolytically etched in a solution of sulfuric acid and aqua regia in Marble's Reagent

Fig. 52. - Microstructure of Inconel 550 specimen that had been fractured by thermal fatigue at 1600/200°F.



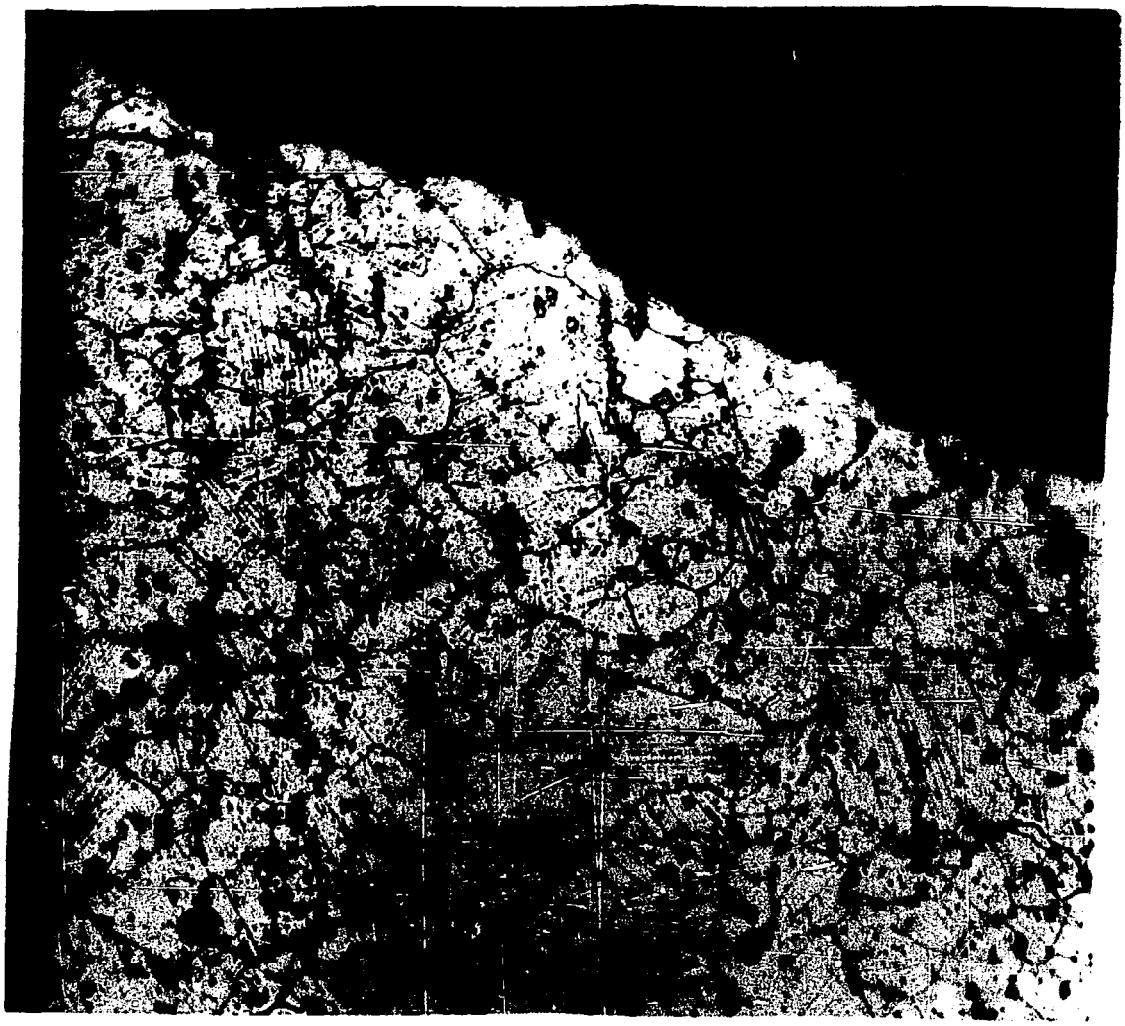
Magnification: 250X
Electrolytically etched in a solution of sulfuric acid and aqua regia in Marble's Reagent

Fig. 53. - Microstructure of Inconel 550 specimen that had been fractured by thermal fatigue at 1550/200°F.



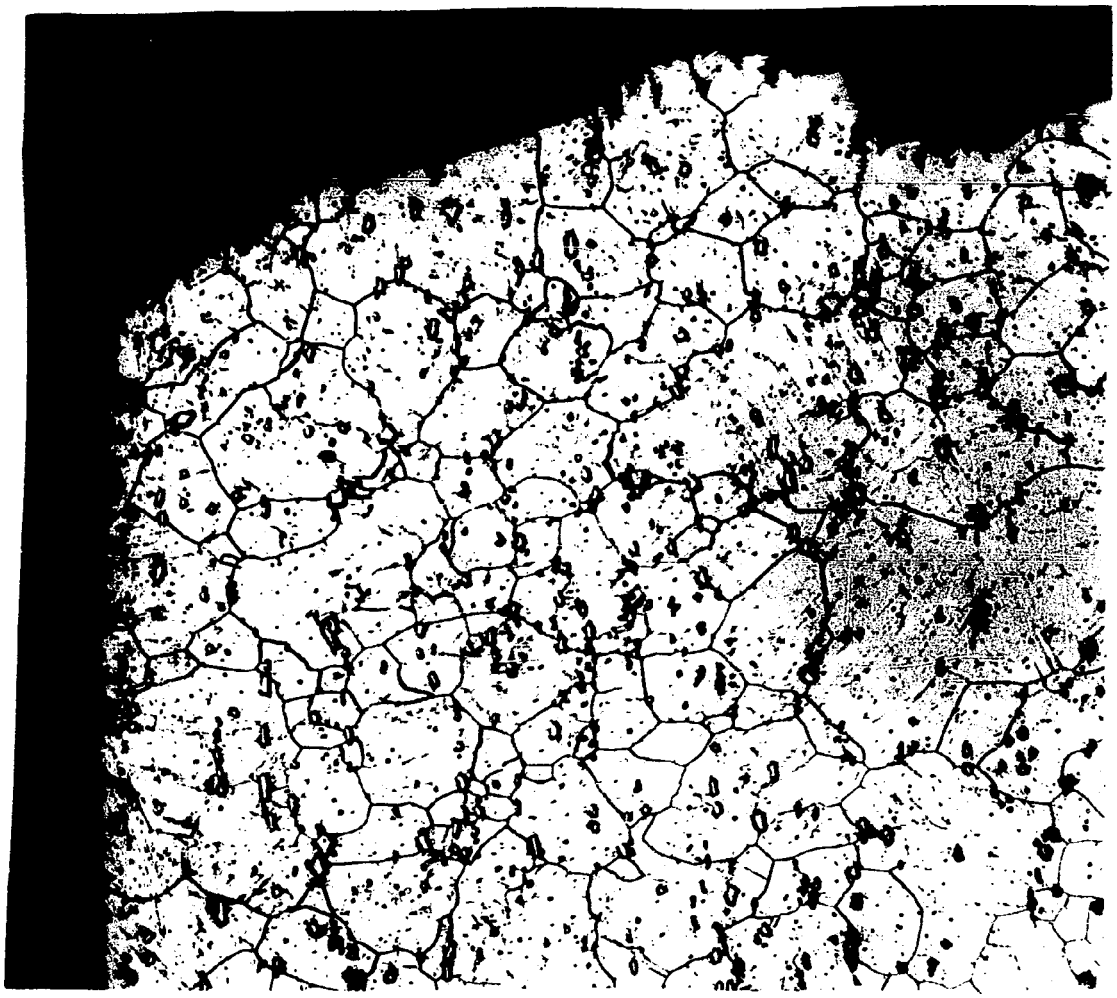
Magnification: 250X
Electrolytically etched in a solution of sulfuric acid and aqua regia in Marble's Reagent

Fig. 54. - Microstructure of Inconel 550 specimen that had been fractured by thermal fatigue at 1450/200°F.



Magnification: 250X
Electrolytically etched in a solution of aqua regia and glycerol

Fig. 55. - Microstructure of S-816 specimen that had been fractured by thermal fatigue at 1450/200°F.



Magnification: 250X
Electrolytically etched in a solution of aqua regia and glycerol

Fig. 56. - Microstructure of S-816 specimen that had been fractured by thermal fatigue at 1200/200°F.